

π^0 PHOTOPRODUCTION FROM DEUTERIUM IN THE
ENERGY RANGE $\frac{1}{2}$ TO 1 BEV

Thesis by
Harry Hobart Bingham Jr.

In Partial Fulfillment of the Requirements
for the Degree of
Doctor of Philosophy

California Institute of Technology
Pasadena, California

1960

ACKNOWLEDGEMENTS

This project was conceived by Dr. A. V. Tollestrup and was under his general direction over most of its course. My thanks go to Dr. Tollestrup also for his guidance during most of my graduate residence. Dr. A. B. Clegg participated in (and was in charge of) the development of the equipment and the early phases of the experiment. Later phases were done in collaboration with Dr. K. Althoff. Dr. R. L. Walker kindly supervised the experiment during the period when Dr. Tollestrup was in Europe.

Many members of the synchrotron staff and crew were of frequent assistance especially during the development of the equipment and the taking of data. Dr. M. Sands and Mr. A. Barna designed the kicksorter and much of the standard synchrotron electronics used in the experiment; the gas target is due particularly to Dr. V. Z. Peterson and Mr. E. Emery; much of the mechanical equipment to Mr. D. Sell and to the synchrotron crew under Mr. L. Loucks and Mr. B. Rule. Mr. A. Neubeiser and Mr. L. Luke operated the synchrotron and were of frequent assistance; Drs. H. R. Myers, G. Neugebauer, W. Wales, M. P. Ernstene and F. P. Dixon were running other experiments

at various times simultaneously with this one. Their cooperation and patience is much appreciated. Many valuable discussions were held with them and with many others, notably Drs. R. Gomez, H. Brody, D. D. Elliott, R. Worlock and S. Berman.

Partial support of the Atomic Energy Commission and the National Science Foundation, and the advice and encouragement of Dr. R. F. Bacher is gratefully acknowledged.

ABSTRACT

Gamma rays from the decay of neutral pions photoproduced in the bremsstrahlung beam of the Caltech synchrotron from high density deuterium and hydrogen gas have been observed with a Thallium Chloride crystal gamma ray spectrometer. Integral gamma ray yields and gamma ray energy spectra have been obtained for several bremsstrahlung endpoint energies from 0.6 to 1.08 Bev at $\theta=60^\circ$ and 120° with respect to the bremsstrahlung beam. The resulting integral D/H ratios show no significant variation with bremsstrahlung energy in this range; the ratio for $\theta=60^\circ$ may be a percent or so lower than that for $\theta=120^\circ$ but the average over energy and angle is consistent with $\gamma_D/\gamma_H = 0.94 \pm 0.02$ per nucleon.

Gamma ray yields for 0.2 Bev ranges of incident photon energy have been calculated from the above integral yields using the photon difference method. The resulting differential D/H ratio may exhibit a broad minimum around 0.8 Bev. The results are consistent, however, with a constant value $\Delta\gamma_D/\Delta\gamma_H = 0.85 \pm 0.05$ per nucleon, averaged over incident photon energy and spectrometer angle.

It was possible to separate to some extent those observed gamma rays coming from the decay of π^0 's photoproduced singly from those from π^0 's multiply photoproduced, on the basis of their different energy spectra. Cross sections for single π^0 photoproduction from hydrogen obtained from the "singles" gamma rays are in general (but not complete) agreement with those obtained by more precise methods by Vette and Worlock. The D/H ratios for singly photoproducing π^0 's may exhibit a maximum for incident photon energy about 0.8 to 0.9 Bev for $\theta=120^\circ$. n/p ratios calculated from the D/H ratios for singly photoproducing π^0 's are equal to the π^-/π^+ ratios from deuterium obtained by Neugebauer et al., within the rather large errors on the n/p for incident photon energy ≥ 0.8 Bev for both $\theta=60^\circ$ and $\theta=120^\circ$. The n/p ratio is significantly lower than the $-/+$ for $\bar{k}=0.7$ Bev, $\theta=120^\circ$, possibly higher for $\bar{k}=0.99$ Bev, $\theta=60^\circ$.

Cross sections for multiply photoproducing π^0 's from hydrogen, obtained from the observed multiples gamma rays, are of the same order of magnitude (possibly somewhat larger) as those obtained for example by Bloch for charged pion pair production from hydrogen, and exhibit similar features: no large variation is apparent with incident photon energy, pion center of mass system angle or pion CMS kinetic energy. The D/H ratio for multiple π^0 photoproduction is in general somewhat less than, but on the order

of one, with possibly a minimum in the region around 0.8 to 0.9 Bev incident photon energy. The observed multiples gamma ray energy spectra are not measured with sufficient precision to distinguish between multiple pion kinetic energy spectra predicted on the bases of various proposed models for pion pair production. Some indication is found, however, that the observed pion kinetic energy spectrum (CMS) may be somewhat peaked toward higher energy for incident photon energies 0.7 and 0.8 Bev, toward lower energy for 0.9 and 0.99 Bev.

CONTENTS

	Page
Acknowledgements	i
Abstract	iii
I. INTRODUCTION	1
A. General	1
B. This Experiment	6
II. OUTLINE OF THE EXPERIMENT	12
A. Apparatus	12
B. Procedure	22
C. Results - D/H Ratios and Absolute Cross Sections	24
i) Integrated Total Counting Rates γ	25
ii) Differential Total Counting Rates $\Delta\gamma, \Delta\gamma$	26
iii) Singly Photoproduced π^0 's	28
iv) Multiply Photoproduced π^0 's	31
SUMMARY TABLE OF RESULTS	41
III. DISCUSSION	43
IV. CONCLUSIONS AND SUGGESTIONS	55
APPENDIX I - EXPERIMENTAL DETAILS	57
A. Synchrotron and Bremsstrahlung Beam	57
B. Gas Target	61
C. Thallium Chloride Crystal Counter	62
i) Characteristics of TiCl_3 , Mounting	62
ii) Development of Crystal Optics, Cosmic Ray Tests	65
iii) Performance of Crystal Counter, Electron Tests	72
iv) Light Collection Efficiency, Energy Resolution	75
D. Gamma Ray Spectrometer	78
i) Electronics	79
ii) Rejection of Particles Other than Gamma Rays	82
iii) Choice of Radiator, Radiator Comparison Runs	85
iv) Efficiency for Detecting Gamma Rays	88
v) Adjustment of the Spectrometer	89

	Page
APPENDIX II - DATA ANALYSIS DETAILS	93
A. Separation of Gamma Rays from Different	
Reactions: Kinematics	93
i) Introduction	93
ii) Expected Pulse Height Spectra from Singly	
Photoproduced π^0 's	97
iii) Expected Pulse Height Spectra from Multiply	
Photoproduced π^0 's	100
iv) Effect of Nucleon Motion in Deuterium	102
B. Data Reduction Details	105
i) Errors	105
REFERENCES	108

I. INTRODUCTION

A. General

The nature and interactions of the fundamental particles in nature is one of the central problems of present day physics. Basic to this study is the probing of nucleons with high energy x-rays currently proceeding at Cal-Tech and at several other laboratories. Some general features of what is known to date about the nucleon through its interactions with photons and with mesons are:

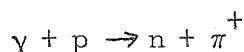
Photons of energy above 145 Mev threshold (approximately the pion mass) can produce pions in collisions with protons and neutrons. The total cross section for single π^0 photoproduction from protons, i. e., for the reaction:



rises near threshold approximately as the cube of the meson momentum,^{1,2} reaches a peak of about $\frac{1}{4}$ mb for incident photons of energy roughly twice the pion mass, then falls to about $\frac{1}{5}$ th of the peak value for gamma rays of about the energy of three pion rest masses.³ The angular distribution is throughout predominantly that expected for a magnetic dipole interaction⁴ with a small interference term (presumably with a small amount of

electric dipole) which changes sign near the peak. This resonance-like behavior indicates the existence of an "excited state" of the proton with angular momentum $3/2$ at an energy about two pion masses above the "ground state."

This conclusion is supported by the data on π^+ photoproduction:



(which is somewhat complicated by the presence of a much larger proportion of s-wave electric dipole production⁶). The ratio 2:1 for the π^0 photoproduction cross section to the p wave part of the π^+ indicates¹⁰ that the isotopic spin of this "first resonance" is $3/2$. Further evidence for the above conclusions is provided by the data on pion scattering.^{1,7}

More recently a second peak has been observed in both the π^0 ⁸ and π^+ ⁹ photoproduction cross sections at photon lab energy near 750 Mev (about four pion masses in the center of mass system of the proton and incident photon). The approximate ratio 1:2 for $\pi^0:\pi^+$ (the reverse of the lower resonance) may indicate isotopic spin $\frac{1}{2}$: contributions of several states are still quite important, in this energy range, however, and are different for π^0 and π^+ .

The angular momentum and parity of the level has been in some dispute⁶ as has indeed the applicability of the "resonance" description of these phenomena in general. It seems that no such simple description as was possible for the first peak can be given

for the second peak. Attempts to fit the available data under various assumptions for the angular momentum and parity of the level and for its interferences with other states have been only partially successful.¹¹ It has not yet been reported possible to fit all the data with the proposed assignments $D(3/2)$, $P(3/2)$ or $P(1/2)$, although probably the best qualitative fit is with $D(3/2)$.

In addition to the peak corresponding roughly to the 750 Mev peak in the photoproduction (about four pion masses CM), the pion scattering data¹³ show another peak about one pion mass higher. Marked changes in the character of both the π^0 and π^+ photoproduction angular distributions beginning above about 900 Mev indicate the influence of angular momentum states of at least $j = 5/2$. (The analysis of the π^+ data is complicated by the presence of the "retardation term" arising from the interaction of the incoming photon with the meson current,¹² which interferes with all states involved in the photoproduction introducing high powers of $\cos \theta$ in the angular distributions.)

The existence of these "resonance levels" or "isobaric states" of the nucleon was predicted by "strong coupling" theories^{7,10,15} which share the assumption that the interaction between a nucleon and the pion field is sufficiently strong that very large numbers of the quanta of the field (pions) are present at any time. Under this assumption one can, for example, treat the field as an unquantized classical field. The errors inherent in the approximation, as well

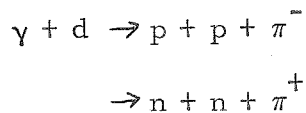
as approximations introduced to date to avoid divergent integrals (such as neglecting nucleon recoil) make the predictions of these theories at most only qualitatively correct, even at low energy.

The opposite approximation, namely that the pion-nucleon coupling is sufficiently weak that only a few quanta are present at any given time has enjoyed better success, particularly in the non-relativistic limit. Restriction to non-relativistic regions in general involves the neglect of nucleon recoil and nucleon-anti-nucleon pair effects and the introduction of a "cutoff" in the momenta involved at a value near the nucleon mass. Thus there are at least two arbitrary parameters in the theory; the value of the cutoff, and the coupling constant. Chew and Low¹⁶ have obtained fair agreement with the pion scattering and photoproduction data around the first resonance using this approach. The general features of the theory are summarized by Wick¹⁷ in a review article.

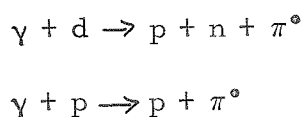
More recently the "dispersion" theory of Goldberger, involving very general conservation and completeness theorems has been used to correlate the low energy data in a reasonably satisfactory manner.¹⁸

The approximations involved in all these theories become less and less applicable as one goes to higher and higher energies. As yet no satisfactory fundamental theory exists to explain the data above the first resonance, although phenomenological correlations of the data have led to some understanding.

The photoproduction and scattering results quoted above were for reactions involving the proton. The corresponding reactions involving the neutron are more difficult to study experimentally because of the unavailability of free neutron targets and in some cases because of the difficulty of identifying and measuring the reaction products. Under the assumption of charge independence (which seems to be applicable to all "strong" interactions) certain relationships can be predicted among the scattering amplitudes involving protons and the corresponding ones involving neutrons for definite angular momentum and parity states.^{7,10} This assumption of charge independence (or conservation of isotopic spin) is of course not applicable to processes involving photons: photons interact specifically with charges and currents. However, the form of the interaction does permit the prediction of some relationships between photoproduction amplitudes from the proton and from the neutron.^{7,10,19,20} These relationships can then be used to predict (under certain conditions) such quantities as the "-/+ ratio from deuterium," i. e., the ratio of the cross sections for:



and the "D/H ratio for single π^0 's", the ratio of the cross sections for:



although there are difficulties in relating the $-/+$ and D/H ratios to the corresponding ratios from free nucleons because of the motion of the individual nucleons in the deuteron and the interaction of the mesons photoproduced from one nucleon with the other nucleon.

Both the $-/+$ and D/H ratios can be measured with better accuracy in general than the individual reactions themselves because of the cancellation of systematic errors. The results of Sands et al.^{7, 21} on the $-/+$ ratio at low energies and of Keck et al.²² on the D/H ratio, along with some more recent measurements²³ are in fair agreement with recent theory.

At higher energies, again, theoretical understanding of the data on these ratios is primarily phenomenological. As at lower energies, however, these data may be of use in clarifying the "states" involved in the photoproduction process and the nature of the interaction. The experiment described in this thesis was begun primarily with the goal in mind to extend knowledge of the D/H ratio to the higher energies presently available with the Cal-Tech synchrotron.

B. This Experiment

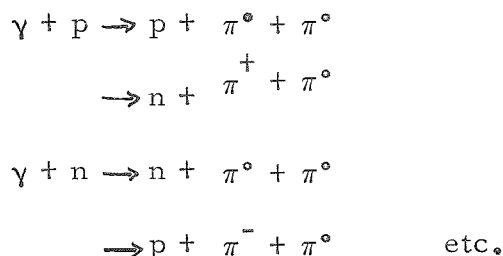
The technique adopted to extend knowledge of the D/H ratio to higher energies is the most direct and simple available (though not necessarily the easiest to interpret): the measurement of the

ratio of the yield of photons from the decay of π^0 's photoproduced in a target of deuterium to the same yield from a target of hydrogen. The technique is in principle the same as that used by Keck et al. for the same measurement at lower energy, with some refinements: a total absorption gamma ray spectrometer was used instead of the scintillation counter telescope used by Keck, and the control of the bremsstrahlung endpoint energy (the principal source of error in the previous work) had been improved considerably in the interim.

Measurement of the gamma ray energy was necessary to separate photons from the decay of π^0 's photoproduced singly (called "singles" gamma rays hereafter):



from photons from the decay of π^0 's photoproduced multiply (called "multiples"):



As many as six π^0 's can be photoproduced from stationary nucleons by 1.08 Bev photons (the maximum energy of the synchrotron at the time of this experiment), but photoproduction of more than two seems to be relatively rare.¹⁴

This separation was not necessary at the lower energies studied by Keck et al. Pair production cross sections²⁴ seem to rise slowly above threshold (about 310 Mev); thus photons from pair produced π^0 's contributed negligible "error" compared with their other sources of uncertainty.

This experiment, the data analysis and the results are described briefly in the next section. Details of the equipment and procedure are in Appendix I, of the kinematics, data analysis, corrections and errors in Appendix II. Results of the experiment are summarized in Table I. D/H ratios are presented for:

i) INTEGRATED TOTAL COUNTING RATE γ

γ is the counting rate of the spectrometer for photons of all energies (within limits set by counter biases and kinematics) from all reactions which may send photons to it (thus called "total"), initiated by bremsstrahlung photons of all energies (thus "integrated" over the bremsstrahlung spectrum). The counting rates are normalized by dividing by the target gas density, thus γ_D/γ_H is the ratio of total gamma ray counting rates per nucleon integrated over the incident bremsstrahlung spectrum.

ii) DIFFERENTIAL TOTAL COUNTING RATES $\Delta\gamma_{12}$ AND $\Delta\gamma_{123}$

$\Delta\gamma_{12}$ is an estimate of the total counting rate of the spectrometer for a range of incident photon energy E_2 to E_1 (thus "differential" in incident photon energy but still "total" in source

and decay photon energy), obtained by subtracting the yield γ_2 (obtained with synchrotron energy E_2) from the yield γ_1 (from E_1) after appropriate normalization.

$\Delta\gamma_{123}$ is obtained by subtracting from $\Delta\gamma_{12}$ a third yield γ_3 (from E_3) appropriately normalized.

The normalizations are so arranged that both $\Delta\gamma_{12}$ and $\Delta\gamma_{123}$ should approximate the "true" differential counting rate from incident photons in the energy range E_2 to E_1 , and should bracket it.

iii) SINGLES

The observed gamma ray energy spectrum $S(E_\gamma)$ obtained by subtracting channel by channel the spectra from two bremsstrahlung endpoints E_2 and E_1 is obtained in a manner analogous to that for $\Delta\gamma_{12}$; $\Delta S(E_\gamma)$ similarly corresponds to $\Delta\gamma_{123}$. The highest energy photons in these spectra are too energetic to have come from the decay of π^0 's photoproduced multiply by incident photons in the energy range E_2 to E_1 , except for the smearing effect of the spectrometer energy resolution. Calculated expected pulse height spectra are fitted to these singles gamma rays and the normalizations of the fits used to estimate the differential cross sections for singly photoproducing π^0 's. The singles gamma ray energy spectra are called $S_1(E_\gamma)$ and $\Delta S_1(E_\gamma)$, the corresponding differential cross sections $\sigma_1(\theta')$ and $\Delta\sigma_1(\theta')$,

iv) MULTIPLES

The multiples gamma rays $S_m(E_\gamma) = S(E_\gamma) - S_1(E_\gamma)$ and $\Delta S_m(E_\gamma) = \Delta S(E_\gamma) - \Delta S_1(E_\gamma)$ are used to estimate differential cross sections $\bar{\sigma}_m(\theta')$ and $\Delta\bar{\sigma}_m(\theta')$ for photoproducing π^0 's in conjunction with one or more other pions.

Results for the D/H ratios are in general consistent with lower energy data and with recent measurements of the $-/+$ ratio^{11, 25} in view of what theory is available. As at lower energy, the D/H ratio is not far from one, indicating that the neutron and proton are about equally efficient in the photoproduction of π^0 's. There are significant departures from one, however, particularly at higher energies. Interpretation of these results is to date primarily speculative.

Results for the absolute singles cross sections are in general but not in complete agreement with results obtained for hydrogen by presumably more accurate methods.⁸ This matter is discussed in Section III.

Results for absolute multiples cross sections are of the same order as those obtained for charged pion pair production,²⁴ and exhibit the same general features: no large variation with incident photon energy, pion angle, or pion kinetic energy (in the center of mass system of incident photon and target nucleon, hereafter called CMS). The precision of the results is not sufficient to permit

detailed comparisons; some speculation relevant to other reported work on pion pairs and to existing phenomenological models is presented in Section III.

II. OUTLINE OF THE EXPERIMENT:

A. APPARATUS

A diagram of the arrangement of the experiment is shown in Fig. 1. The bremsstrahlung beam of the synchrotron passes through the gas target filled with high density hydrogen or deuterium (as well as through targets associated with other experiments) and is monitored with an ionization chamber. π^0 's are photoproduced by the bremsstrahlung gamma rays from the hydrogen or deuterium nuclei and decay in the gas target. The decay photons are detected and their energy measured by the gamma ray spectrometer placed at a variable angle with respect to the bremsstrahlung beam. A brief description of the gamma ray spectrometer follows. A more detailed description of the equipment, its development and its performance in various tests is given in Appendix I.

The gamma ray spectrometer is shown in Fig. 2, along with a block diagram of the associated electronics. The heart of the spectrometer is the thallium chloride crystal counter, which consists of a large single crystal of TlCl* optically coupled to a 5" diameter photomultiplier tube. The phototube detects the

*Supplied by Mr. N. F. Blackburn, Engineer Research and Development Laboratories, Fort Belvoir, Virginia.

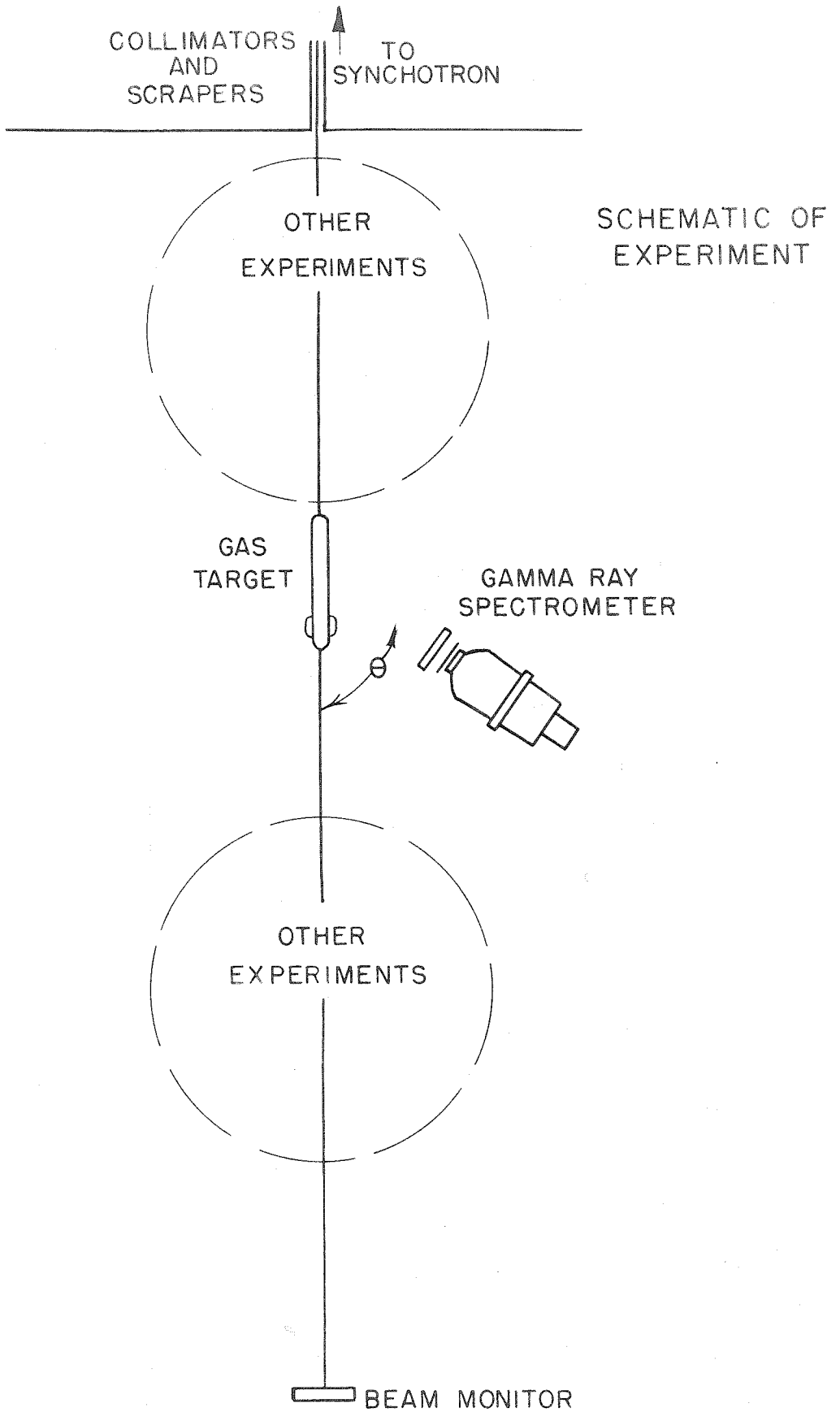
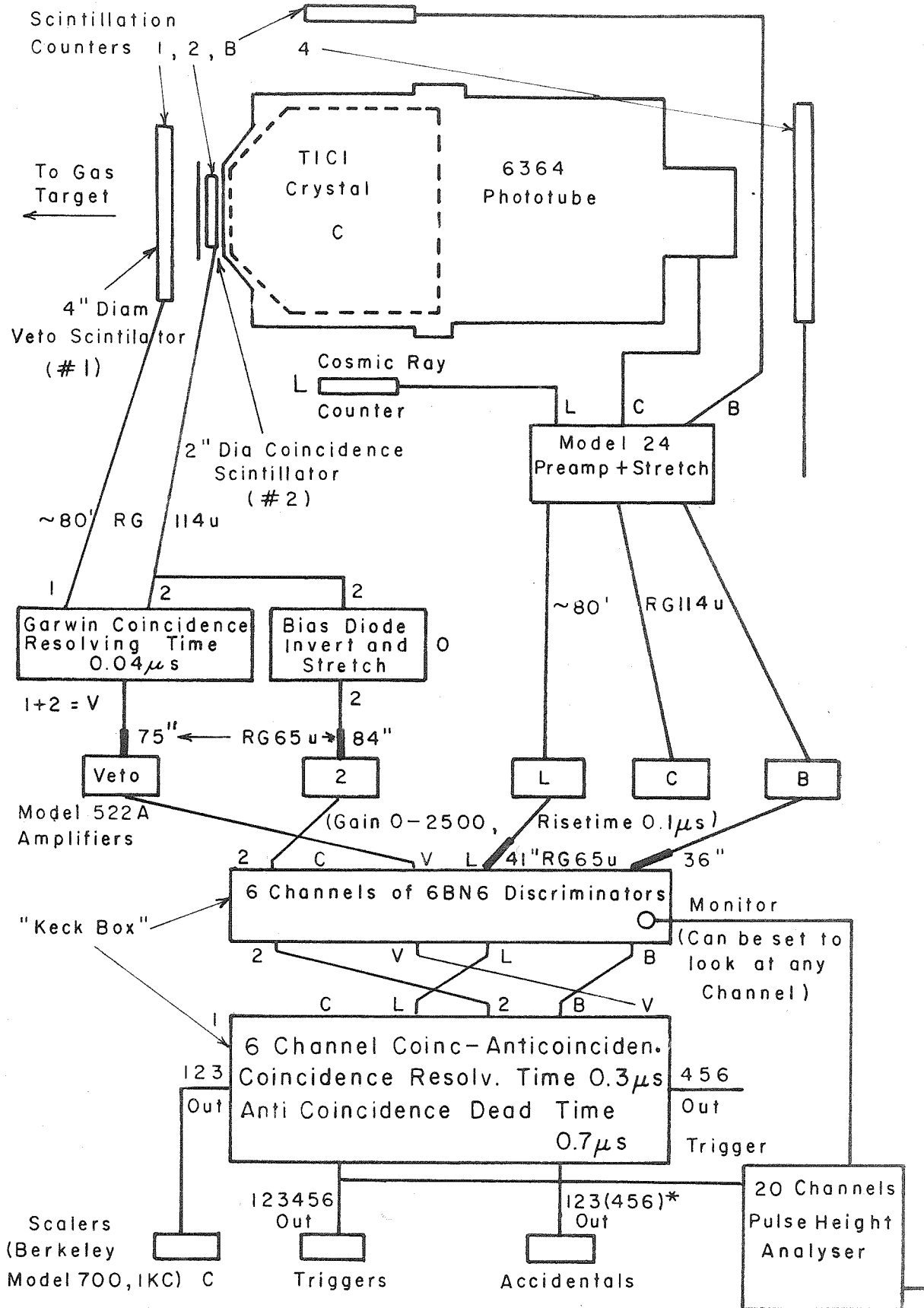


Fig. 1

FIG. 2 TELESCOPE & ELECTRONICS



Cerenkov light emitted by the electrons in the electron-photon shower produced in the crystal by an incident high energy gamma ray (or electron). Since the crystal is some 14 r.l. (radiation lengths) long by 13.4 r.l. in diameter, a large proportion of the shower is contained in the crystal for gamma rays with energies in the Bev range. The output pulse of the phototube is thus a measure of the energy of the incident photon.

In order to improve the rejection of particles other than photons, and to avoid the poor energy resolution of the edge regions of the crystal counter, it was used behind two conventional scintillation counters²⁴ in a counter telescope. The first counter of the telescope (#1 in Fig. 2) vetos charged particles incident axially (those incident from other directions are blocked by lead shielding). This is followed by a lead "radiator" (normally 2/3 r.l. thick) in which gamma rays convert to electron pairs, a second scintillator to detect the pairs, and the crystal to detect the shower proper. In normal running the pulses from the crystal counter (suitably amplified) are sorted by the kicksorter into its 20 channels when it is gated by an output pulse from the 6 channel slow coincidence-anticoincidence circuit (the "Keck box") set to respond to the event $2+c-V$, where 2 refers to a pulse from the 2" diameter coincidence scintillator (#2) next to the crystal counter (c), and V is effectively a pulse from the 4" diameter veto scintillator (#1)

in front. (Actually a fast coincidence between 1 and 2 is fed to the Keck box to reduce the counting rate in the veto channel to that of the relatively small 2" diameter scintillator. The signature $2+c-V$ is equivalent to $2+c-1$, if $V=1+2$.) Thus the spectrometer responds to neutral particles incident within 1" of the crystal axis (those further out do not trigger the 2" diameter scintillator) which make showers in the radiator which continue into the crystal. That the rejection of particles other than gamma rays was successful was checked by comparing counting rates as the thickness and atomic number of the radiator were varied: the counting rates were found to vary in the manner expected for gamma rays converting in the radiators (Appendix IDiii and Table 4). The efficiency of the charged particle veto was checked periodically by observing a "plateau" in the counting rate as the gain (or discriminator bias) for the veto scintillator was varied.

The calculated efficiency of the spectrometer for detecting gamma rays when used with the normal 2/3 r.l. thick radiator is shown in Fig. 3. This efficiency is mainly the probability of electron pair production in the lead, with approximate corrections (estimated largely by Dr. A. B. Clegg) for the possibility of conversion in material between the gas target and the veto scintillator and for the possibility that one or both of the pair electrons not trigger the coincidence scintillator because of energy loss or wide angle scattering in the lead.

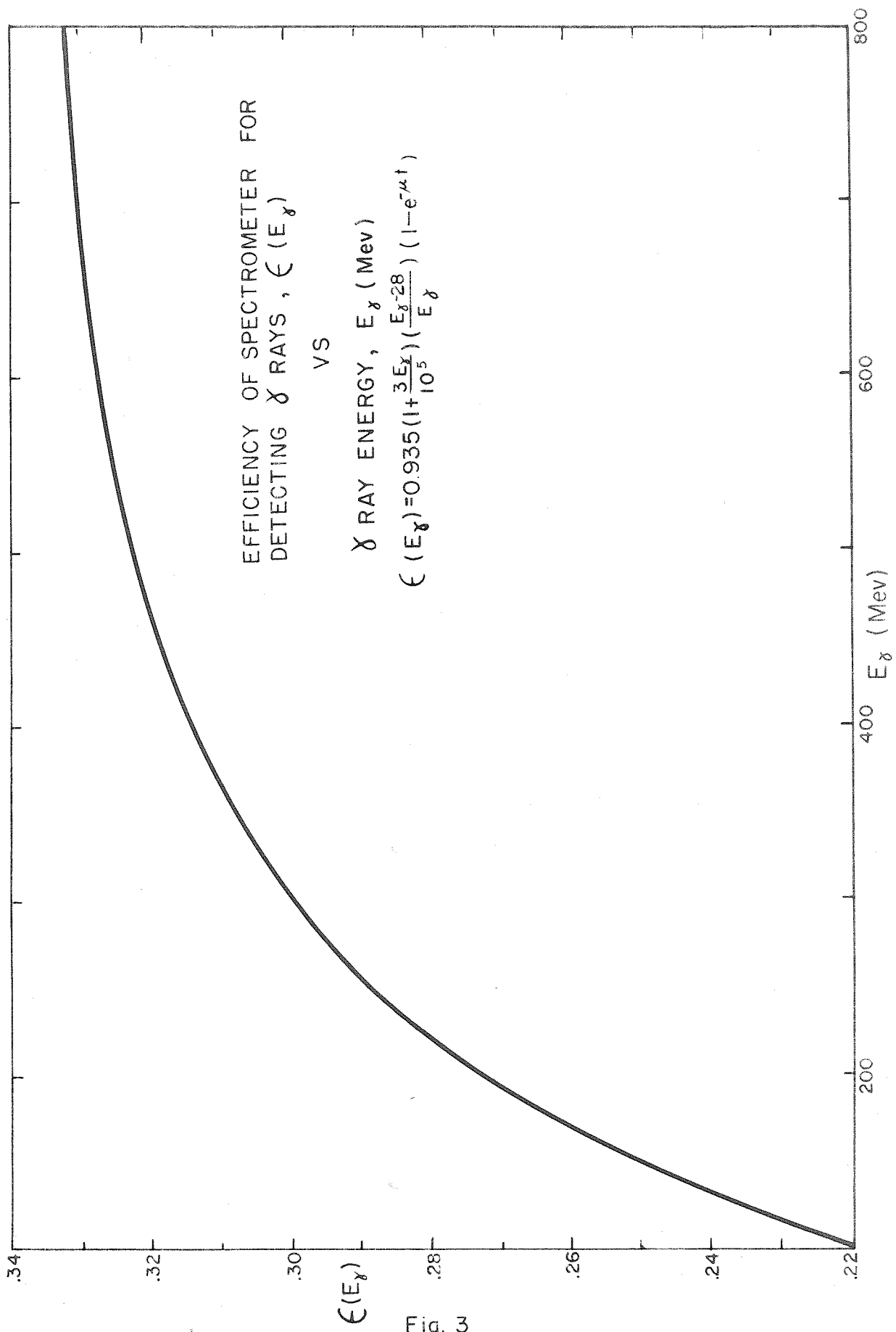


Fig. 3

Fig. 4 shows the energy calibration of the crystal counter obtained by observing the average pulse height from showers caused by electrons of known momentum as this momentum was varied (Appendix ICiii). Note that the crystal response is linear with electron momentum up to the highest momentum observed.*

The energy calibration of the crystal counter was reestablished from time to time during the course of the experiment by observing the average height of the pulses made in the crystal counter by cosmic ray muons passing through it. (To ensure that the muons passed entirely through the crystal a coincidence between the crystal and two scintillation counters, one above, one below it, was required to gate the kicksorter.) Cosmic ray muons passing through the crystal in a diametrical direction make pulses in it the same height as those from the showers made by 110 ± 5 Mev electrons (as observed during the electron tests). One such point reestablishes the whole calibration curve (within this 5%), since the energy response of the

*Extrapolation of the results of Kantz and Hofstadter²⁶ on the spatial extent of showers and comparison with the calculations of Yamagata and Yoshimine²⁷ would indicate that an increasing proportion of the energy of the shower should escape as its energy is increased. Thus one might expect the energy response of the crystal counter to fall below a straight line as the energy is increased. A compensating effect comes from the energy dependence of the light collection efficiency of the crystal, which would be expected to increase with shower energy as more of the light would be emitted closer to the cathode of the phototube for showers penetrating more deeply into the crystal. This interpretation is corroborated by the shower escape calculations and cosmic ray tests of the crystal optics discussed in Appendix IC.

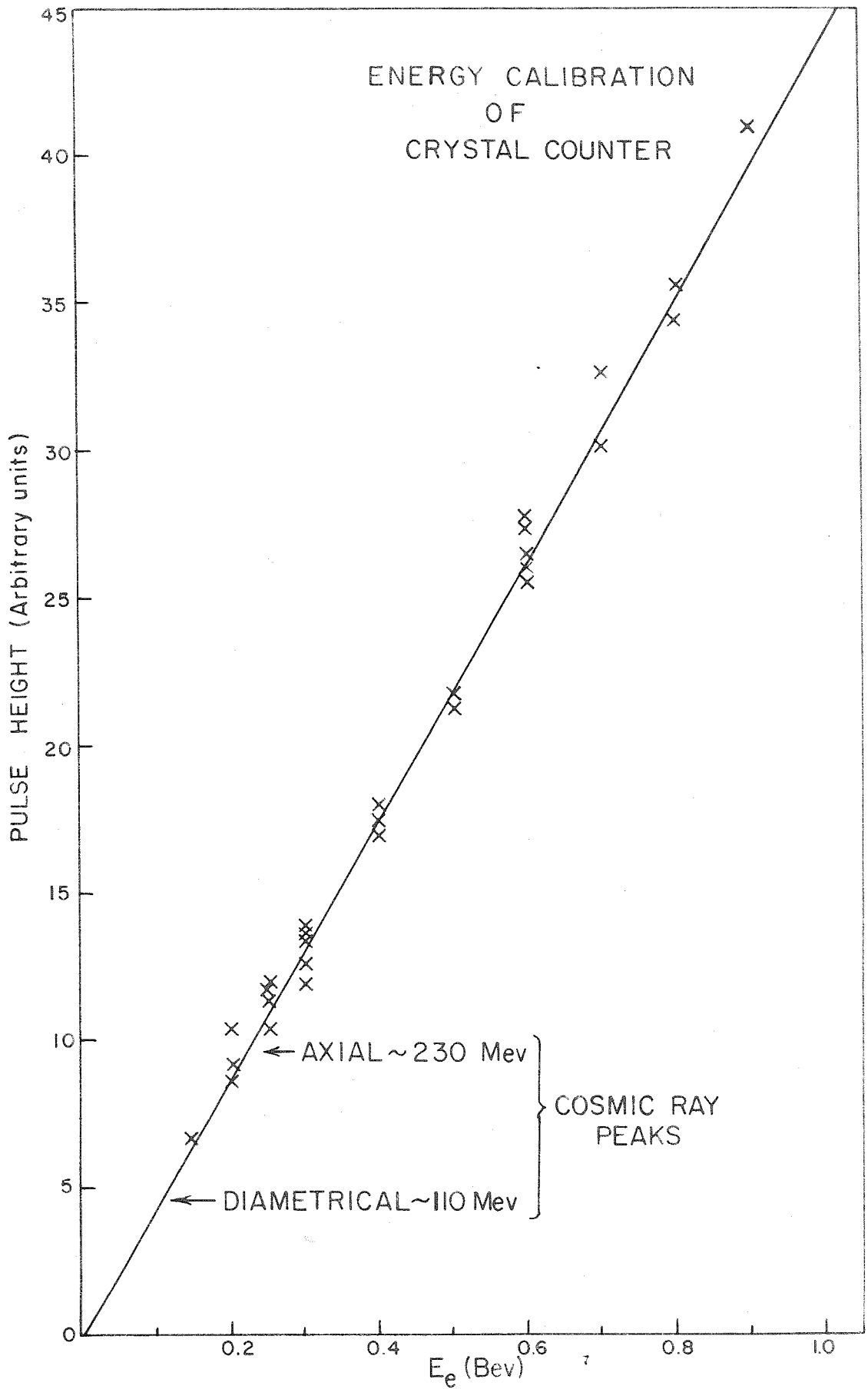


Fig. 4

crystal counter is linear and effectively zero for zero energy.

The width of the peak in the pulse height spectrum made by electrons of a given momentum incident on the crystal is a measure of the energy resolution of the crystal for that energy shower. This width seems to be due primarily to statistical fluctuations in the number of photoelectrons released at the cathode of the phototube by the Cerenkov light from the shower electrons. Smaller contributions to the width come from fluctuations in the energy escaping from the crystal, in the light produced and in the multiplication ratios at the dynodes of the phototube. The energy resolution of the spectrometer for gamma rays is calculated from the observed crystal resolution for electrons and plotted in Fig. 5. For this calculation it was assumed that each of the pair electrons made in the radiator by the gamma ray has equal probability of any energy from zero to the photon energy (minus 1 Mev), and loses constant energy per unit length in the lead through ionization alone. Inspection of the actual pair energy distribution²⁸ indicates that the first assumption would contribute negligible error. Monte Carlo calculations, such as that of Yamagata and Yoshimine²⁷ indicate that the second assumption may lead to an underestimate of the gamma ray widths.

The angular resolution of the spectrometer in the line source geometry of this experiment ($\pm 2^\circ$ or so) contributes another effective source of energy resolution ($\pm 5\%$ or so), as does the distribution of nucleon momenta in the deuteron ($\pm 2\%$ or so). Approximate

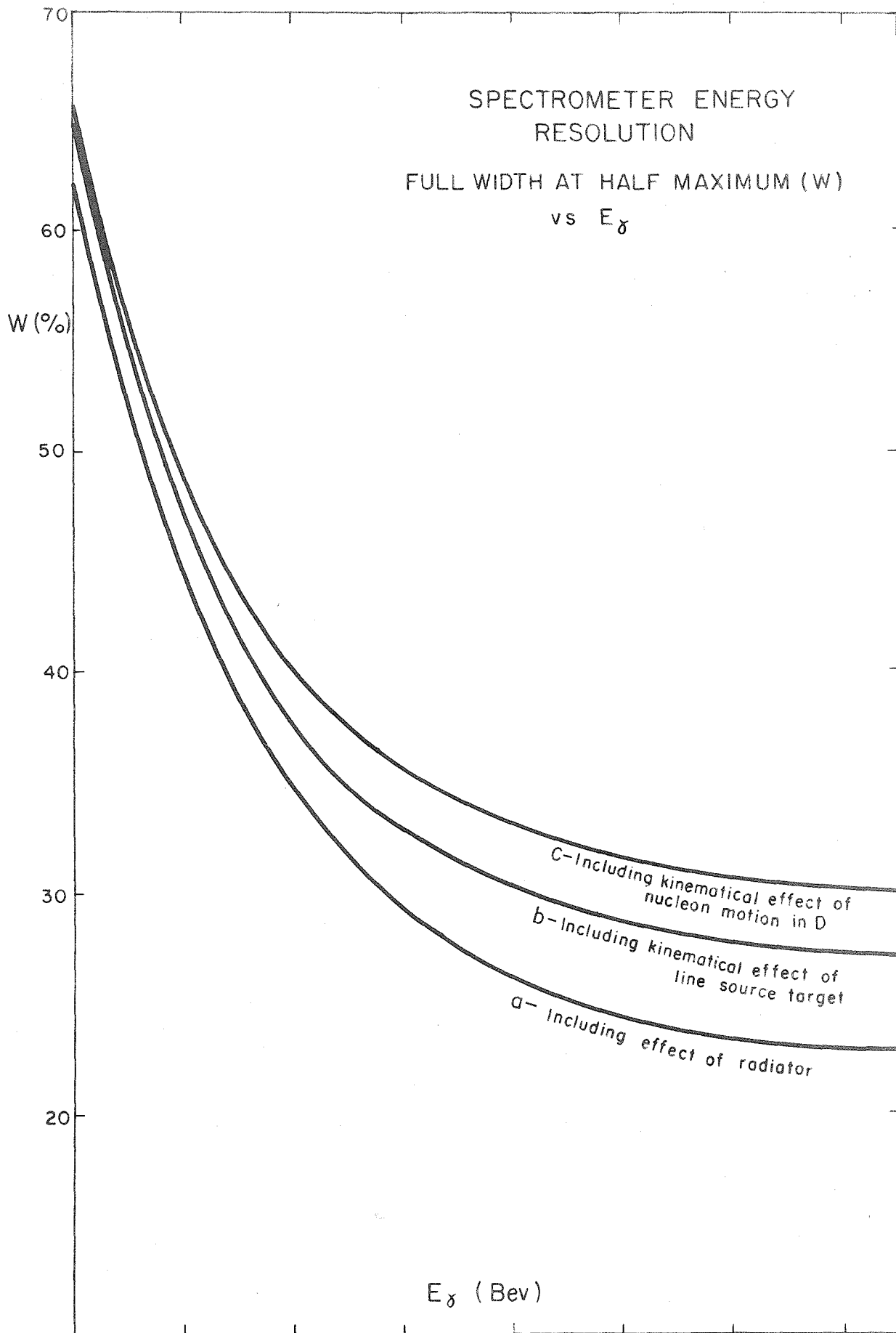


Fig.5

inclusion of these effects leads to curves b and c of Fig. 5 (See Appendices I and II).

B. PROCEDURE

The spectrometer was adjusted (Appendix IDv) to observe photons coming at a given angle θ relative to the bremsstrahlung beam of the synchrotron (mainly from the decay of π^0 's photo-produced in the gas target). The pulse height in the crystal counter (displayed in the kicksorter) is a measure of the photon energy. For a two body process, the energy and angle of one of the product particles gives sufficient information to calculate all the kinematics of the process. The energy and angle of one of the decay photons does not, however, determine the energy and angle of the π^0 which decayed: the other decay photon which is not observed carries off an unknown amount of momentum. If the energy of the incident photon which created the π^0 is known in addition, however, the π^0 energy* (and that of the nucleon from which it was created) can be calculated (Appendix IIA). Since the decay photon energy is known only within

*For a stationary target nucleon, the incident photon energy fixes the CMS energy of the π^0 and the LS to CMS transformation for the gamma ray energy and angle. Thus the π^0 energy and gamma ray energy and angle are known in the CMS. The π^0 direction must then lie on a cone of known apex angle relative to the gamma ray. If the gamma ray energy is large, this apex angle is small. Thus the π^0 angle is roughly the same as the gamma ray angle.

the energy resolution of the spectrometer (typically $\pm 30\%$) and the angle only within the angular divergence from the line source gas target ($\pm 12^\circ$ or so), it would suffice to know k (the incident photon energy) within perhaps 20 or 30%. This is accomplished in principle by subtracting the yield, properly normalized, obtained when the synchrotron is run at a given energy from the yield from a higher energy to obtain the yield from the range of incident photon energy between the two bremsstrahlung endpoints.

Deuterium, hydrogen and empty target yields were thus obtained for several synchrotron energies and two spectrometer angles. The yield of gamma rays converting in the radiator is assumed to be (Appendix IDv) the yield with radiator out (or in front of the veto counter) subtracted from the yield with radiator in. Care was taken to symmetrize the alternation between in and out runs not only in time but also with respect to what changes in the experimental conditions (such as targets associated with other experiments, and stray magnetic fields) were known.

When compatible with other experiments the synchrotron was alternated symmetrically a few times a day between the two energies E_1 and E_2 being subtracted: $E_1 E_2 E_1$ (or sometimes three energies: $E_1 E_2 E_3 E_2 E_1$). This procedure permitted estimation of drifts and served to cancel unobserved drifts of some time constants at least, in the average of a day's runs at a given energy.

D and H targets were alternated typically only a few times a month. It is likely that more frequent alternation would have reduced uncertainties due to electronics drifts and changing experimental conditions. Synchrotron energy scheduling difficulties would have been worse, however, if more frequent alternation had been attempted, making optimal time division among D, H and BG runs at the several energies more difficult.

Calibrations and tests of the equipment were made periodically in an effort to minimize the effects of drifts. In general the most serious drifts were in the kicksorter, thus it was calibrated every few hours with a precision pulser. The energy calibration of the crystal counter was checked every few days with a cosmic ray run, the preamps and amplifiers occasionally with a pulser.

C. RESULTS; D/H YIELD RATIOS AND ABSOLUTE CROSS SECTIONS

Table 1 summarizes the results of the experiment: D/H ratios for integrated total counting rate γ , differential total counting rates $\Delta\gamma$ and $\Delta\gamma$, and counting rates due mainly to singly photoproduced π^0 's; absolute differential cross sections for singly and multiply photoproducing π^0 's from hydrogen and deuterium.

The reduction of the spectrometer counting rate to the above quantities is described in brief below; further details are in Appendix

II. The quoted errors are due mostly to counting statistics. Other sources of uncertainty (see Appendix IIB) limit the precision to:

$$\begin{aligned} \gamma & \text{ about } \pm 3\%, & \gamma_D/\gamma_H & \text{ about } \pm 2\% \\ \Delta\gamma & \text{ and } \Delta\gamma & \text{ " } \pm 20\%, & \Delta\gamma_D/\Delta\gamma_H & \text{ " } \pm 5\% \\ \sigma_1(\theta') & \text{ and } \sigma_1(\theta') & \text{ about } \pm 30\%, & \sigma_{1D}(\theta')/\sigma_{1H}(\theta') & \text{ about } \pm 15\% \\ \sigma_m(\theta') & \text{ " } \sigma_m(\theta') & \text{ " } \pm 40\% \end{aligned}$$

i) Integrated Total Counting Rate γ :

The actual counting rate for gamma rays from the gas in the target which convert in the radiator is obtained by subtracting some backgrounds from the raw spectrometer counting rate:

Radiator OUT - typically some 10%, averaged over a given series of runs and subtracted from the average IN counting rate of the series.

Individual runs are normalized to standard bips (Appendix IA) to correct for variations in the beam monitor sensitivity. Average IN-OUT counting rates for a given series of runs are divided by the gas density for the series. All "averages" are weighted means with the individuals weighted inversely as their errors squared.

Empty Target - typically less than 5% of the corresponding IN-OUT rates with gas in the target, subtracted from average D and H counting rates.

The resulting integrated total counting rates (for each configuration) were averaged over each period of time between changes of target material. The final average γ_D/γ_H are listed in Table 1, plotted vs. the bremsstrahlung endpoint energy (E_0) in Fig. 6. Note that some 90% of the counts comprising the γ come from the 300 Mev resonance. Thus it is not surprising that γ varies little with E_0 . γ_D/γ_H is consistent with the average value 0.947 ± 0.007 for $\theta = 120^\circ$, 0.928 ± 0.005 for $\theta = 60^\circ$ (with a few percent additional possible systematic error).

ii) Differential Total Counting Rates $\Delta\gamma$, $\Delta\gamma$:

The total counting rate for a range of incident photon energy (thus "differential" in incident photon energy but still "total" in source and gamma ray energy) is obtained by subtracting the yield γ_2 obtained with the synchrotron energy E_2 from the yield γ_1 from E_1 after appropriate normalization. The normalization is arranged to approximately cancel the yields from incident photons of energy less than E_2 in the two spectra. (The normalization factor would be the ratio E_2/E_1 if the beam monitor response were independent of machine energy. Correcting for the monitor response gives the normalization factors of Table 3, Appendix IA.)

Since the lower energy parts of the two bremsstrahlung spectra do not fit exactly, there is a contamination to the yield desired (that from incident photons of energy between E_1 and E_2)

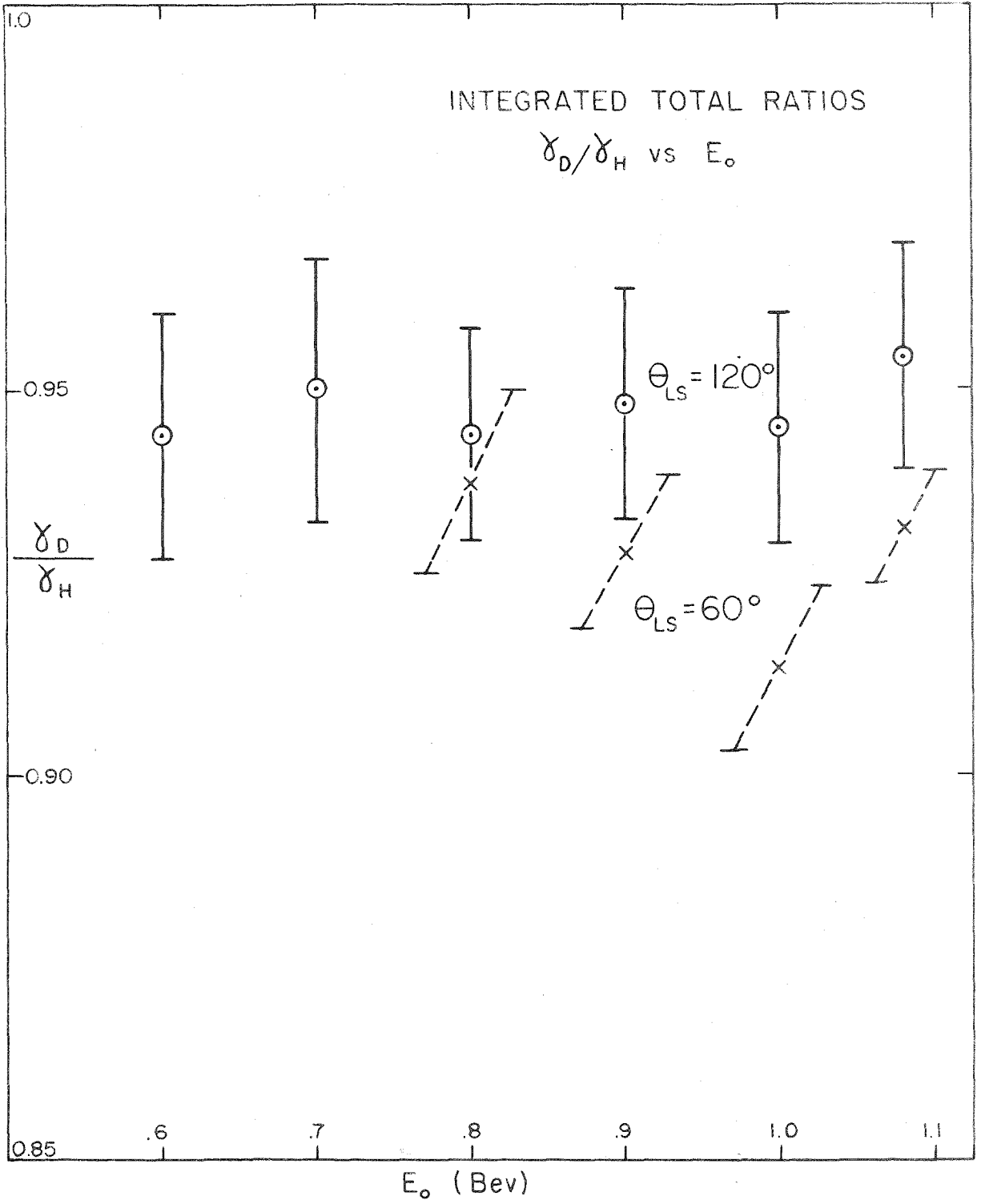


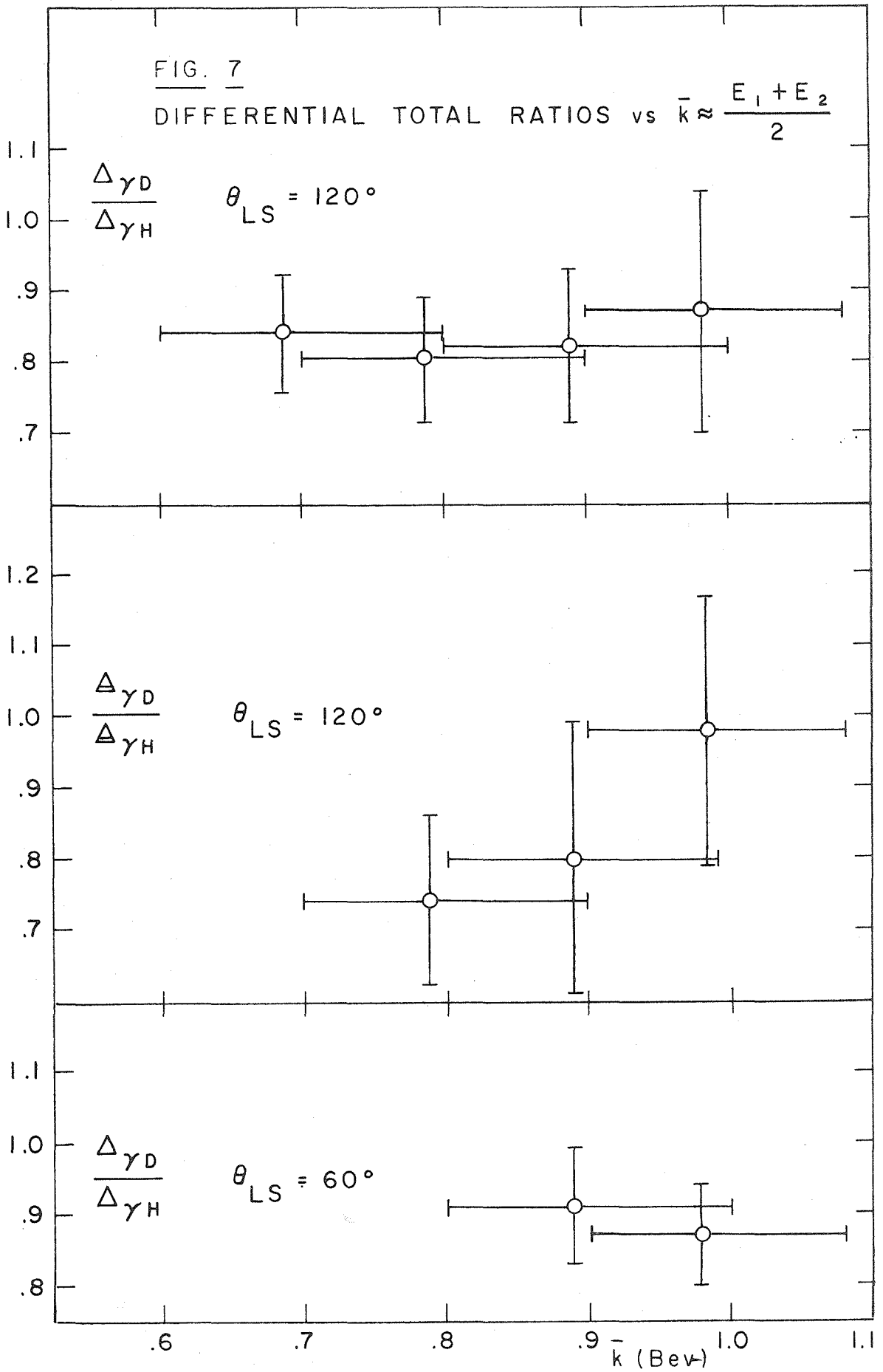
Fig. 6

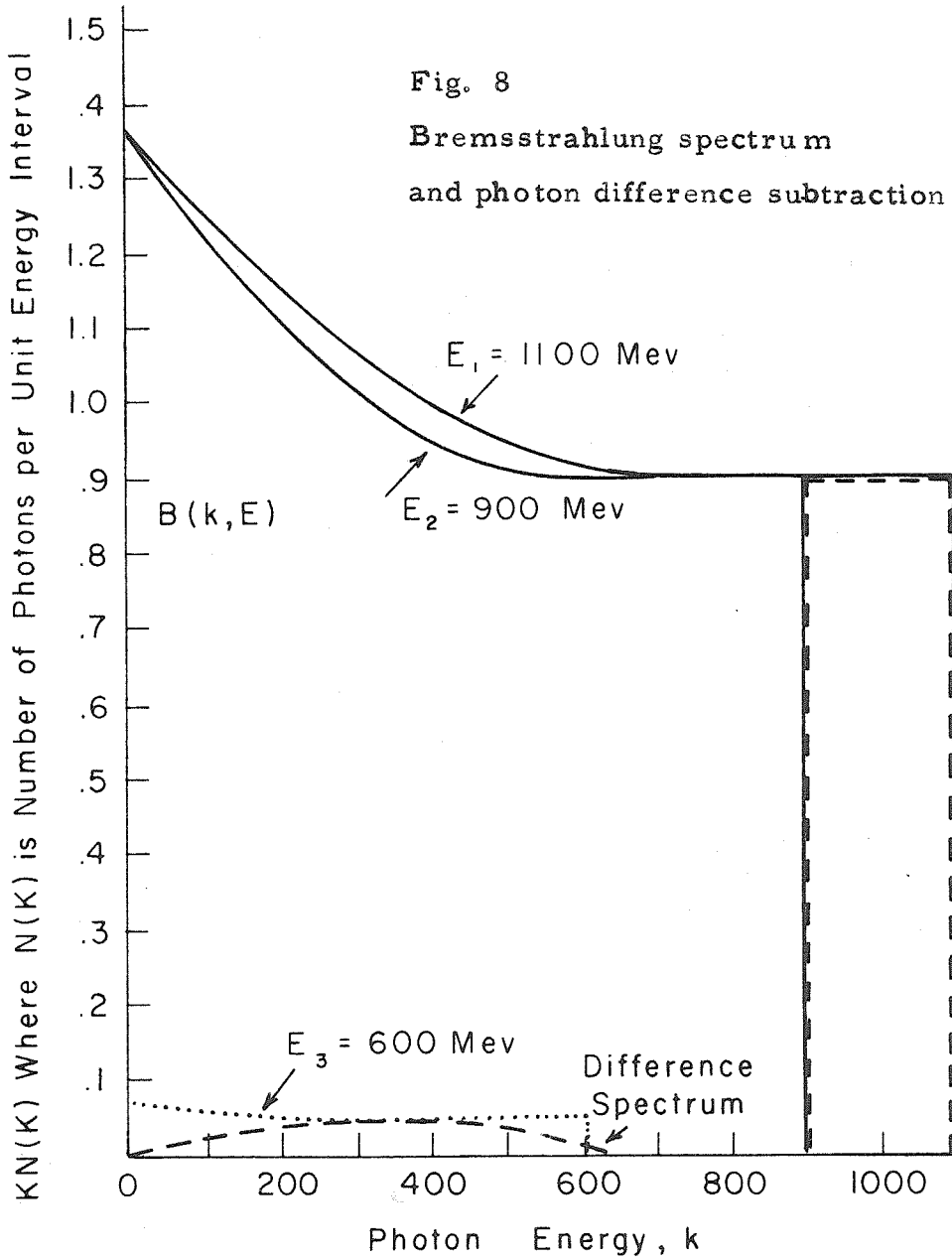
from the incompletely cancelled lower energy photons (see Fig. 8). This contamination can be estimated (as suggested by Dr. A. B. Clegg) by running the synchrotron at some lower energy E_3 . Subtracting the appropriately normalized yield γ_3 from the difference $\Delta\gamma_{12}$ gives $\Delta\gamma_{123}$.

Yields $\Delta\gamma_{12}$ were calculated for each day's runs, also average $\Delta\gamma_{12}$ over the several days during a period of time with a given target, for each k range and spectrometer angle. Backgrounds were subtracted and the individual $\Delta\gamma D/\Delta\gamma H$'s computed. Average $\Delta\gamma D/\Delta\gamma H$ are summarized in Table 1, plotted in Fig. 7 vs. average incident photon energy \bar{k} .

The yields $\Delta\gamma_{123}$ were obtained for each day's runs by subtracting from the yields $\Delta\gamma_{12}$ the yields γ_3 (with $E_3 = 0.6$ Bev) so normalized that there should be no contribution to a yield $\Delta\gamma_{123}$ from incident photons of energy 0.3 Bev (near the peak of the first resonance). Inspection of the subtracted bremsstrahlung spectra (Fig. 8) indicates that this procedure results in the subtraction of an overestimate of the yield from the incompletely cancelled lower energy part of the bremsstrahlung spectra. Thus $\Delta\gamma_{12}$ and $\Delta\gamma_{123}$ should bracket the "true" yield from the k range E_2 to E_1 . Resulting averages are summarized in Table 1, plotted in Fig. 7.

$\Delta\gamma_{12}$ and $\Delta\gamma_{123}$ do not in general differ appreciably. Also little variation is evident with \bar{k} or θ . The $\Delta\gamma D/\Delta\gamma H$ are consistent with a constant value 0.85 ± 0.05 from $\bar{k} = 0.7$ to 0.99 Bev.





One could in principle calculate the small correction to the yield γ_3 which would reduce it to the yield from the incomplete low k cancellation using the known π^0 cross sections and low k D/H ratios. This was not felt worthwhile in view of the large errors on the differences $\Delta\gamma_{12}$, and possible uncertainties in the exact bremsstrahlung spectrum shape at the gas target.

iii) Singly Photoproduced π^0 's:

The spectrometer pulse height spectrum is presumed to be the energy spectrum primarily of the decay gamma rays from π^0 's photoproduced in the target gas when the radiator out and empty target backgrounds have been subtracted (Appendix IIA). The reduction of the spectrum data follows (for each channel of the kick-sorter individually) the procedure for the differential total counting rate $\Delta\gamma$: IN runs (corrected to counting rate per standard hectabip) are averaged over a given series of runs and OUT runs similarly corrected and averaged are subtracted. The resulting 20 channel pulse height spectrum is presumed to be that of gamma rays converting in the radiator. After the empty target background spectrum (usually quite small) has been subtracted out, the resulting spectrum for a given synchrotron energy corresponds to the integrated total counting rate γ .

The spectrum $S(E_\gamma)$ resulting from the subtraction channel by channel of the spectra (properly normalized) from two different

synchrotron energies E_1 and E_2 , which corresponds to the differential total counting rate $\Delta\gamma_{12}$, is used to estimate differential cross sections for π^0 photoproduction, $\sigma_1(\theta')$. In most cases the spectrum $\Delta S(E_\gamma)$ corresponding to $\Delta\gamma_{123}$ differed negligibly from the corresponding $S(E_\gamma)$ in the upper channels used to determine the singles cross section. The cross sections labelled $\Delta\sigma_1(\theta')$ are obtained from the $\Delta S(E_\gamma)$.

The separation of the singles and multiples gamma rays is based on the number of high energy gamma rays found in the spectrum; because of the energy taken by the other pion(s) in multiple production, the decay photons from π^0 's photoproduced multiply have a maximum energy which is typically 50 to 100 Mev lower than the maximum energy photons from the decay of π^0 's photoproduced singly (for a range of incident photon energy of some 200 Mev). The smearing effect of the counter energy resolution destroys this separation to some extent, but in any case the highest energy photons come mainly from "singles" pions.

The observed gamma ray energy spectrum from singles, $S_1(E_\gamma)$ is related to the differential cross section for photoproducing single π^0 's, $\sigma_1(\theta')$ (see Appendix IIA):

$$S_1(E_\gamma) = \sigma_1(\theta') N_t 2\Omega \frac{W}{E_1} I(\bar{k}, \theta, E_\gamma) = \sigma_1(\theta') N$$

Here N is the spectrum normalization factor, composed of N_t , the number of target nucleons/cm² of beam, Ω the lab solid

angle subtended by the spectrometer, W , the total beam energy of the run, E_1 and E_2 , the bremsstrahlung endpoint energies of the integrated spectra subtracted, $\bar{k} \approx \frac{1}{2}(E_1 + E_2)$ the average incident photon energy*, θ , the lab angle of the spectrometer with respect to the beam, θ' , the corresponding CMS angle, and I , the integrated weighting function (Fig.9, see Appendix IIA):

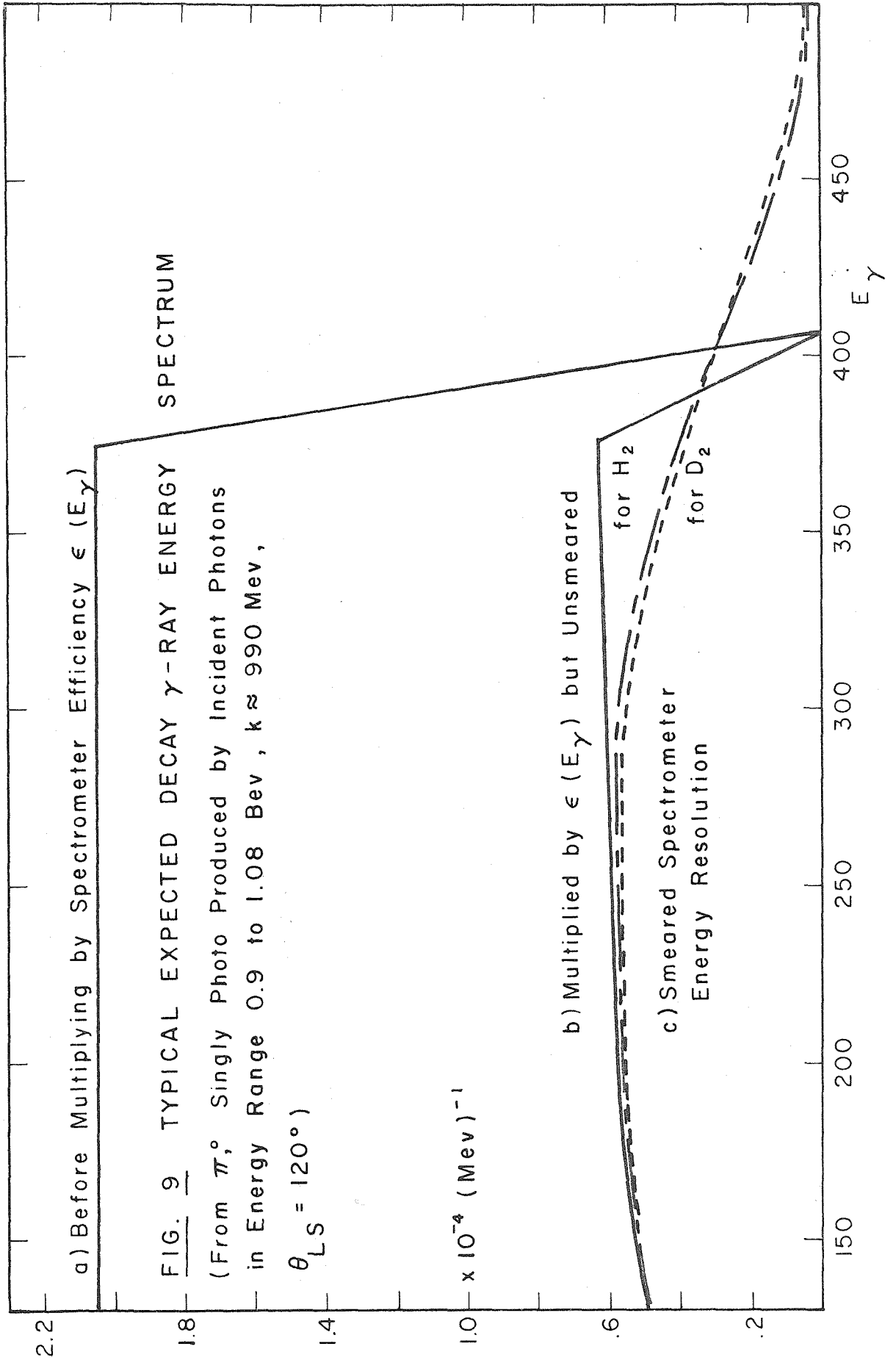
$$I(\bar{k}, \theta, E_Y) = \epsilon(E_Y) \int_{E_1}^{E_2} \frac{\sqrt{1 - \beta_c^2}}{1 - \beta_c \cos \theta} \frac{B(k, E_1)}{p'_\pi} \frac{dk}{k}$$

where $\epsilon(E_Y)$ is the spectrometer efficiency for detecting photons of energy E_Y , $\beta_c = k/k+M$ is the speed of the CMS relative to the LS for a stationary nucleon of mass M being hit by a photon of energy k , B/k is the bremsstrahlung energy spectrum with endpoint energy E_1 (Appendix IA) and p'_π is the photo-pion momentum in the CMS.

Integrating the observed spectrum over the high energy photons and comparing with the corresponding integral of the spectrum normalization factor N gives the cross section $\sigma_1(\theta)$. Cross

$$* \bar{k} = \int_{E_1}^{E_2} \frac{1 - \beta_c^2}{1 - \beta_c \cos \theta} \frac{B(k, E_1)}{p'_\pi} dk \bigg/ \int_{E_1}^{E_2} \frac{1 - \beta_c^2}{1 - \beta_c \cos \theta} \frac{B(k, E_1)}{p'_\pi} \frac{dk}{k}$$

gives	E_1	E_2	\bar{k}_{60°	\bar{k}_{120°	$\frac{1}{2}(E_1 + E_2)$
	1.08	0.9 Bev	0.979	0.983	.99
	1.0	0.8	0.889	0.890	.90
	0.9	0.7	0.787	0.788	.80
	0.8	0.6	0.686	0.688	.70



sections were obtained in this way for each day's runs; average cross sections and D/H ratios are summarized in Table 1, plotted in Fig. 11 vs. \bar{k} .

A not untypical fit to a measured pulse height spectrum is shown in Fig. 10. The fit is good to the upper channels of the kick-sorter which correspond to photons which could not have come from π^0 's photoproduced in conjunction with one or more other pions, except for the counter resolution smearing. This is an indication that the counts in the upper channels come mainly at least from the decay of π^0 's photoproduced singly. The possibility that some of the counts come from the decay of some hypothetical particle which also decays into two gamma rays cannot be ruled out.

Such fits do imply, however, that elastically scattered gamma rays do not contribute largely to the counting rates. Compton photons from a given incident photon energy coming out at a given lab angle would all be of the same energy, nearly the same as the peak energy photons from π^0 decay. The absence of such a "line" in the observed spectrum implies that the photon Compton effect is perhaps 1/5th or less as probable as single π^0 photoproduction. Theoretical estimates place it much lower than this.⁴⁸

iv) Multiply Photoproduced π^0 's:

When one subtracts the singles γ ray energy spectrum $S_1(E_\gamma)$ from the measured spectrum $S(E_\gamma)$ there remains a large

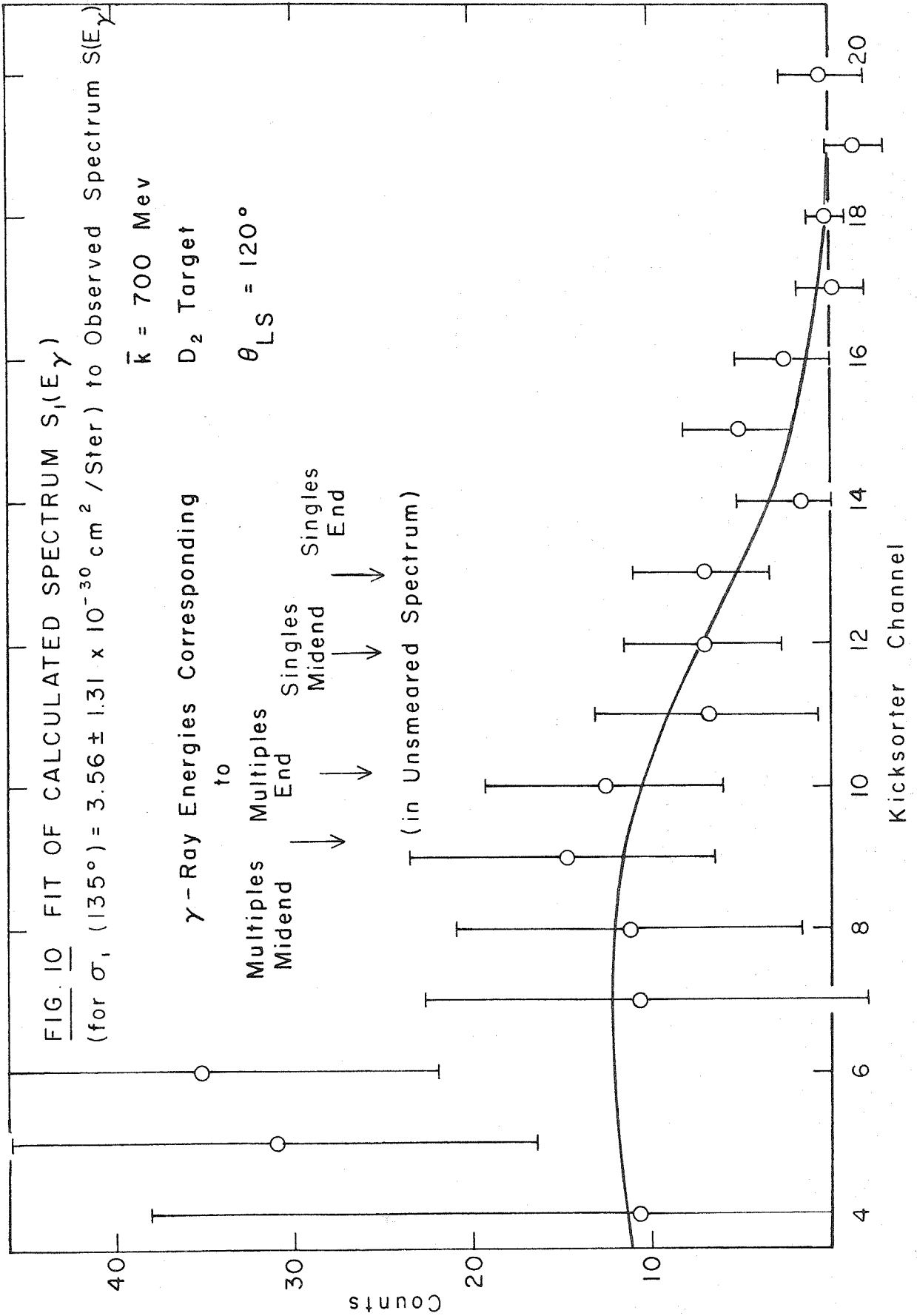
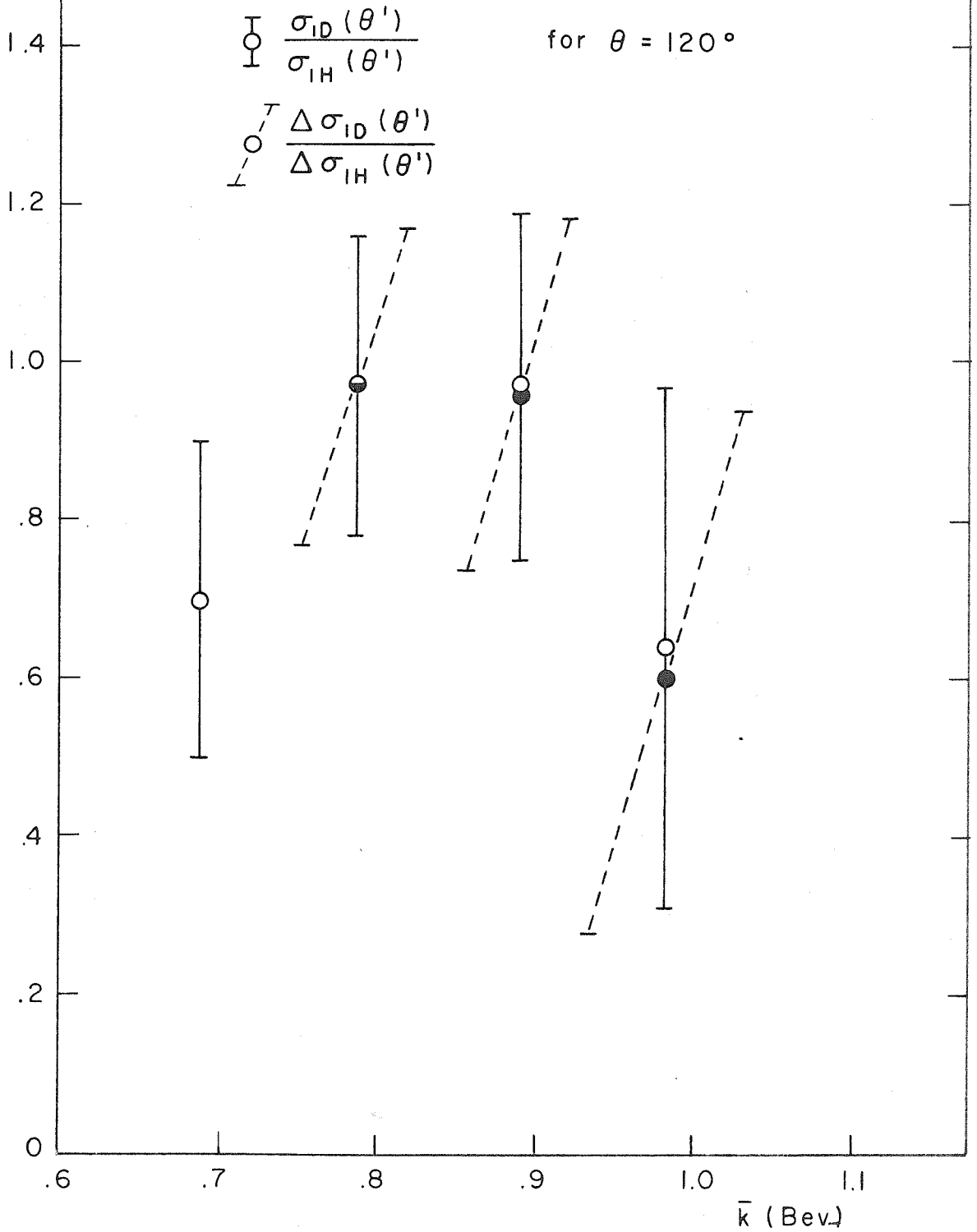


FIG. II

$\frac{D}{H}$ RATIO OF SINGLY PHOTOPRODUCED π^0_s
VS. INCIDENT PHOTON ENERGY



residue of low energy photons, $S_m(E_\gamma)$. These are presumed to come mainly from the decay of π^0 's photoproduced multiply; some, however, result from the imperfect subtraction of the yields from incident photons of energy below E_2 . Thus $S_m(E_\gamma)$ is an overestimate of the yield of multiples γ rays from incident photons in the energy range E_2 to E_1 between the endpoints of the subtracted bremsstrahlung spectra. An underestimate of this "true" yield comes from the spectrum $\Delta S_m(E_\gamma)$ remaining after the subtraction of $\Delta S_1(E_\gamma)$ from the spectrum $\Delta S(E_\gamma)$. Thus $S_m(E_\gamma)$ and $\Delta S_m(E_\gamma)$ should bracket the true multiples gamma ray spectrum. The poor statistics on the S_m and ΔS_m after the several subtractions, however, (and the imperfectly known bremsstrahlung spectrum shape, particularly at the gas target position) preclude any very ambitious attempt to estimate from them the energy spectrum of the parent multiply photoproduced pions.*

To improve the counting statistics on the S_m and ΔS_m the channels (of the kicksorter) have been bundled in twos and many days' runs in a given configuration have been averaged. (In some

*Multiple pion photoproduction is a three (or more) body reaction. Thus even for a single incident photon energy the pions which come out at a given angle in the LS will in general have a distribution of energies. Estimation of the form of this distribution requires a model for the multiple photoproduction process. As yet no satisfactory model for the process exists, although several have been proposed. 23, 43, 49

cases interpolations were necessary because of kicksorter drifts from day to day.) In Figs. 12 the resulting γ ray energy spectra are plotted vs. E'_γ , the CMS γ ray energy. The spectra have been reduced to CMS differential cross sections $\sigma_{\gamma m}(\theta, E'_\gamma)$, $\text{cm}^2/\text{Ster-Mev}$, using

$$S_m(E'_\gamma) = \epsilon(E'_\gamma) \frac{dE'_\gamma d\Omega'}{dE_\gamma d\Omega} \Omega N_t N_\gamma \sigma_{\gamma m}(\theta, E'_\gamma)$$

where $\epsilon(E'_\gamma)$ is the spectrometer efficiency, N_t the number of target atoms/ cm^2 , $\frac{W}{E_1} \frac{B(k, E_1)}{k} \Delta k = N_\gamma$ the number of incident bremsstrahlung photons and Ω the solid angle subtended by the spectrometer. Note that

$$\frac{d\Omega'}{d\Omega} = \left(\frac{E'_\gamma}{E_1} \right)^2 = \frac{1 - \beta_c^2}{(1 - \beta_c \cos \theta)^2}$$

where $\beta_c = k/k+M$ is the CMS velocity relative to the LS and θ the spectrometer lab angle relative to the bremsstrahlung beam.





Cross sections for photoproducing π^0 's above the CMS kinetic energy corresponding to the minimum observed photon energy are obtained by integrating the S_m and ΔS_m (adding also those photons of lower energy which would be present in addition even if only pions of energy above the lowest photon observed were present - namely those photons in a rectangular spectrum extending down in energy from the minimum observed, E'_{\min} , to about

$m_\pi^2/4E'_{\min}$ (for $E'_{\min} \gg m_\pi$) which then tails off to zero along a

curve corresponding to that along which it tails to zero at the high energy end). The resulting differential cross sections $\sigma_m(\theta')$ and $\Delta\sigma_m(\theta')$ and the pion kinetic energy range to which they correspond (typically 1/2 to 4/5 of the total kinematically available in the CMS) are summarized in Table 1. (See Appendix IIA): Each π^0 gives two photons, so:

$$\sigma_m(\theta') = \frac{1}{2} \int_0^{E'_\gamma/\max} \sigma_{\gamma m}(\theta', E'_\gamma) dE'_\gamma$$

Some idea of the form of the multiple pion energy spectrum giving rise to the observed S_m and ΔS_m can be gleaned from a comparison with them of expected gamma ray energy spectra calculated for several assumed pion energy spectra (Appendix IIAiii). Fig. 13 shows a typical S_m (reduced to $\sigma_m(\theta', E'_\gamma)$) compared with the gamma ray pulse height spectra which would result if the pion CMS energy spectrum were:

-  i) independent of energy from minimum to maximum kinematically available;
-  ii) increasing linearly toward the high energy side;
-  iii) increasing linearly toward the low energy side;
-  iv) increasing linearly up to the midpoint energy, then decreasing linearly to the maximum energy.

Even much grossly featured spectra as these yield gamma ray spectra which are qualitatively similar after the smearing by

the π^0 decay kinematics and the spectrometer energy resolution. Thus fits were not attempted for the more detailed pion energy spectra which might be expected on the basis of various models for multiple pion photoproduction. As is discussed in Section III, however, some conclusions relevant to such models can be drawn on the basis even of these simple spectra.

The measured multiples spectra plotted in Figs. 12 have been fitted with each of the above calculated pulse height spectra (by requiring that the areas of the calculated and measured spectra agree in the measured energy region). Differential cross sections $\sigma_{mt}(\theta')$ and $\Delta\sigma_{mt}(\theta')$ obtained from the fitting normalizations are listed in Table 1. These are estimates of the cross section for multiply photoproducing π^0 's, integrated over all pion energy (and of course over all kinematically available angles and energies of the other particles), summed over all reactions, weighted by the number of π^0 's yielded in each. The cross section obtained from the spectrum which best fits the measured spectrum (estimated by eye only) is starred in Table 2; this spectrum is also run through the measured points in Figs. 12. Since there is little difference between the gamma ray spectra from the rectangular pion energy spectrum and from the one peaked in the middle, when one is starred the other would fit nearly as well. In most cases, however, it was possible to distinguish the forward and backward peaking spectra. In Fig. 13,

for example, the best fit is clearly to the backward peaking one. The best fitting (of forward and backward) is checked in the table if not already starred.

The fact that the observed multiples spectra go to zero near the kinematically expected spectrum end is primarily due of course to the method of estimating the singles spectra which are subtracted from the measured spectra to obtain them: a calculated singles spectrum is run through the experimental points above a point corresponding to the endpoint energy of the multiples photons. The $\theta = 60^\circ$ multiples spectra are quite consistent with zero all through the energy range above this multiples bias, some indication that the calculated spectrum has the correct shape (and that no other reactions such as elastic photon scattering contribute significantly) and that the residual counts are indeed due to multiply photoproduced π^0 's. The averaged $\theta = 120^\circ$ spectra, however, exhibit a systematic negative region near the multiples endpoint and positive region further out in energy, (although they are still quite consistent with zero in the energy range above the multiples endpoint). This matter is further discussed in the following section.

FIG. 12a

MULTIPLES γ -RAYS
 $\sigma_{\gamma m}(\theta', E'_\gamma)$ vs E'_γ (CMS)

$\bar{k} = 0.7$ Bev $\theta_{LS} = 120^\circ$

DEUTERIUM

$\sigma_{\gamma m}(\theta', E'_\gamma)$

— \bar{I} for $\sigma_{mt}(\theta') = 2.9 \mu\text{b}/\text{Ster}$

$\times 10^{-31} \text{ cm}^2 / \text{Ster} - \text{Mer}$

Multiples
Midend \rightarrow

E'_γ (Bev)

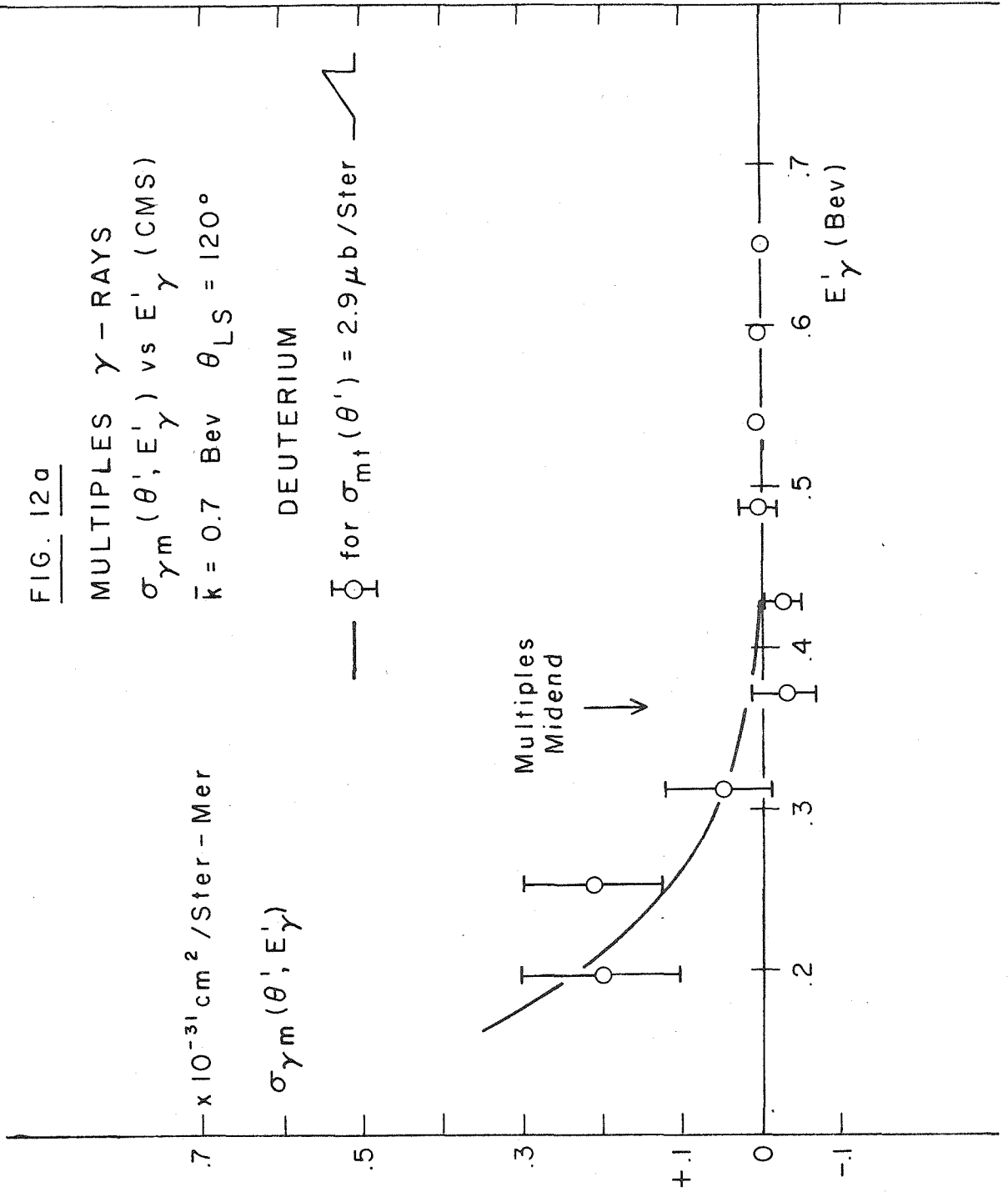


FIG. 12b

MULTIPLES γ -RAYS
 $\sigma_{\gamma m}(\theta', E'_\gamma)$ vs E'_γ (CMS)
 $\bar{k} = 0.7$ Bev $\theta_{LS} = 120^\circ$

$\times 10^{-31}$ cm² / Ster - Mer

$\sigma_{\gamma m}(\theta', E'_\gamma)$

HYDROGEN

— $\bar{\sigma}$ for $\sigma_{mt}(\theta') = 5.7 \mu\text{b}/\text{Ster}$ \wedge

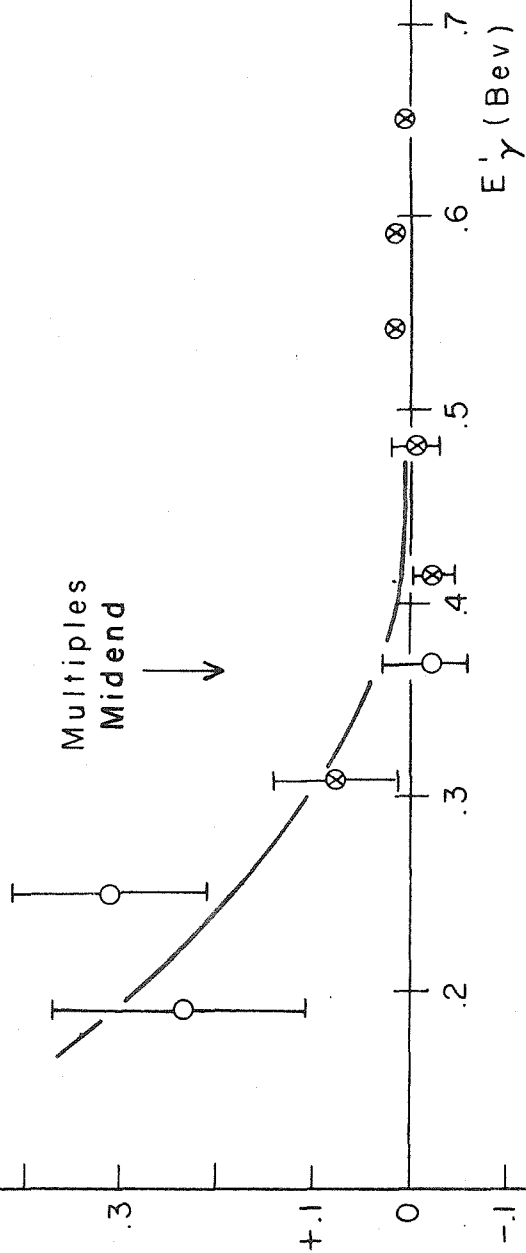


FIG. 12c

MULTIPLES γ -RAYS $\sigma_{\gamma m}(\theta', E'_\gamma)$ vs E'_γ (CMS) $\bar{k} = 0.8$ Bev $\theta_{LS} = 120^\circ$

DEUTERIUM



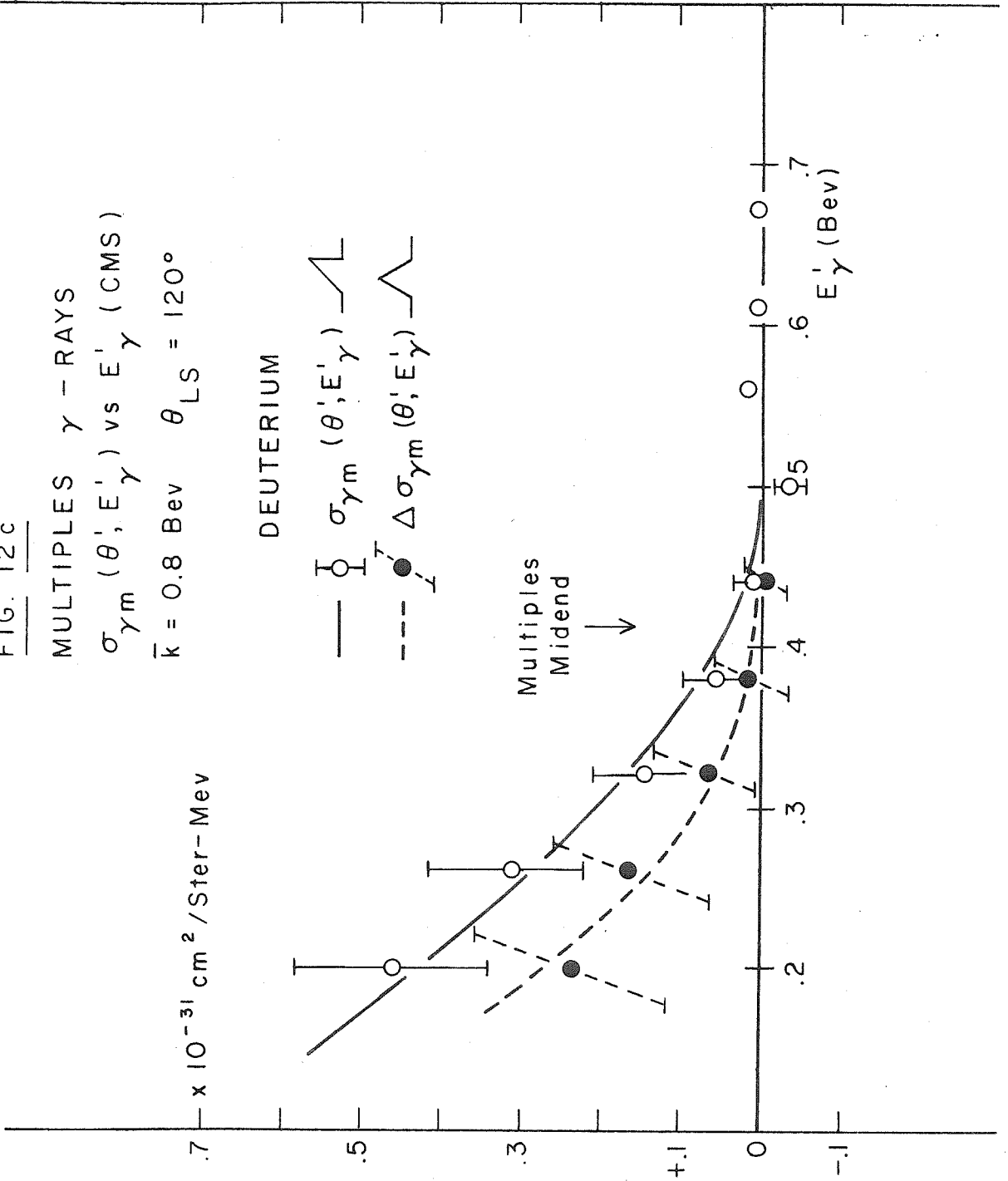
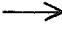
— $\sigma_{\gamma m}(\theta', E'_\gamma)$ - - - $\Delta\sigma_{\gamma m}(\theta', E'_\gamma)$  $\times 10^{-31}$ cm²/Ster-Mev E'_γ (Bev)Multiples
Midend 

FIG. 12 d

MULTIPLES γ - RAYS $\sigma_{\gamma m}(\theta'; E'_\gamma)$ vs E'_γ (CMS) $\bar{k} = 0.8$ Bev $\theta_{LS} = 120^\circ$

HYDROGEN

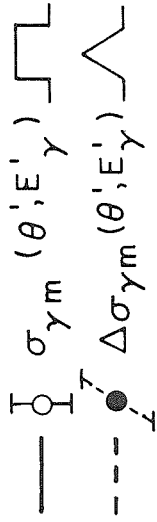
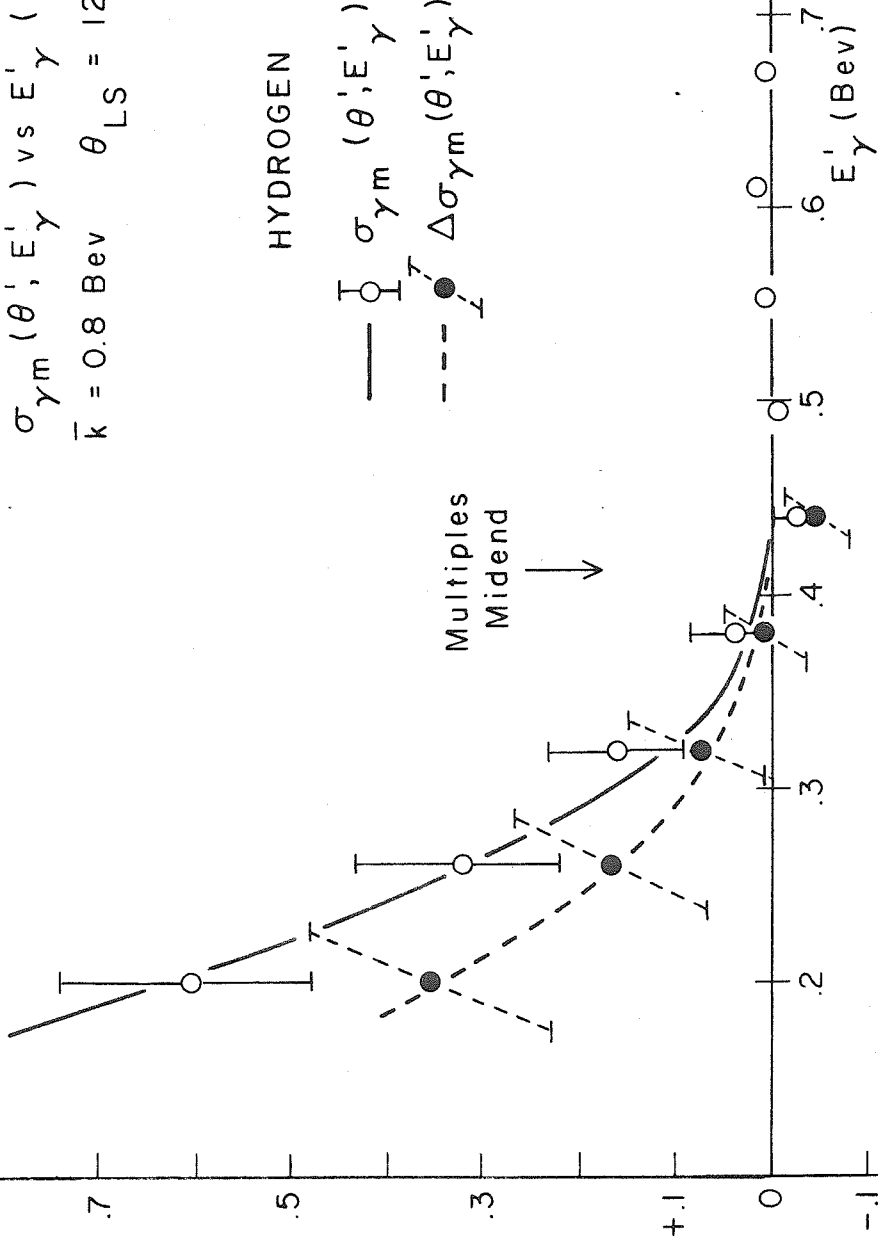
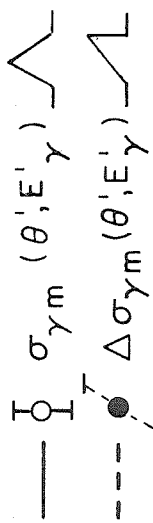
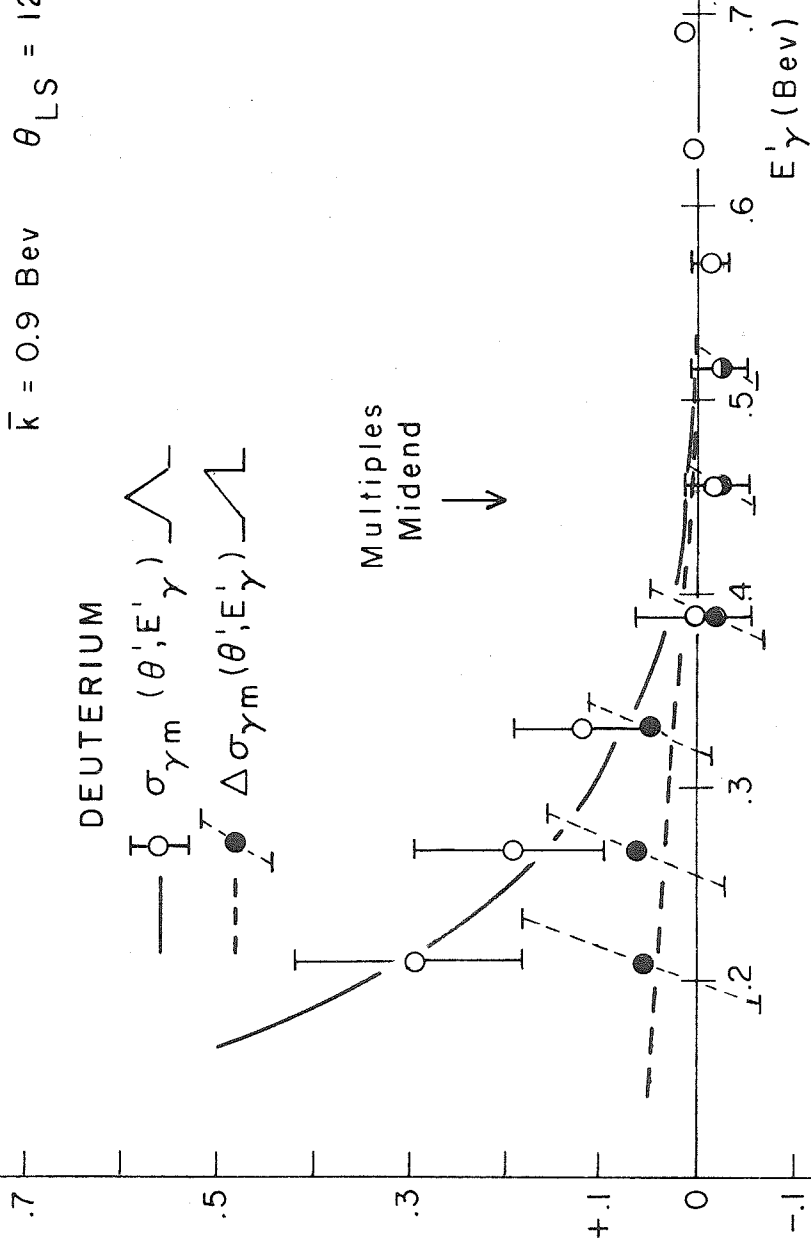
 $\times 10^{-31}$ cm²/Ster - Mer

FIG. 12e

MULTIPLES γ - RAYS $\sigma_{\gamma m}(\theta; E'_\gamma)$ vs E'_γ (CMS) $\bar{k} = 0.9$ Bev $\theta_{LS} = 120^\circ$ $\times 10^{-31} \text{ cm}^2 / \text{Ster-Mev}$

DEUTERIUM

Multiples
Midend \rightarrow 

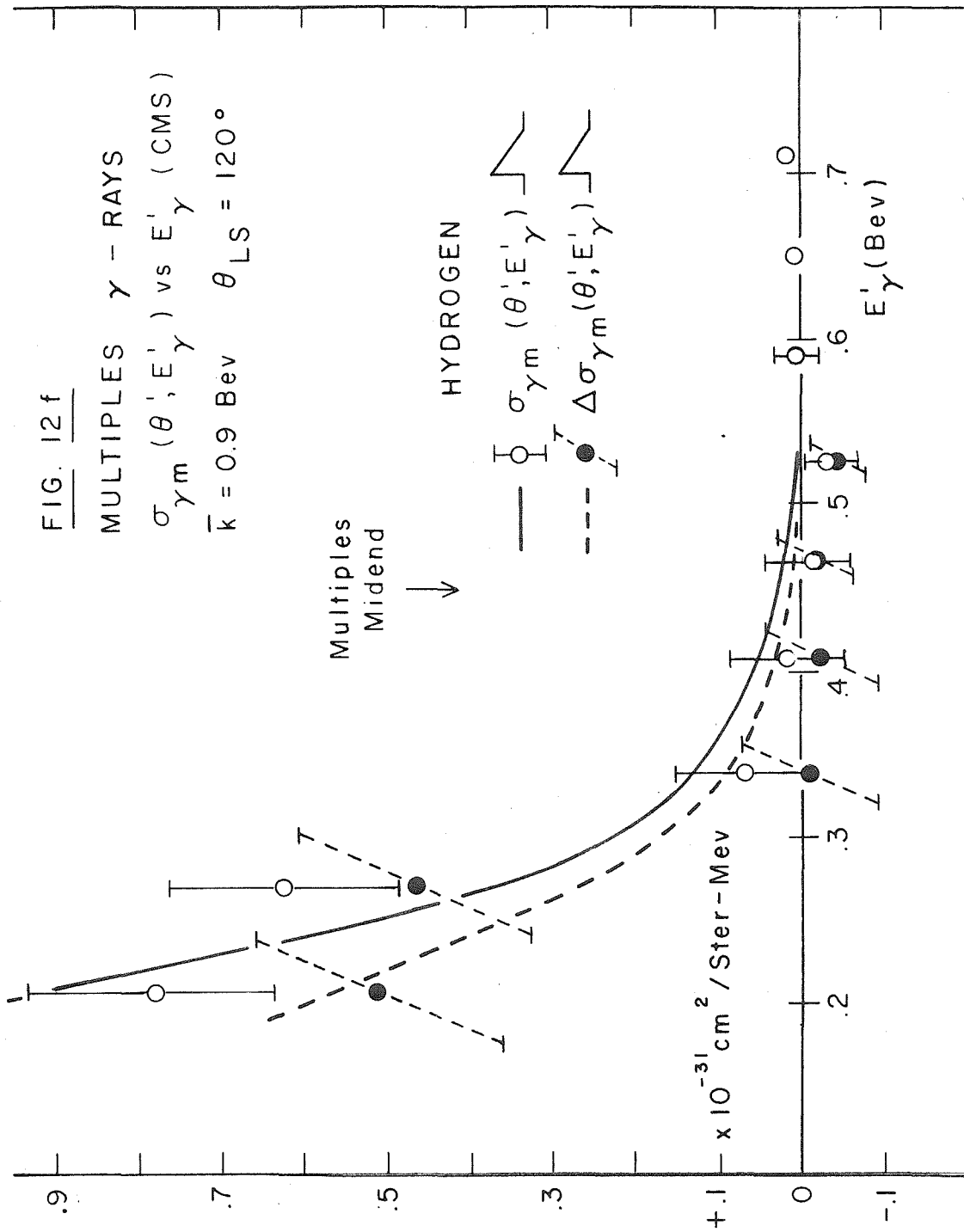


FIG. 12g

MULTIPLES γ - RAYS $\sigma_{\gamma m}(\theta', E'_\gamma)$ vs E'_γ (CMS) $\bar{k} = 0.99$ Bev $\theta_{LS} = 120^\circ$

DEUTERIUM

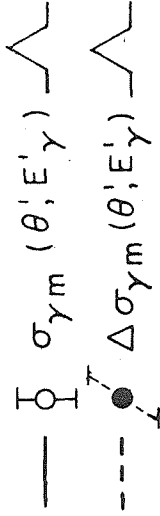
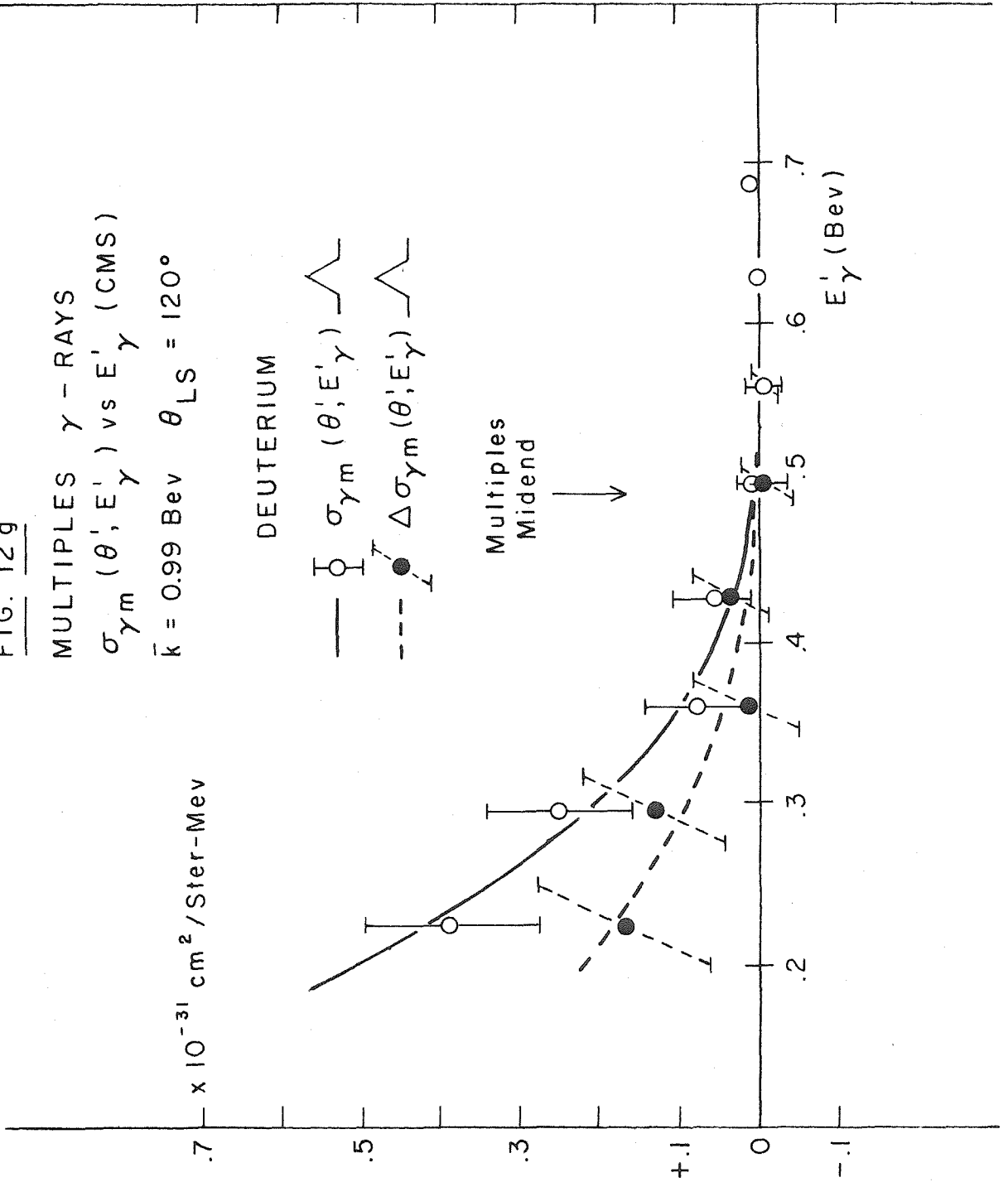
Multiples
Midend \rightarrow $\times 10^{-31} \text{ cm}^2 / \text{Ster-Mev}$ E'_γ (Bev)

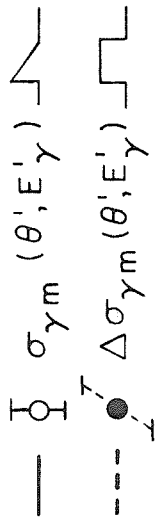
FIG. 12 h

MULTIPLES γ - RAYS

$\sigma_{\gamma m}(\theta', E'_\gamma)$ vs E'_γ (CMS)

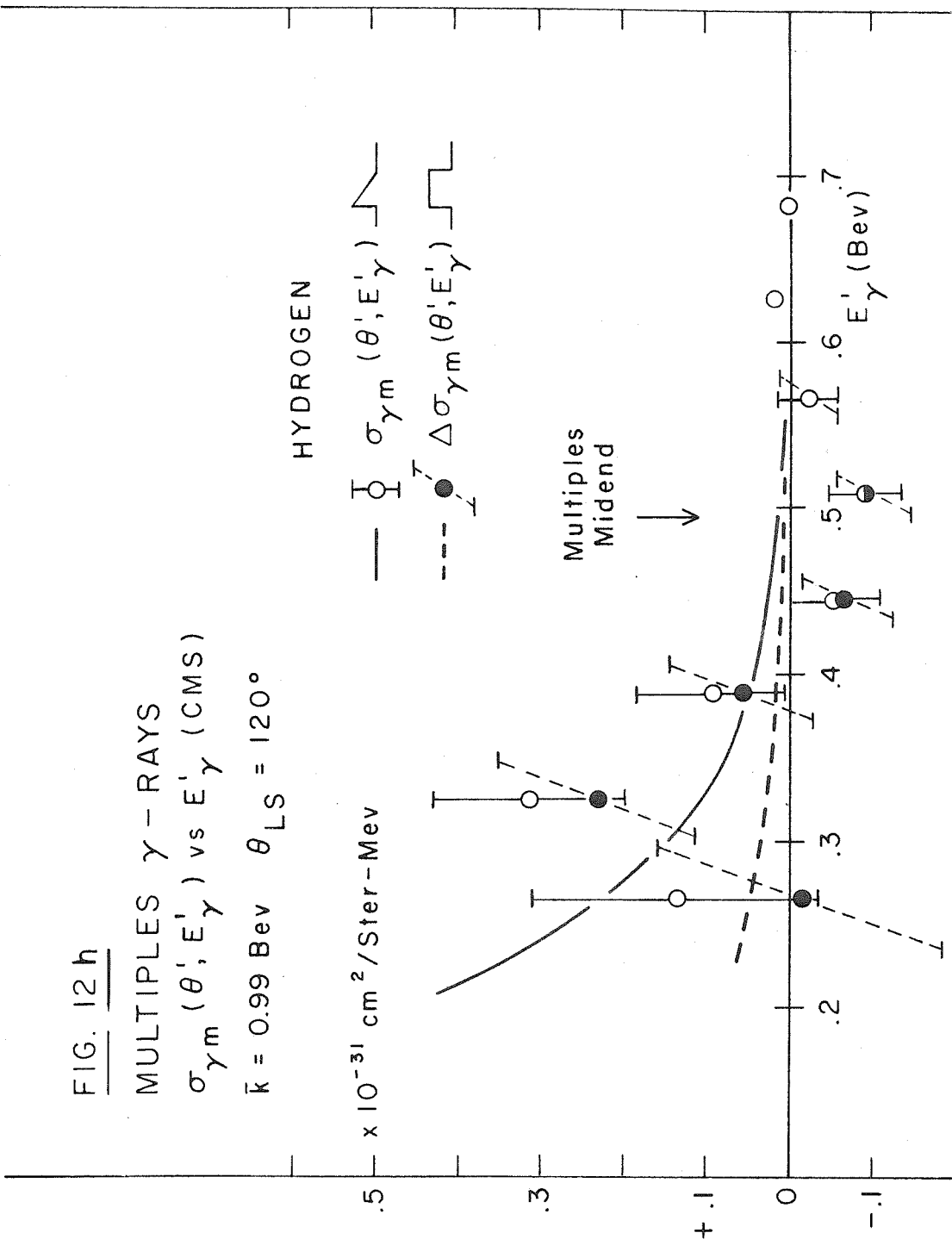
$\bar{k} = 0.99$ Bev $\theta_{LS} = 120^\circ$

HYDROGEN



$\times 10^{-31} \text{ cm}^2 / \text{Ster-Mev}$

Multiples
Midend \rightarrow



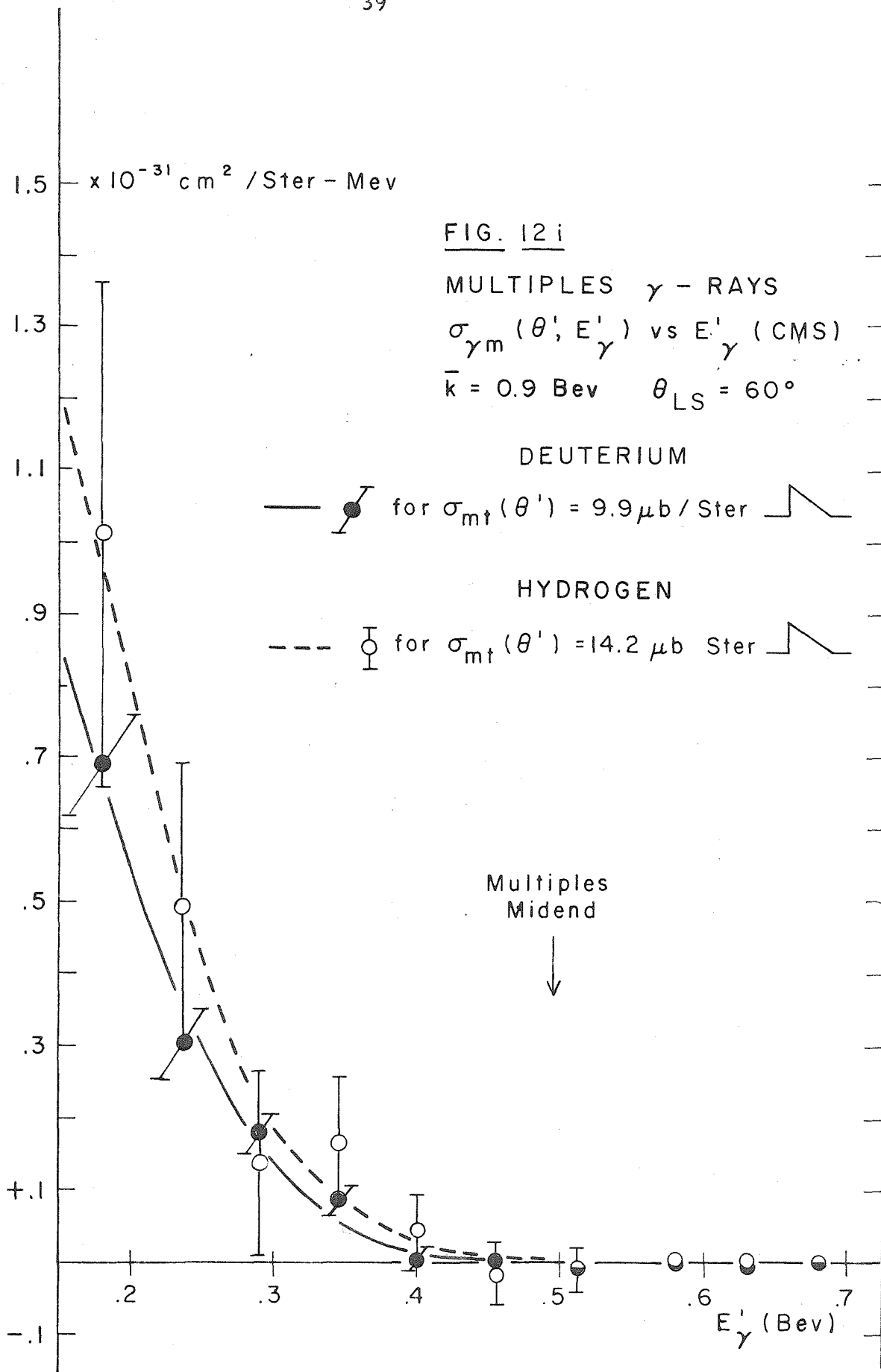


FIG. 13

FIT OF TYPICAL MULTIPLES γ -RAY SPECTRUM
TO EXPECTED PULSE HEIGHT SPECTRA

\bar{k} DEUTERIUM $\sigma_{\gamma m}(\theta', E'_\gamma)$ vs E'_γ

$\bar{k} = 0.9 \text{ Bev}$ $\theta_{LS} = 60^\circ$

$1.0 \times 10^{-31} \frac{\text{cm}^2}{\text{Ster Mev}}$

$\sigma_{\gamma m}(\theta', E'_\gamma)$

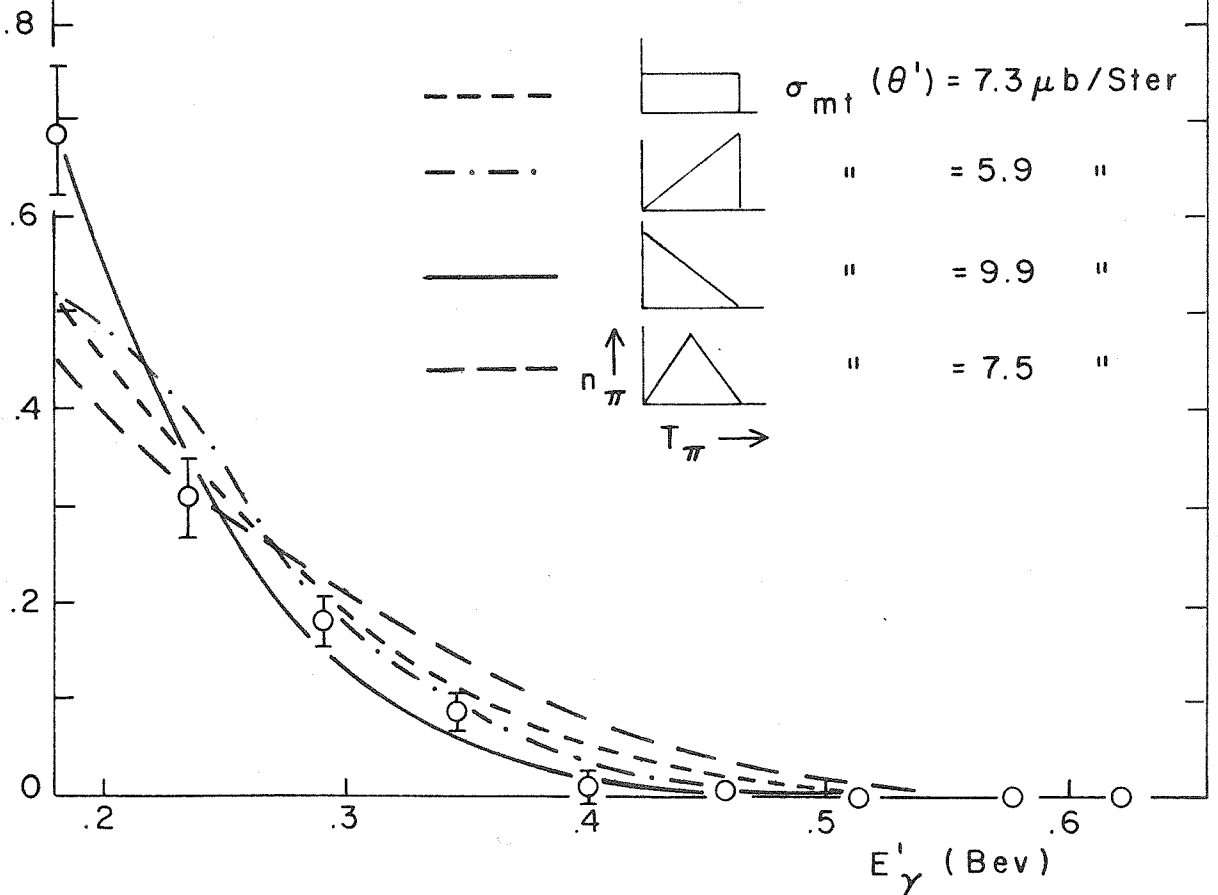


TABLE I

Summary of Results

E_0 (Bev)	1.08	1.0	0.9	0.8	0.7	0.6	av
$\gamma D / \gamma H$							
$\gamma D / \gamma H$ $\theta_L = 120^\circ$	0.954+0.015	0.945+0.015	0.948+0.015	0.944+0.014	0.950+0.017	0.944+0.016	0.947+0.007
$\gamma D / \gamma H$ $\theta_L = 60^\circ$	0.932+0.007	0.914+0.011	0.929+0.010	0.938+0.012			0.928+0.005
$E_1 - E_2$	1.08-0.9		1.0-0.8		0.9-0.7		0.8-0.6
$\Delta \gamma D / \Delta \gamma H$ 120°	0.87+0.17		0.82+0.11		0.80+0.09		0.84+0.08
$\Delta \gamma D / \Delta \gamma H$ 120°	0.98+0.19		0.80+0.19		0.74+0.12		
$\Delta \gamma D / \Delta \gamma H$ 60°	0.87+0.07		0.91+0.08				
Mainly Singles							
$\sigma_{1D}(\theta') / \sigma_{1H}(\theta')$							
$E_1 - E_2$	1.08-0.9		1.0-0.8		0.9-0.7		0.8-0.6
$\sigma_{1D}(135^\circ) / \sigma_{1H}(135^\circ)$	0.64+0.33		0.97+0.22		0.97+0.19		0.70+0.20
$\Delta \sigma_{1D}(135^\circ) / \Delta \sigma_{1H}(135^\circ)$	0.60+0.33		0.96+0.22		0.97+0.20		
$\sigma_{1D}(90^\circ) / \sigma_{1H}(90^\circ)$	0.98+0.30		0.96+0.4				
Mainly Singles Absolute $\sigma_1(\theta')$ ($\mu\text{b}/\text{ster}$)							
\bar{k} (Bev)	0.98		0.89		0.79		0.69
$\sigma_{1D}(135^\circ)$	2.6+0.9		5.2+0.7		4.9+0.7		3.0+0.7
$\Delta \sigma_{1D}(135^\circ)$	2.4+0.9		5.0+0.7		4.5+0.7		
$\sigma_{1H}(135^\circ)$	4.1+1.6		5.4+1.0		5.0+0.7		4.2+0.9
$\Delta \sigma_{1H}(135^\circ)$	4.0+1.6		5.2+1.0		4.7+0.8		
$\sigma_{1D}(90^\circ)$	3.7+0.8		2.3+0.4				
$\sigma_{1H}(90^\circ)$	3.8+0.9		2.3+1.0				

TABLE I (cont'd.)
Multiples Cross Sections ($\mu\text{b}/\text{ster}$)

\bar{k}	$T\pi_0$ mid- end	$T\pi_0$ min	$1 - \frac{T'mE}{T'm}$	$\theta = 60^\circ$ ($\theta' \approx 90^\circ$)		
				$\sigma_m(\theta')D$	$\Delta\sigma_m(\theta')D$	$\sigma_m(\theta')H$
990	360Mev	127	0.65	5.2+1.1		
900	325	127	0.61	4.8+0.5		7.4+2.2
				$\theta = 120^\circ$ ($\theta' \approx 135^\circ$)		
990	360	144	0.60	4.1+1.1	2.0+1.1	3.8+1.8
"	"	87	0.76	5.6+1.0	2.4+1.0	
900	325	124	0.62	2.9+1.1	1.4+1.1	8.6+1.7
"	"	72	0.78	4.0+1.1	0.8+1.1	10.3+1.4
800	281	118	0.58	4.6+1.1	2.3+1.1	4.7+1.1
"	"	64	0.77	6.0+1.1	3.0+1.1	7.4+1.1
700	236	81	0.66	2.6+0.9		4.0+1.0
"	"	36	0.85	2.6+0.8		3.3+1.0

$\sigma_{mt}(\theta')$ and $\Delta\sigma_{mt}(\theta')$ from fits to spectrum shapes [$(T\pi^0)_{\min} = 0$]

\bar{k}	Target θ	$\theta = 60^\circ$			$\theta = 120^\circ$		
		$\sigma_{mt}(\theta')$	$\Delta\sigma_{mt}(\theta')$	$\sigma_{mt}(\theta')$	$\Delta\sigma_{mt}(\theta')$	$\sigma_{mt}(\theta')$	$\Delta\sigma_{mt}(\theta')$
990							
	D	6.8+1.6	3.0+1.6	5.5+1.3	2.4+1.3	9.7+2.2	4.2+2.2
	H	4.4+2.0	1.1+2.2	3.4+1.7	0.8+1.7	*8.2+4.1	2.0+4.1
900	D	7.3+0.5		5.9+0.4		*9.9+0.7	7.5+0.5
	H	10.5+2.5		8.4+2.0		*14.2+3.5	10.7+2.6
	D	4.8+1.5	1.0+1.5	3.9+1.2	*0.8+1.2	7.2+2.2	1.5+2.2
	H	12.0+2.0	7.4+2.0	9.6+1.6	5.9+1.6	*17.9+2.9	11.0+2.9
800	D	8.1+1.5	3.8+1.1	*6.1+1.1	2.9+1.1	11.4+2.1	5.4+2.1
	H	*9.3+1.6	4.8+1.6	7.2+1.2	3.6+1.2	13.1+2.2	6.7+2.2
700	D	3.8+1.4		*2.9+1.0		6.3+2.3	3.9+1.4
	H	5.5+1.6		*4.2+1.2		9.1+2.6	5.7+1.6

III. DISCUSSION

Although there is as yet no fundamental theory to explain pion photoproduction, particularly above the first "resonance," the results of this experiment can be correlated to some extent with other data.

The integral ratios are not inconsistent with the lower energy results of Keck et al.²² Keck's results are consistent with the constant value $\gamma_D/\gamma_H = 0.9 \pm 0.02$ for $\theta = 73^\circ$ and 140° and $E_0 = 0.3, 0.4, 0.5$ Bev. The integral ratios γ_D/γ_H quoted in Table 1 are consistent with the constant value 0.94 ± 0.02 (with a few percent additional possible systematic uncertainty), for $\theta = 60^\circ$ and 120° and $E_0 = 0.6^*, 0.7^*, 0.8, 0.9, 1.0, 1.08$ Bev. Since π^0 's from the first resonance would be expected to cause the major part (80-90%) of the integrated total counting rates even up to 1.08 Bev, it is not surprising that there is no large variation with E_0 . There is some indication γ_D/γ_H may be lower (by a percent or so) for $\theta = 60^\circ$ than for $\theta = 120^\circ$. (An increase for backward angles is observed also in the $-/+$ ratio.^{21, 25})

The differential ratios $\Delta\gamma_D/\Delta\gamma_H$ and $\Delta\gamma_D/\Delta\gamma_H$ are in general somewhat lower than the corresponding integral ratios, indicating that the D/H ratio may be lower in the $\frac{1}{2}$ to 1 Bev range than over the resonance, with possibly a minimum around 0.8 Bev.

The quoted differential ratios are consistent, however, with the

*Data taken only at 120° .

average value 0.85 ± 0.05 (with possible additional systematic uncertainty of a few percent) for $k = 0.6$ to 1.08 Bev. Note that these differential ratios are "total" in the sense that they may include contributions from all reactions which can yield photons, including multiple pion photoproduction.

Rather than a minimum in the energy region around 0.8 Bev, the D/H ratio of gamma rays from singly photoproduced pions may exhibit a maximum, particularly for $\theta = 120^\circ$. (The statistics are not good enough for a definite conclusion, however.) Thus it may be that the multiples cross sections behave oppositely to those for singles: σ_1^{no} exhibiting a maximum relative to σ_1^o where $\sigma_2^{-o} + 2\sigma_2^{noo}$ exhibits a minimum relative to $\sigma_2^{+o} + 2\sigma_2^{ooo}$.**

This maximum around $\bar{k} = 800$ Mev in the singles D/H ratio is in qualitative agreement with the results of Neugebauer et al.²⁵ on the -/+ ratio. At forward angles the -/+ ratio decreases monotonically (from 1.4 at threshold to about 0.5 at 0.9 Bev), but at backward angles it increases from 1.4 at threshold to a maximum as high as 2.8 around 0.7 to 0.8 Bev (after which it decreases as at forward angles). There need be no simple relation between the -/+ and D/H ratios if the photoproduction takes place through a mixture

**The subscripts refer to the number of pions produced, the superscripts to their charge. The superscript n distinguishes reactions from target neutrons where charge conservation does not remove the ambiguity. Photoproduction of more than two pions is here assumed relatively unlikely.¹⁴

of states of different angular momentum and isotopic spin, as the evidence seems to indicate it does. In the region around 0.8 Bev, however, the approximate ratio 2:1 is found for $\sigma_1^+ : \sigma_1^0$ indicating that states with total isotopic spin $I = \frac{1}{2}$ may dominate in this region. (See, however, Wetherell's analysis.⁶⁾

Thus, one would expect:^{10,19 *}

$$\frac{\sigma_1^-}{\sigma_1^+} = \frac{\sigma_1^{\text{no}}}{\sigma_1^0}$$

Fig. 14 shows the results of Neugebauer et al.²⁵ for the $-/+$ ratio for $\theta' = 90^\circ, 120^\circ$ and 150° plotted vs. \bar{k} in comparison with the singles n/p ratio computed from the D/H results of this experiment (Table 1). It was assumed that the nucleons in the deuteron act independently as though they were free, i.e., that:

$$2 \frac{D}{H} - 1 = \frac{n}{p}$$

The n/p results for $\theta' = 135^\circ$ fall between the $-/+$ curves for $\theta' = 120^\circ$ and $\theta' = 150^\circ$ for $\bar{k} = 0.8$ Bev and 0.9 Bev. For 0.99 Bev the n/p results are lower than the $-/+$ (but not significantly); for 0.7 Bev the n/p ratio is some 3 probable errors below the $-/+$. For both $\bar{k} = 0.9$ and 0.99 the $\theta' = 90^\circ$ n/p and $-/+$ ratios roughly agree. Thus it seems that for $\bar{k} \geq 0.8$ Bev the n/p and $-/+$ ratios are equal within the rather large errors on the n/p.

*Watson¹⁹ has shown that the four photoproduction amplitudes can be written in terms of three matrix elements (at least if the electromagnetic interaction is linear in the particles present) for each angular momentum and parity state:

$$T^- = \sqrt{2} T_3 + \frac{1}{\sqrt{2}} [T_1 + \delta_1] \quad T^{n0} = 2 T_3 - \frac{1}{2} [T_1 + \delta_1]$$

$$T^+ = \sqrt{2} T_3 + \frac{1}{\sqrt{2}} [T_1 - \delta_1] \quad T^0 = 2 T_3 - \frac{1}{2} [T_1 - \delta_1]$$

Hence:

i) If only the $I=3/2$ matrix element (T_3) is non zero (or in general if only one of the three matrix elements is non zero):

$$\sigma^-(\theta)/\sigma^+(\theta) = \sigma^{n0}(\theta)/\sigma^0(\theta) = 1$$

for each angular momentum and parity state separately, and also for the sum over all states (contributing to the given T). Note that this implies that the angular distributions for the four reactions would be the same.

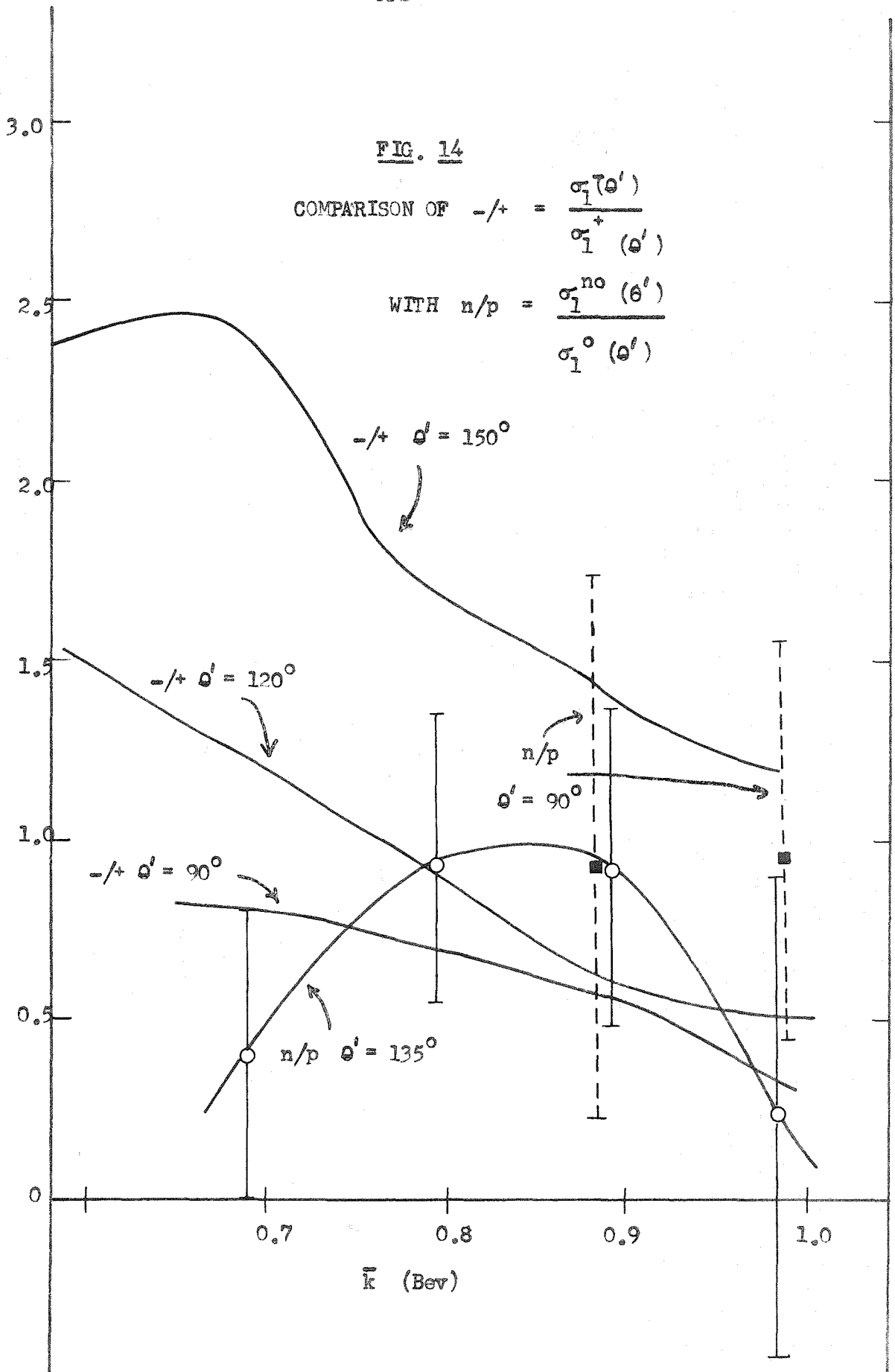
ii) If only the $I=1/2$ matrix elements T_1 and δ_1 are non zero, the ratios need not be one, but still:

$$\sigma^-(\theta)/\sigma^+(\theta) = \sigma^{n0}(\theta)/\sigma^0(\theta)$$

again for each state separately and for the sum over states; again the angular distributions would be the same.

iii) If all three matrix elements are non zero the ratios need not be equal, nor in general equal to one, and the angular distributions need not be the same.

iv) If the $-/+$ ratio is greater than one δ_1 must have the same sign as the larger of T_3 and T_1 . If the n/p ratio is larger than one δ_1 must have sign opposite $2T_3 - \frac{1}{2}T_1$.



This may lend some support to the hypothesis that only one isotopic spin state is important at these energies. The disagreement at lower energy may be due, for example, to effects of the 3-3 resonance, or to S wave charged pion photoproduction.

The assumption that the nucleons in the deuteron act independently is of course not strictly correct. Although near threshold the $-/+$ ratio, (but not the D/H) is affected somewhat by nucleon exclusion (the Pauli Principle "prevents" the final nucleons, which are identical, from being in the same state) and by differences in the coulomb interaction of the product particles, both the coulomb and Pauli effects would be expected to be quite small for energies this far above threshold. Both the n/p and $-/+$, however, should be affected by interactions of the product mesons with the "spectator" nucleon in the deuteron. W. Wales²⁵ has compared absolute cross sections for π^+ photoproduction from hydrogen and deuterium and found that the π^+ from deuterium cross section is on the average some 5% lower than from hydrogen in the $\frac{1}{2} - 1$ Bev range, an amount he finds consistent with the elastic photodisintegration of the deuteron cross sections,⁵⁰ and the probability that excitation of the deuteron will lead to elastic photodisintegration, as estimated by Fermi⁵¹ from phase space arguments. It is impossible to separate the similar effect for π^0 's from the n/p "effect" simply by measuring the D/H ratio: without detecting the recoil nucleons one

cannot say which π^0 's come from the proton and which from the neutron. If one assumes the effect for π^0 's from deuterium is similar to that for π^+ 's, however, one would expect the absolute cross sections to be depressed by the same percentage - thus the n/p results plotted in Fig. 14 may be some 10% too low.

Table 2 gives a comparison of the results of this experiment for the absolute differential cross sections for single π^0 photoproduction from hydrogen with the results of Vette and Worlock⁸ (who detected the recoil proton with a magnetic spectrometer and counter telescope respectively). The agreement is good for $\theta = 60^\circ$ ($\theta' \approx 90^\circ$). This is an indication that the high energy gamma rays observed do indeed come from singly photoproduced π^0 's; that other possible gamma ray sources such as elastic photon scattering, K meson and hyperon decay, and the decay of other hypothetical particles (such as Nambu's meson⁵²) are not large relative to π^0 photoproduction, (as might be expected). The shape of the gamma ray spectrum above the multiples kinematical endpoint is well predicted under the assumption that it is due to single π^0 's alone. Figs. 12 show that the difference between the measured and predicted spectra for $\theta = 60^\circ$ is zero for some 300 Mev above the expected endpoint of the multiples gamma ray spectra.

The results for $\theta = 120^\circ$ ($\theta' \approx 135^\circ$) are systematically larger than the results of Vette and Worlock and the spectrum shape

is not perfectly fitted by the calculated spectrum. Figs. 12 show that the difference between the measured and calculated spectra is consistent with zero but systematically shows a negative region near the multiples endpoint and a positive region beginning some 100 Mev higher in energy. Thus it seems that the measured spectrum is slightly "flatter" than the predicted. This is probably not due to the inclusion of some multiples photons (which would be expected because of the rather poor spectrometer energy resolution) - inclusion of multiples should steepen the spectrum. If the counter resolution were broader than believed in the low energy regions, however, the predicted spectrum would be flatter. It is quite possible that the counter resolution was indeed not as good as assumed in the low energy regions. The measured resolution for electron showers could easily be in error by 15%; the resolution for gamma ray showers calculated from the electron resolution may include theoretical errors as well, which would be expected to be worst in the low energy regions. In particular, the assumption that the radiator only broadens the resolution by the spread in ionization energy loss of two electrons is undoubtedly an underestimate, worse for lower energy.²⁷ It was not felt worthwhile to improve the calculation in view of the uncertainty in the measured electron resolution, and the insensitivity of the D/H ratios to the details of the spectrum shape.

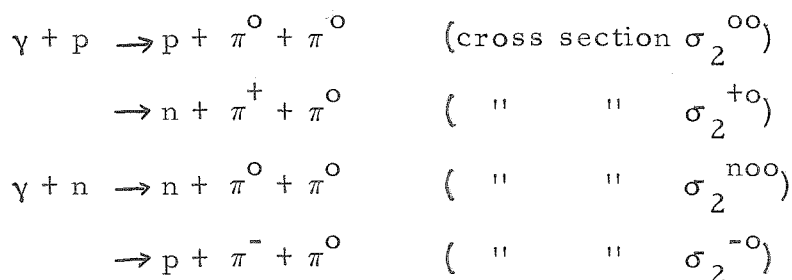
A systematic error in the energy calibration of the kick-sorter could also account for the predicted spectrum being slightly

too steep (and giving too high cross sections) - contraction of its horizontal scale by some 10% would steepen it sufficiently to account for the discrepancy. An anomalously large Compton cross section for backward angles could also explain the "extra" high energy photons.

The multiples cross sections quoted in Table 1 are of the same order of magnitude as those found for charged pion pair production:²⁴



Sellen et al.¹⁴ have found that photoproduction of more than two pions is relatively rare for incident photons from $\frac{1}{2}$ - 1 Bev. Thus it is likely that the multiples gamma rays observed in this experiment come mainly from the decay of π^0 's photoproduced in the reactions:



Although the large uncertainties in the results of this experiment preclude any very detailed comparison with other work or with existing phenomenological theory, some general remarks can be made:

i) as was found for charged pion pair production, there is no evident large variation either with pion angle or incident photon energy (in the ranges observed);

ii) the D/H ratio for multiples is in general somewhat less than, but on the order of one, with possibly a minimum in the region around 900 Mev incident photon energy (perhaps right between the second and third "resonances");

iii) the kinetic energy spectrum of the pions (in the CMS) is never inconsistent with a constant spectrum or with one peaked in the middle, but may be peaked toward higher energy for $\bar{k} = 0.7$ and 0.8 Bev, toward lower energy for $\bar{k} = 0.99$ Bev, probably also for $\bar{k} = 0.9$ Bev.

As yet little theoretical interpretation of pion pair production has been attempted for these energy ranges. The calculations of Cutkosky and Zachariasen⁴⁹ on the basis of Chew-Low theory are not expected to be relevant this far above threshold. The assumption that the matrix elements for pion pair production are independent of the relevant kinematical parameters, so that the pion kinetic energy distributions are governed simply by the densities of final states leads to poor agreement with the charged π pair distributions.²⁴ Both the C-Z and the density of states pion kinetic energy distributions would lead to γ ray spectra which could be fitted to the curves shown in Fig. 12: these spectra would be bracketed between those from the rectangular distribution and the distribution peaked in the middle (both of which are in general consistent with the measured distributions). Thus one cannot say that the pure

density of states or the C-Z distributions are in general inconsistent with the multiples π^0 kinetic energy spectra "observed" in this experiment.

It is fashionable also to consider pion pair production in terms of "isobar models" in which the attraction between a pion and a nucleon in the 3-3 "state" is assumed to be sufficiently strong that the compound state plays the role of a particle (the "isobar"). The width of the 3-3 resonance indicates that the lifetime of the isobar should be only some 10^{-23} sec (during which time it would separate only some 10^{-13} cm from the other pion); some semiquantitative agreement with inelastic pion scattering data has nevertheless been obtained⁵³ under this assumption.

Since the isobar and the "recoil pion" must have equal (and opposite) momentum in the CMS, one would expect the CMS pion kinetic energy spectrum at a given CMS angle to exhibit a peak corresponding to the recoil pion, at higher energy, and a broader low energy distribution corresponding to the isobar pion (if the total CMS energy is \gg the excitation energy of the isobar ~ 140 Mev). In the case of (π^0, π^+) pair production, for example, one might then expect a π^0 kinetic energy spectrum peaked toward higher energies if the π^0 is the recoil pion, toward lower energies if it is the isobar pion (cf. iii above).

If more than one state is important in the photoproduction it is difficult to predict which pions would be isobar and which recoil,

and which reactions would be most probable. It seems, however, that only one $I = 1/2$ state may be important in the region of the second "resonance," for single π photoproduction. If this were so also for multiple photoproduction one would expect the ratios³² 9:4:2:2:1 for $\sigma_2^{+-} : \sigma_2^{oo} : \sigma_2^{+o} : \sigma_2^{o+} : \sigma_2^{-+}$, where the first superscript refers to the isobar pion, the second to the recoil pion in pion pair production from hydrogen.* Bloch²⁴ has found the neutral isobar hypothesis gives better agreement than the doubly charged with his observed π^- kinetic energy spectra above 820 Mev; thus interferences must be important at least by 820 Mev in the pair production. A pure $I = 3/2$ state* would give the ratios 18:16:8:2:1 for $\sigma_2^{+-} : \sigma_2^{o+} : \sigma_2^{-+} : \sigma_2^{oo} : \sigma_2^{+o}$. (Only states with $I = 1/2$ and $I = 3/2$ can be reached by a gamma ray incident on a single nucleon.¹⁹) Thus also for $I = 3/2$ the suppression of the recoil π^- 's must be due to some interferences (cf. Clegg's calculation³²). One can note, however, that iii above would indicate that the π^0 's for $\bar{k} = 0.8$ Bev seem to be recoil, strongly suggesting $I = 1/2$, while those at higher energy may be isobar, which would be consistent with both $1/2$ and $3/2$. (For $\bar{k} = 0.7$ Bev the recoil and isobar peaks are nearly coincident.)

*In pion pair production from the neutron the corresponding $I = 1/2$ ratios are: 9:4:2:2:1 for $\sigma_2^{n-+} : \sigma_2^{noo} : \sigma_2^{-o} : \sigma_2^{o-} : \sigma_2^{n+-}$; for $I = 3/2$, 18:16:8:2:1 for $\sigma_2^{n-+} : \sigma_2^{o-} : \sigma_2^{n+2} : \sigma_2^{noo} : \sigma_2^{-o}$. Thus for any pure state the π^0 's from the neutron would have the same spectrum shape as those from the proton.

$I = 1/2$ would favor a pair correction in the single π^0 data midway between that assumed by Vette,⁸ whose data seemed to indicate $\sigma_2^{00} \ll \sigma_2^{+-}$ and that of Worlock⁸ which was consistent with $\sigma_2^{00} = \sigma_2^{+-}$. $I = 3/2$ would favor Vette. This experiment is of course unable to distinguish σ_2^{+0} and σ_2^{00} , but the results of Table 1 require at least one of them to be comparable to σ_2^{-+} (and with σ_1^0).

For comparison with other results, the multiples cross sections obtained from the normalizations for the spectrum fits have been "averaged," arbitrarily weighting equally the normalization for the flat spectrum, the middle peaked and the better fitting of the forward and backward peaked and the poorer fitting of the forward and backward half as much. The resulting "average" $\sigma_{mt}(\theta')$ and $\Delta\sigma_{mt}(\theta')$ for each configuration have then simply been averaged to obtain the numbers quoted in Table 2. It is clear that these multiples cross section estimates could easily be in error by at least the variation among the fitting normalizations: hence the quoted errors of 50% or more. Note that the resulting average cross sections are of the same order as those obtained by Bloch for σ_2^{-+} ; but possibly somewhat larger. $2\sigma_2^{00} + \sigma_2^{0+} + \sigma_2^{+0}$ { somewhat greater than } $\sigma_2^{-+} + \sigma_2^{+-}$ would be predicted for { $I = 1/2$ } : { $I = 3/2$ } : less than

viz, 12:10 for $I = 1/2$, 21:26 for $I = 3/2$.

TABLE 2

Comparison of Results with Other Experiments

$\sigma_1(\theta')_H$ Single π^0 's from H_2 ($\mu\text{b/ster}$)				
$\theta' \approx 90^\circ$ (CMS)				
\bar{k}	Vette (magnet)	\bar{k}	Worlock (counter) (telescope)	This Experiment
490	5.43 \pm .41			
585	3.27 \pm .26	600	3.50 \pm .20	
690	3.88 \pm .41	700	4.50 \pm .28	
785	4.07 \pm .21	800	3.86 \pm .26	
940	2.27 \pm .21	900		2.3 \pm 1.0
		990		3.8 \pm 0.9
$\theta' \approx 135^\circ$ (CMS)				
690	2.77 \pm .41	700	2.37 \pm .39	4.2 \pm 0.9
785	2.34 \pm .41	800	3.02 \pm .42	4.8 \pm 0.8
940	3.64 \pm .38	900		5.3 \pm 1.0
		990		4.0 \pm 1.6
π Pairs				
$\theta = 60^\circ$				
\bar{k}	This Experiment $2\sigma_{2^{00}} + \sigma_{2^{+0}} + \sigma_{2^{0+}}$		\bar{k}	Bloch $\sigma_{2^{-+}} + \sigma_{2^{+-}}$
	D	H		H
	$\mu\text{b/ster}$			
900	6.7 \pm 3	9.3 \pm 5	1000	4.2
			820	4.2
$\theta = 120^\circ$				
990	5.1 \pm 2 $\frac{1}{2}$	3.8 \pm 3 $\frac{1}{2}$	1000	4.2
900	3.3 \pm 2 $\frac{1}{2}$	10.8 \pm 5		
800	5.6 \pm 3	7.2 \pm 3 $\frac{1}{2}$	820	4.2
700	3.5 \pm 2 $\frac{1}{2}$	5.2 \pm 2 $\frac{1}{2}$	660	3.9

IV. CONCLUSIONS AND SUGGESTIONS

The results of this experiment (summarized in Table I and discussed in Section III) for the integral and differential total D/H ratios lead to the conclusion that the neutron is somewhat less efficient than the proton in combined single and multiple photoproduction of π^0 's, by incident photons of energy less than 1.1 Bev. Integral total D/H ratios were obtained with a precision of a few percent, differential total D/H ratios (for some 0.2 Bev ranges of incident photon energy) good to perhaps 7%.

Rather than to improving the above integral and differential total ratios, it would seem that further effort would better be devoted to improving the separation of the several reactions contributing to counting rates for gamma rays from hydrogen and deuterium targets. There are serious limitations to the subtraction techniques which were used in this experiment to separate the several reactions (in addition to the inherent limitation of detecting only one gamma ray): subtraction of one set of data from another in general "magnifies" their relative errors, also magnifies requirements for stability and calibration of equipment; subtraction of fitted calculated curves from the data also magnifies errors, strains calibrations and stability, sometimes introduces errors from approximations in the theories.

Measurement of D/H ratios with a view to deducing the corresponding n/p ratios also has disadvantages: alternation of

targets introduces problems for example with electronics drifts, backgrounds, and target density monitoring; interpretation of D/H ratios in terms of the corresponding n/p ratios is not yet without theoretical uncertainties.

If it were desired, for example, to extend this experiment to other angles and/or energies, the technique could be improved in several ways: reduction particularly of counting statistical errors could be realized using a larger spectrometer with several phototubes (for coincidences to dispense with the radiator); a counter with better energy resolution would somewhat simplify the separation of singles and multiples (and Compton) gamma rays; effects of drifts could of course be reduced by more stable electronics, particularly a more stable kicksorter, also by more frequent alternation among targets and synchrotron energies; a calibrated light source built into the spectrometer could provide better energy calibration; more accurate beam monitor calibration and bremsstrahlung spectrum shape data for the precise conditions of the experiment would particularly improve the absolute multiples cross sections; a "point source" liquid target would simplify changing of angle and some shielding problems and slit scattering uncertainties, also improve the angular resolution for a given counting rate.

APPENDIX I - EXPERIMENTAL DETAILS:

A. SYNCHROTRON AND BREMSSTRAHLUNG BEAM:

The Cal-Tech synchrotron accelerates electrons to a peak energy variable from about 1/2 to 1 Bev and at the end of the acceleration period causes them to spill out uniformly in time onto a tantalum radiator producing a uniform pulse of bremsstrahlung gamma rays some 20 msec long. Typically some 10^9 electrons are accelerated per pulse (one pulse per second) and a bremsstrahlung beam intensity of about 2×10^{11} Mev per pulse is achieved. The beam is collimated in emerging from the synchrotron through a rectangular aperture in a lead wall and its edges are scraped (of scattered particles) in passing through somewhat larger apertures in succeeding lead walls. The resulting beam at the gas target position has a cross section of about $1'' \times 1 \frac{1}{2}''$.

The bremsstrahlung spectrum has been measured with a pair spectrometer.²⁹ In the center of the beam the spectrum is approximately that expected from a thin radiator, as shown in Fig. 8. The edges of the beam exhibit a somewhat thicker target spectrum (essentially the same except for more rounding off at the high energy end) but not the spectrum expected from a target 0.02 r.l. thick (the full thickness of the tantalum radiator).

Fig. 8 includes a plot of the bremsstrahlung spectrum $B(k, E_0)$ vs. k/E_0 where the number of photons in the photon energy

interval Δk in a bremsstrahlung beam of maximum energy E_0 is:

$$N(k) \Delta k = \frac{W B(k, E_0)}{E_0} \frac{\Delta k}{k}$$

$B(k, E_0)$ is normalized so that:

$$\int_0^{E_0} B(k, E_0) dk = E_0$$

The total energy in the beam is:

$$\int_0^{E_0} kN(k) dk = W$$

The total beam energy is monitored as a function of time with a 1" thick copper walled air filled ionization chamber placed in a cavity in the beam catcher. The current from this chamber is integrated electronically on a precision capacitor (Beam Integrator Model 3, #0196). Charge collected is recorded on a mechanical register as number of beam integrator pulses ("bips"). The total beam energy in a given time is then proportional to the number of bips:

$$W = (\#bips) Q (\text{coulombs/bip}) R (\text{Mev/coulomb})$$

The integrator calibration (Q) was checked periodically by Mel Daybell. It varied only some 1/2% during the course of the experiment (and cancels out in the D/H ratio); its variation was thus neglected in the data reduction.

The ionization chamber calibration (R) is a combination of two factors: the energy response of the chamber relative to a supposedly energy independent quantameter of the type described by Wilson,³⁰ and the beam attenuation between the gas target position and the position of the ion chamber. The product of the two factors (R) is measured simultaneously by placing the quantameter at the gas target position and measuring the ratio of the ionization chamber output to that of the quantameter (normalized by a thin walled ionization chamber placed in front of both) with various targets in between. Results obtained by a team headed by Dr. R. Gomez at the end of this experiment are summarized in Table 3.

The response of the copper ionization chamber depends also on the density of the air in it. This density was monitored during the calibration (and during the course of the experiment) and used to correct the measured beam intensity in bips for each run to that for standard temperature and pressure (i.e., to "standard bips"). The ratio of bips to standard bips for a run was typically 1/1.11; day to day variations in the correction amounted to at most a few percent. All counting rates in this experiment have been reduced to per standard Hectabip, (HB).

TABLE 3

Ion Chamber Calibration

$$R_{\text{quantameter}} = 4.88 \times 10^{18} \text{ Mev/coulomb}$$

$$Q_{\text{integrator}} = 0.2163 \times 10^{-6} \text{ coulombs/bip}$$

E_0	R_Q at Gas Target Position		R_{ion} Chamber without Carbon				
	Rion Chamber in Normal Position		Rion Chamber with t ¹¹ Carbon				
	Liquid Target Between		t ¹¹ c between				
			t = 1"	$\perp 30^\circ$	$1\frac{1}{2}"$	$\perp 2\frac{1}{2}"$	\perp
600Mev	.9383						
700	.9731		1.054	1.059	1.077		
800	1.008		1.047	1.054	1.071		
900	1.042		1.044	1.051	1.066	1.14	
1000	1.073		1.042	1.049	1.064		
1080	1.100		1.041	1.047	1.062	1.129	

Normalizations for Subtractions $\Delta\gamma_{12}$

E_2/E_1	R_1/R_2	$\frac{B(E_2, E_1)}{B(E_2, E_2)}$	$\frac{E_2 R_1 B}{E_1 R_2 B}$
900/1080	1.100/1.042	1	0.879
800/1000	1.073/1.008	1	0.852
700/900	1.042/.9731	1	0.834
600/800	1.008/.9383	1	0.808

Normalizations for Subtractions $\Delta\gamma_{123}$

E_3/E_1	$R_1 R_3$	$E_3 R_1 / E_1 R_3$	$\frac{B(300, E_3)}{\Delta B}$	$\frac{E_3 R_1 \Delta B}{E_1 R_3 B}$
600/1080	1.100/.9383	0.651	23.8	0.0274
600/1000	1.073/.9383	0.686	17.5	0.0392
600/900	1.042/.9383	0.741	16.0	0.0463

B. THE GAS TARGET:⁴⁷

The gas target is the same as that used by Elliott²⁴ and by Bloch.²⁴ The hydrogen or deuterium is contained in a 2" diameter, 17" long steel cylinder with 30 mil thick walls which is kept in contact with a liquid nitrogen reservoir and thermally insulated with a few inches of styrofoam. The gas density is measured every few hours during the course of the experiment. A precision gauge reads the pressure of the gas in the "bomb"; the temperature is measured with thermocouples, one near the tip of the bomb, one at the base where it contacts the liquid nitrogen reservoir. The average of these two temperatures (which typically differ by some 5°K) is used in determining the density (from the data of state of Johnston,³¹ et al.). To minimize variations in the density, the bomb was sealed off during times when data were being taken. For safety, the seal was made at the remote control panel some 40' away from the bomb itself. Thus slight changes in the density of gas in the bomb were possible as its temperature varied (due to variations in the level of nitrogen in the reservoir and in the room temperature), causing more or less gas from the lines to the seal to flow into the bomb. The magnitude of this density variation as the bomb temperature (T_1) varies is:

$$\frac{dp_1}{p_1} = \frac{dT_1/T_1}{1 + V_1 T_2 / V_2 T_1} \quad (3)$$

assuming the gas obeys $PV=nRT$ and neglecting variations in the line

temperature (T_2) which was assumed equal to room temperature. Using $T_1 = 85^\circ\text{K}$, $T_2 = 300^\circ\text{K}$, $V_1 = 930\text{ cc}$, $V_2 = 110\text{ cc}$ and $\Delta T_1 = 12^\circ\text{K}$ one finds $\Delta\rho_1/\rho_1$ is about 1/2%. Apparently random density variations of a few % were observed during the course of typical runs, but these are probably due to temperature and pressure measurement errors of a few %. In analyzing the data, the average of all the density measurements made at random times over a whole period when the bomb was sealed off was used. The average density during a typical run of several days is thus known relatively to perhaps 1%, absolutely to about 3%.

The bomb was aligned with respect to the beam using photographs of it in the beam x-rays with the collimators and scrapers removed so that the diameter of the beam was some 3" at the gas target position, followed (or preceded) by a second exposure on the same film in the normal beam ($1\frac{1}{2}'' \times 1''$) with primary collimator replaced. The alignment was periodically rechecked in the same manner (and occasionally adjusted slightly). Background runs also served as frequent and sensitive checks.

C. THE THALLIUM CHLORIDE CRYSTAL COUNTER*:

i) Characteristics of TlCl , Mounting:

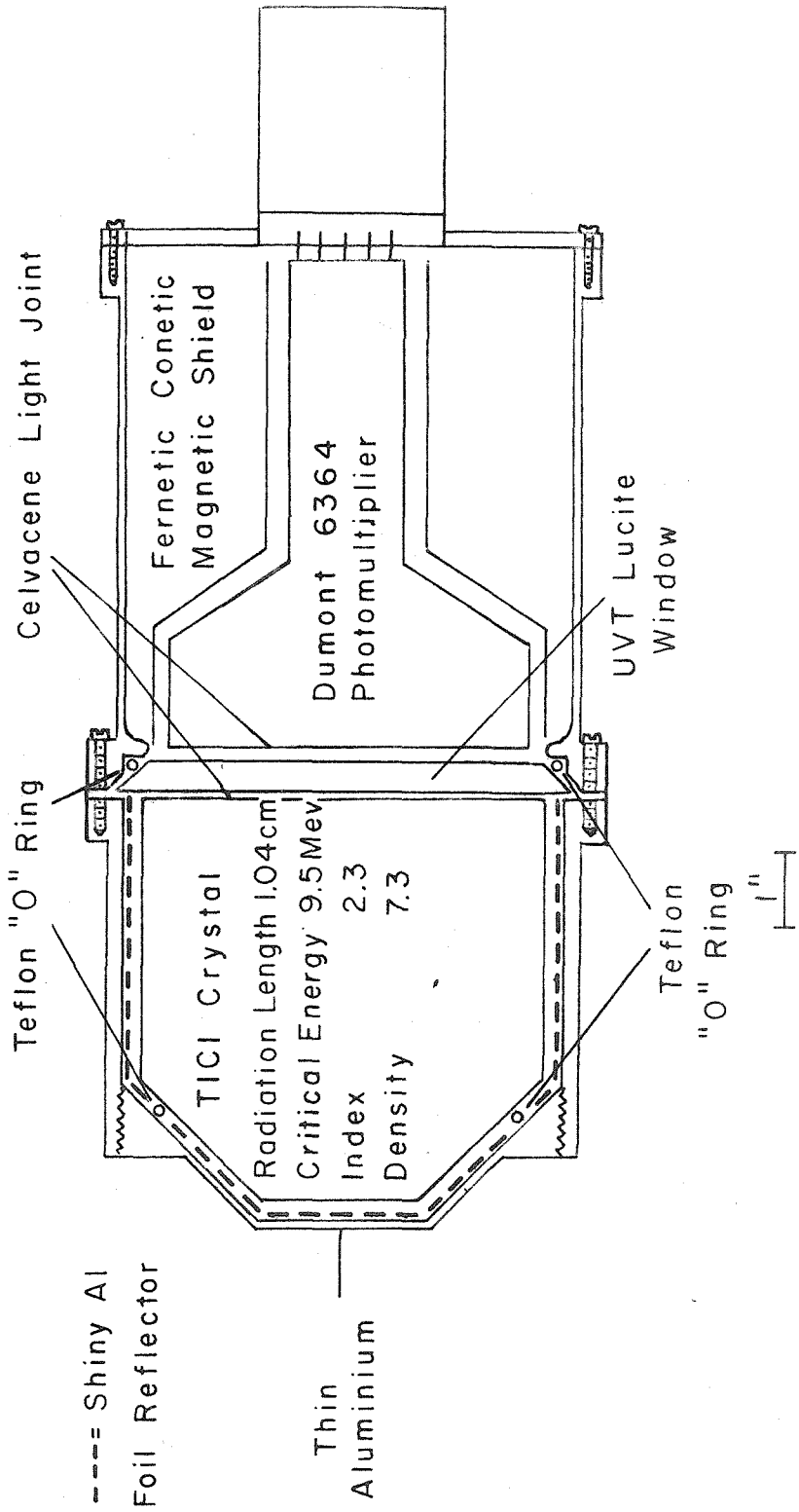
*Most of the development of the crystal counter and telescope was done in collaboration with Dr. A. B. Clegg. This and the following section (D) owe much to some unpublished summaries of this work by Dr. Clegg.

The crystal and its mounting are shown in Fig. 15. It is cylindrical (5½" dia, 5 3/4" overall length) with a truncated conical tip. (The truncated face is 2" in diameter.) Since the radiation length in TlCl is 1.04 cm (calculated with formula 1, p. 220 of Rossi,²⁸) the overall length is about 14 r.l. and the diameter 13.4 r.l. The critical energy is about 9.5 Mev. The refractive index varies from 2.4 for blue light to 2.2 for red, giving a critical angle of about 27°. Wavelengths down to about 3900 Å are transmitted quite well but the absorption increases rapidly for shorter wavelengths. When polished, TlCl is clear, with a slight yellowish tinge. It is soft (easily scratched with fingernail), and dense (7.0 gm/cc). It seems not to scintillate appreciably.

Successive grades of emery paper down to 600 were used to polish the crystal as it rotated slowly on a sort of potter's wheel. This was followed by 400 grit emery powder, then Linde fine abrasive (both used wet with a felt pad) and finally a commercial silver polish. The crystal appeared to have a fine polish at this stage while still wet, but upon drying the surface became crazed. It was found possible to avoid the crazing by burnishing the surface while still wet (and drying it while doing so) with sodium oleate (soap) powder on a felt pad. (This technique was suggested by Dr. A. V. Tollestrup.) The face toward the photomultiplier (the large flat face) was left rough (360 grit emery paper) to provide for diffuse reflection.**

**Cerenkov radiation from particles travelling axially toward the phototube has a momentum component in the forward direction.

FIG. 15 SCHEMATIC OF THALLIUM CHLORIDE CRYSTAL AND MOUNTING



After polishing, the surface was sprayed with DuPont Krylon (while rotating on the potter's wheel) for mechanical protection and as a safety precaution. (TlCl is poisonous and easily absorbed through the skin.)

The crystal was wrapped loosely with shiny aluminum foil and potted in a steel cylinder (with a thin aluminum cap for the conical end). Light joints to the plexiglass window and to the phototube were made with celvacene light vacuum grease. No attempt was made to find a coupling liquid with the optimum index of refraction of 1.8 to match TlCl ($n=2.3$) to plexiglass ($n=1.5$). The presence of the coupling liquid makes no difference to the critical angle (as long as its n is intermediate), which is determined solely by the first and last media. It does affect the transmission coefficient somewhat ($T=0.956$ direct from $n=2.3$ to $n=1.5$; $T=0.976$ with a layer of $n=1.8$ in between, for normally incident light) but not enough to make it worthwhile to sacrifice some transmission or to attempt to work with a liquid of viscosity inappropriate for forming a bubble-free and stable optical joint.

Since the spectrometer was used near the synchrotron and various analyzing magnets used in other experiments and the 5"

This component is preserved by providing specular reflection by the polished cylindrical wall of the crystal. This Cerenkov light would be totally internally reflected at the face to the phototube as well, however, if this surface were polished also. To prevent this, it was left rough.

photomultiplier (DuMont 6364) is sensitive to magnetic fields, it was quite extensively magnetically shielded. The phototube was surrounded by a "fernetic-conetic" shield (obtained from Perfection Mica Co., Chicago, Ill.) and by the mild steel of the pot. When mounted as part of the spectrometer, the crystal counter sat on aluminum brackets which were clamped to a steel counter cart. The cart supported also the other two counters of the spectrometer, the converter and several inches of lead shielding. The whole assembly was then boxed in with mild steel plate. No effect was found on the spectrometer gamma ray counting rate for any but the highest magnet currents, which were rarely used. Even for these high currents the effect was barely noticeable: perhaps 1% in counting rate and thus was observed only after many runs were averaged. Another layer of magnetic shielding in the pot would probably have eliminated observable effects of external magnetic fields.

ii) Development of Crystal Optics; Cosmic Ray Tests:

An extensive series of tests was performed to optimize the energy resolution of the crystal counter.* Since the intensity of the

*This work and most of the spectrometer development were done with Dr. A. B. Clegg under Dr. A. V. Tollestrup's general direction ; valuable discussion took place with Drs. R. F. Bacher, I. Bowen, R. Gomez, Mr. B. Rule and Mr. D. Sell during the crystal development.

Cerenkov light produced by the shower electrons is not large, the major source of energy uncertainty is statistical fluctuations in the number of photoelectrons released at the photocathode by the shower light. Since the average amount of shower light produced by a given energy gamma ray is fixed by the material and size of the crystal, this source of uncertainty can be reduced only by optimizing the light collection efficiency and the photocathode efficiency.

Available 5" tubes were tested for photocathode efficiency by the standard technique of measuring the width of the peak in the pulse height spectrum observed by the tube from a NaI(Tl) crystal irradiated by the 664 Kev gamma rays from a Cs¹³⁷ source. When tested in this way, our best DuMont K1198's and 6364's were found comparable to our best RCA C7170's and 7046's. It was decided to use the more convenient 6364's. A slightly larger diameter tube (perhaps with a photocathode some 6" in diameter) would have been better than either but none was available at the start of this experiment.

The best K1198's on hand were used for the early work with the crystal counter.³² For this experiment a 6364 (actually labelled K1438) with a special high efficiency cathode was obtained from DuMont, but it proved no better and somewhat noisier than the best tubes we had had on hand. Linearity of tube response with light level was checked crudely by comparing average pulse heights (and widths) made in an NaI(Tl) crystal by the radiation from Cs¹³⁷, Na²² (1.28 Mev) and RaTh (2.1 Mev).

Light collection efficiencies for various optical arrangements ("pottings") of the crystal were compared by comparing the pulse height and width of the peak in the pulse height spectrum in the crystal when cosmic ray muons were required to pass through the crystal axially (by requiring a coincidence among the crystal and two scintillation counters, one above and one below the crystal to gate the kicksorter analyzing the pulses from the crystal). A typical "cosmic ray peak" is shown in Fig. 16a. The pulse height corresponding to the maximum of this peak is a measure of the amount of Cerenkov light emitted along the path of the muon which manages to reach the photocathode (within the known gain of the amplifiers) and the relative width of the peak is a measure of the average number of photoelectrons liberated at the photocathode.

Several possible mountings of the crystal were tested in this way. Although the method does not yield precise conclusions, some indication was found that better light collection efficiency is obtained using aluminum foil as a reflector, placed some 1/4" away from the surface of the crystal, rather than wrapping the crystal more closely with aluminum or packing it in MgO. Possibly the slight superiority of the specularly reflecting aluminum, in spite of the lower light absorption of the diffusely reflecting MgO powder, is due to the preservation of the forward component of the Cerenkov light momentum by the aluminum; some marring of the crystal

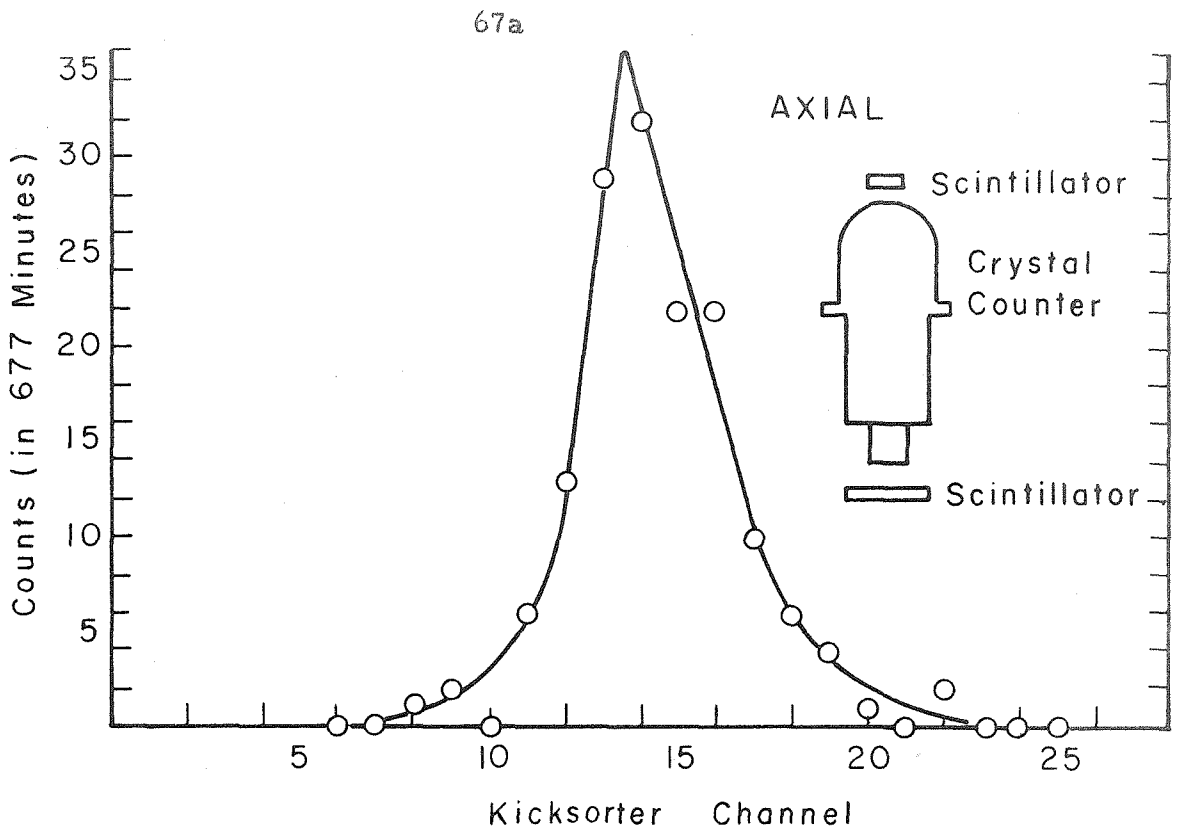
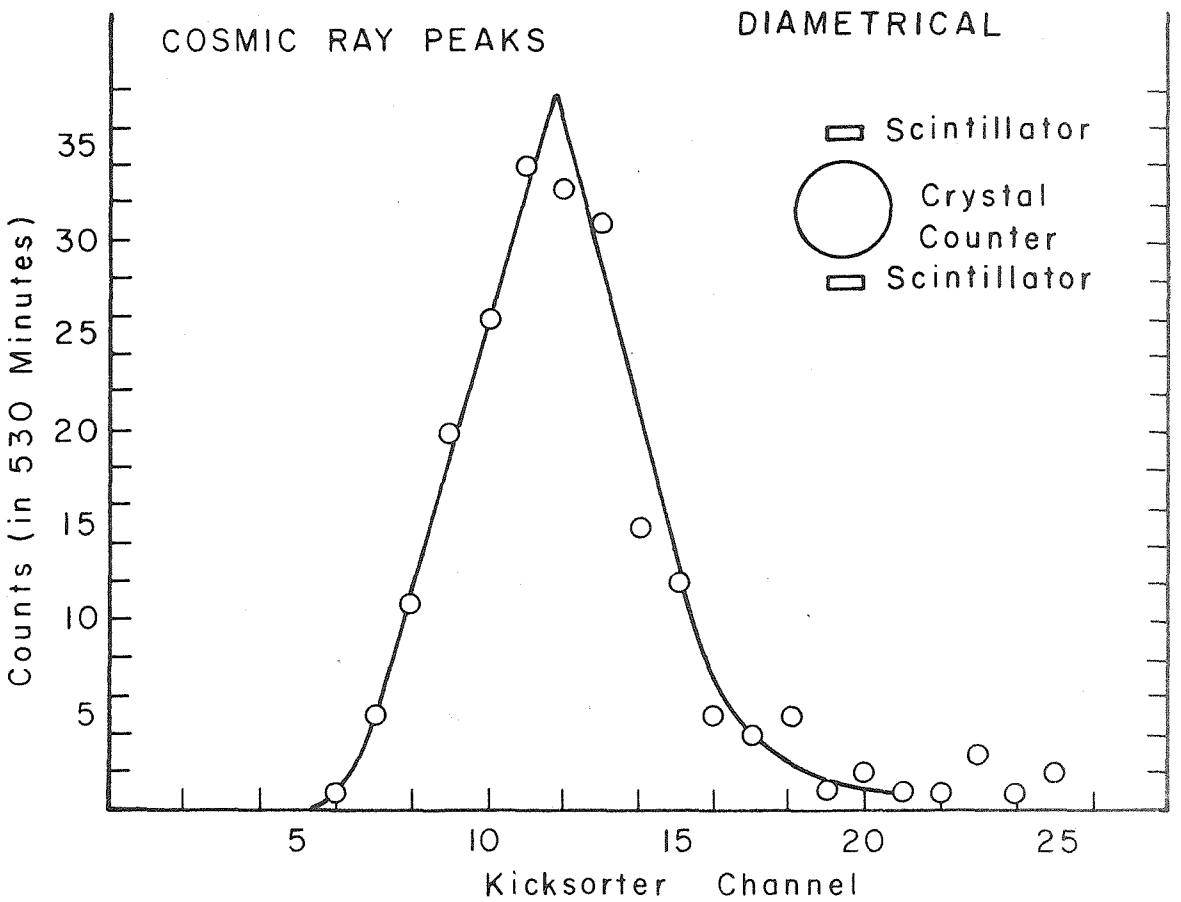


FIG. 16



polish through the packing of the MgO would also explain it, however. That the opposite effect, the superiority of MgO, is found in the case of NaI(Tl) scintillator crystals, is possibly explained by the less directional character of scintillation light.

Fig. 17 illustrates a possible reason for the slight improvement gained by putting the aluminum reflector some 1/4" away from the sides of the crystal rather than in contact with it. A large fraction of the Cerenkov light which escapes into the air from the crystal sides will have been incident at approximately the critical angle (since the critical angle and the angle of the Cerenkov cone are the same if the source particle moves nearly at the speed of light parallel to the surface). Thus the light will emerge nearly parallel to the crystal surface. An oversized, bevelled window will direct much of this light to the photocathode (Ray a).* If returned to the crystal (Ray b) the light would suffer absorption over the long path to the flat face against which the window of the phototube is mounted, and in addition would in part be reflected back into the crystal at this interface. If this face were not rough, it would be totally internally reflected there. It was found that the presence of the window did indeed apparently improve the resolution (as would be expected

*One might expect that a light pipe of area greater than the phototube face would gain nothing in light collection, but the arguments presented, for example, by Garwin³³ assume a diffuse source of light, and do not apply, for example, to a collimated beam.

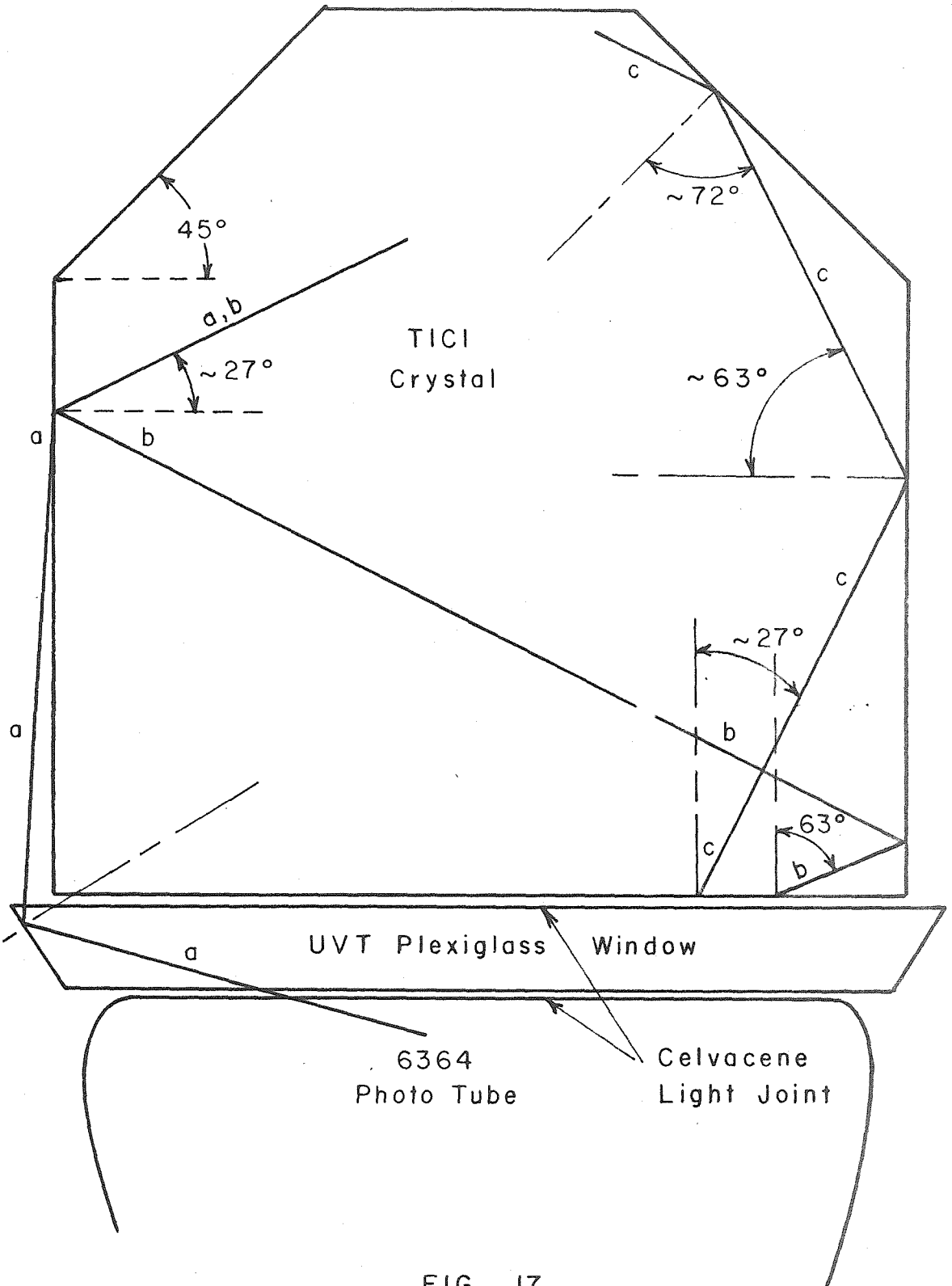


FIG. 17
 RAYS IN CRYSTAL

from the above argument) over mounting the tube directly against the crystal face. It was also found that a UVT plexiglass window may be better than UVA.

Some unsuccessful attempts were made by Dr. Clegg to silver the surface of a small sample of $TlCl$ by conventional chemical silvering processes. The lack of success is thought to be due to the considerable solubility of $TlCl$ in water (1/3 gm/ml at $20^{\circ}C$) along with the considerable insolubility of $AgCl$. In view of the results of the cosmic ray tests it was felt that silvering would not improve the optics anyway, so no further attempts were made.

A verification of the above interpretation of the crystal optics was obtained by requiring cosmic ray muons to go through the crystal diametrically (rather than axially as above), by laying it on its side and putting the scintillators above and below. The average muon path length in the crystal for the diametrical arrangement is 0.90 that in the axial, yet the pulse height obtained is smaller by a factor 2.08 ± 0.04 (also the width of the peak is worse; 45% vs. 33% - Fig. 16b). Thus light from muons travelling toward the photocathode is 1.9 times as likely to reach it as light from muons travelling diametrically across the crystal. Fig. 17 illustrates some reasons for this effect. Particles travelling in the axial direction produce Cerenkov light which for $v=c$ would be incident at the critical angle upon a cylindrical surface whose axis is the particle track. For a cylindrical surface parallel but not coaxial with

the track, most of the light would be incident at greater than the critical angle and thus would be totally internally reflected. Thus if the crystal surface is well polished there should be almost no loss of light from axially travelling particles except for absorption in the crystal and reflection at the diffuse joint to the phototube. Diametrically travelling particles, on the other hand, start only half their light toward the phototube. The other half must travel on the average some three times as far to reach the tube even if properly reflected at the conical end. In addition, some of the light which does start toward the tube would escape through the cylindrical face. That as much as half as much light is collected from diametrical particles as from axial in spite of the above is probably due to the somewhat shorter average path length and smaller average angle of incidence at the tube face of the "totally internally reflected almost half" of the diametrical light.

Since much of the light from showers is produced by axially travelling electrons, it was felt that the improvement which would result from covering more of the crystal surface with phototubes would be only slight, certainly not enough to justify the considerably greater awkwardness of the resulting counter.

The diametrical muon peak served as a day to day gain calibration for the crystal counter as it was used in the spectrometer telescope during the neutral pion experiments. Whenever the synchrotron was shut off for more than a few hours, this cosmic ray peak

would be observed using scintillators permanently in place above and below the horizontally lying crystal counter (for the coincidence requirement to assure that the muons had passed completely through the crystal). In some cases the peak was observed also while the synchrotron was operating, by gating the apparatus on only at quiet times during the synchrotron cycle; a gate of about 1/2 sec was used allowing observation of cosmic rays roughly half the time.

An attempt was made to use particles passing axially through the crystal for a more continuous energy calibration (for reasonable statistics a cosmic ray run takes several hours) under "beam on" conditions. The spectrum in the crystal was observed, gating the kicksorter with the signature $1+2+c+4$, where 1 and 2 are the veto and coincidence scintillators previously referred to (Fig. 2) in front of the crystal counter (c) and 4 was another scintillator placed behind the crystal counter. (Actually $V=1+2$ and $R=2+4$ were fed to the Keck box instead of 1 and 4 respectively, to reduce the counting rate in these channels to that of the relatively small counter #2.) A peak was observed, presumably due to pions passing through the crystal, but it was quite broad (perhaps because of the large probability of pion stars or electron showers also triggering #4) and the counting rate so low as to make the information less useful as a calibration of the crystal counter than the gamma ray counting rate itself.

iii) Performance of the Crystal Counter; Electron Tests:

The performance of the crystal counter as an electron-photon shower detector was checked by observing the pulses in it due to showers caused by electrons of known momentum. A small button of lead was placed at one focus of a magnet* and the crystal counter at the other focus. Ray tracing indicated that by suitably blocking the magnet aperture, a beam of particles with a momentum spread $\Delta p/p$ of some 8% would be sent through the central 2" of the crystal. The particles observed were required to enter the crystal through the 2" diameter scintillator (placed on its nose) by gating the kick-sorter which recorded the crystal counter pulse height spectrum with a coincidence between this scintillator and the crystal. Setting the magnet at a small angle to the bremsstrahlung beam ensured a preponderance of electrons over pions (or protons if positive particles were observed). Pulses from pions would be expected to be smaller in any case (see section Dii) since at these energies they do not radiate enough to make appreciable showers. Electrons were observed with energy ranging from 125 to 1000 Mev. The pulse height of the resulting peak is plotted vs. electron energy in Fig. 4 (Section II).

Before and after the electron tests, cosmic ray runs were taken.

The pulse height for the axial and diametrical peaks is also plotted

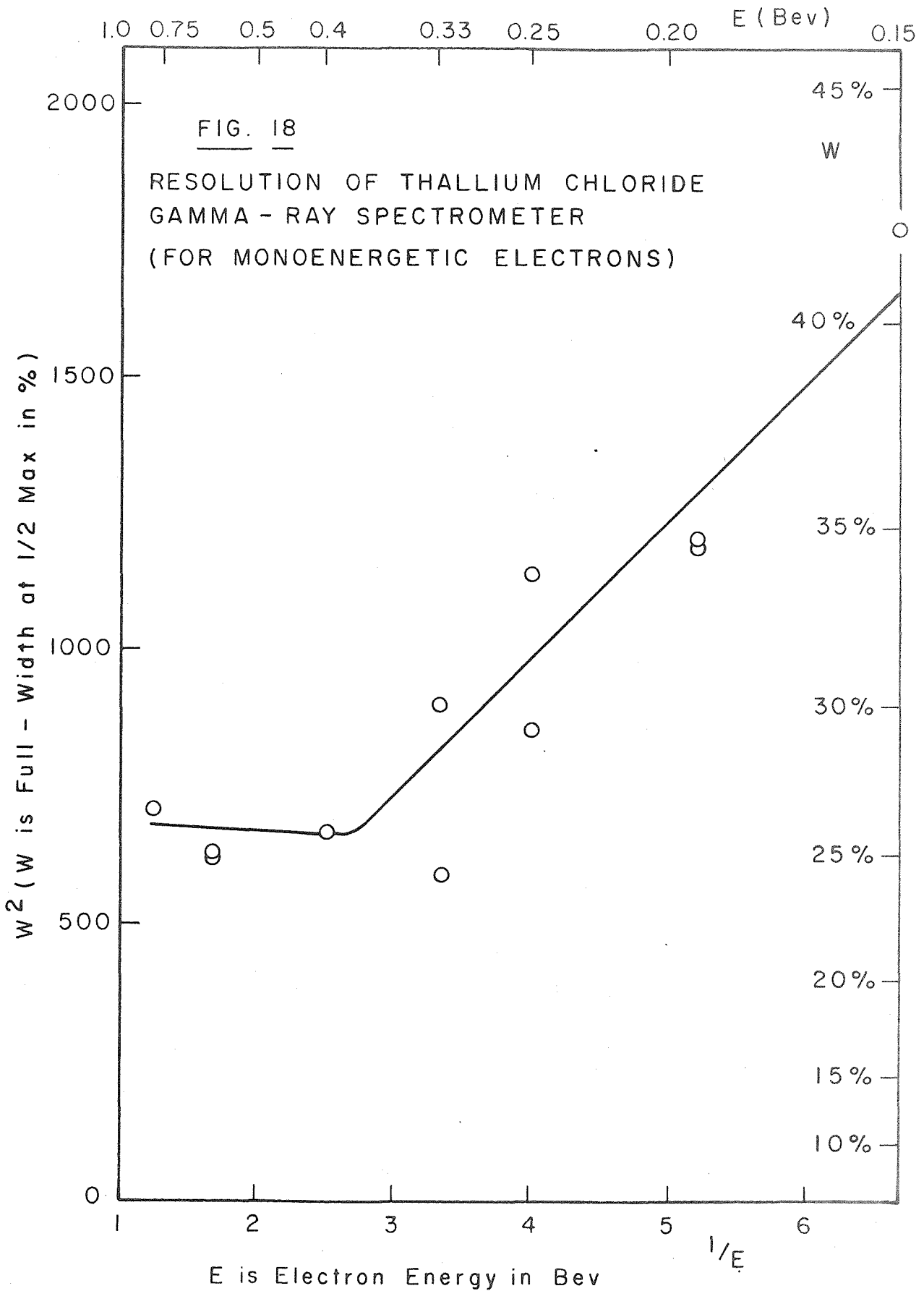
*This magnet was kindly lent by Dr. R. L. Walker. These tests were done at several times, in collaboration with Dr. A. B. Clegg, Dr. K. Althoff and Mr. J. Kilner. Some of the data was reduced by Mr. R. Diebolt.

in Fig. 4. The axial peak corresponds to electron showers of energy 230 ± 7 while diametrical peak corresponds to 110 ± 5 Mev.

The full width at half maximum of the electron peaks is plotted against electron energy (actually w^2 vs. $1/E$) in Fig. 18. A small correction has been applied to w for the estimated momentum spread of the incident electrons. Although the energy calibration of the crystal was found to be linear each time it was measured, considerable variation in the results for w was found from time to time. Fig. 18 shows the results of the best day's runs.

If the number of photons incident on the photocathode is proportional to the energy of the shower and if the width is due entirely to statistical fluctuations in the number of photoelectrons emitted from the cathode of the phototube, the points should lie on a straight line through the origin. w^2 vs. $1/E$ should also be a straight line if the energy escaping from the crystal is proportional to the energy of the shower and if the energy escapes primarily as gamma rays at the energy of the minimum in the absorption curve for gamma rays in TlCl .²⁶ (Fluctuations in the number of such gamma rays would cause fluctuations in the light output of the shower.)

The magnitude of the second effect would be considerably less than the first at low energies. By integrating the shower



spreading curves of Kantz and Hofstadter²⁶ one finds that a cylinder of tin 7 r.l. in radius by 10 r.l. long should contain 90% of the shower from a 185 Mev gamma ray and a similar cylinder of lead should contain 86% of a 185 Mev shower. Normalizing the energy by the respective critical energies (7.8 Mev for lead, 9.5 Mev for TlCl, 12.6 Mev for tin) one finds that the TlCl crystal should contain 90% of a 140 Mev shower and 86% of a 225 Mev one. Thus perhaps 25 Mev should escape the crystal from a 200 Mev shower, on the average as about 2 or 3 gamma rays ($\pm 1\frac{1}{2}$ or 2). Statistical fluctuations in the number of gamma rays escaping should thus correspond perhaps ± 15 Mev in the energy dissipated in the crystal or to a full width at half maximum of 10 to 15%. Since w for a 200 Mev shower is observed to be perhaps 35% one can conclude that for low energies shower escape fluctuations are not the primary source of width. It is probable, however, that shower escape fluctuations contribute significantly to the widths of the highest energy peaks, perhaps causing the possible departure from linearity of the w^2 vs. $1/E$ curve at high energies.

In addition to the pulse height spectra obtained for electrons entering the central 2" of the crystal axially, spectra were obtained 1) for the 2" scintillator 1/2" to one side of the axis, and 2) for the crystal making an angle of about 7° with respect to the electron beam. The peaks from the electrons entering at the 7° angle with respect to

the crystal axis were not significantly broader than the normal central axial ones (a desirable result for a counter being used with a "line source" target), but as would be expected the resolution deteriorated when the showers were started sufficiently off center that a significant fraction of a shower could escape the sides of the crystal.

iv) Light Collection Efficiency; Energy Resolution for

Gamma Rays:

The axial cosmic ray peaks average about 32% in full width at half maximum. Correcting for the dynode multiplication fluctuations³⁴ (a factor of about 1.4 for a 10 stage phototube with gain 6×10^5) this means the σ for the photocathode itself is about 10% (neglecting fluctuations in the light output of the muons, which should be smaller by about a factor $1/\epsilon^{\frac{1}{2}}$ where ϵ is the quantum efficiency of the cathode, about 10%). Thus the light from a muon traversing the crystal axially releases on the average some 110 photoelectrons. However, 880 photoelectrons would be released by such a muon if all its light were incident on the cathode (assuming the Cerenkov light emission probability formula, given p. 265 of Schiff,³⁵ with $n = 2.3$, $v = c$, and integrating over the S11 photocathode frequency response, normalizing to 0.158 photoelectrons per incident photon at $\lambda = 440 \text{ m}\mu$). Thus the light collection efficiency is about 14% for particles travelling axially (some 14.6 cm) through the crystal at about the speed of light. The diametrical

muon peak width of 45% gives similarly a light collection efficiency of about 8% for diametrically travelling particles. Light from a diametrical muon has thus only about half the likelihood of being collected as light from an axially travelling one.

Minimum ionizing particles lose about 9.3 Mev/cm in TlCl. Thus a 100 Mev shower would have about 9.7 cm of electron track in the crystal (if 90% of the shower energy is dissipated in the crystal by the electrons as estimated from Kantz and Hofstadter's curves). A shower from a 150 Mev gamma ray would thus have about the same total electron path length as a muon passing axially through the crystal and a 135 Mev photon the same as a diametrical one. However, an axial muon makes a pulse looking like a 230 Mev shower and a diametrical one like a 110 Mev shower. Light from a shower has therefore only about 2/3 the likelihood of being collected as light from an axial muon. This is probably a combination of two effects: most of the shower energy is dissipated near the entrance point of the electron (in regions far from the cathode); part of it by the less efficient diametrically travelling particles.

The energy resolution of the crystal counter for gamma rays can be estimated from that for electrons assuming the gamma ray produces a pair of electrons, a given one of which is equally likely to have any energy from zero to the gamma ray energy (minus 1.02 Mev). (Inspection of the actual distribution functions²⁸ indicates that this approximation would not cause noticeable error.) Gamma

ray widths were calculated from the individual electron widths (Fig. 18) assuming:

$$w^2 = \frac{(2.35 \sigma)^2}{E_\gamma^2} = \frac{(E_1 w_1)^2 + (E_2 w_2)^2}{E_\gamma^2}$$

and averaging over the energy split ($E_1 + E_2 = E_\gamma - 1 \text{ Mev}$).

When the crystal counter is used in the gamma ray spectrometer, conversion of the gamma rays at different depths in the radiator contributes to the width. Assuming the electrons lose 0 to w' (Mev) in the lead and that the probability of conversion is uniform over the depth of the lead gives:

$$\sigma_{\gamma a}^2 = (\sigma + w')^2$$

to a rather crude first approximation, only satisfactory to the degree that w' (assumed due to ionization energy loss only since a large fraction of the radiated energy should go on into the crystal) is small (9.6 Mev). Curve a in Fig. 5 is the width corresponding to $\sigma_{\gamma a}$.

Curve b in Fig. 5 comes from curve a assuming a constant width of 15% due to the kinematical effects of the $\pm 12^\circ$ angular resolution from the line source gas target (i. e., assuming

$$w_{\gamma b}^2 = w_{\gamma a}^2 + 225).$$

Curve c is calculated from $w_{\gamma b}$ assuming the motion of the nucleons in the deuteron contributes a constant width of 12% (Appendix IIAiv).

Each of the assumptions above is quite crude, but since the electron widths themselves are typically 30% or more and rather poorly known (perhaps to no better than 15%), the above assumptions probably do not cause the major uncertainties in the spectrometer energy resolution function.

D. THE GAMMA RAY SPECTROMETER:

In order to improve the rejection of particles other than gamma rays and to avoid the poor energy resolution of the edge regions of the crystal counter it was used behind two conventional scintillation counters in a counter telescope. A diagram of the telescope and a block diagram of the associated electronics is given in Fig. 2, section II.

The telescope consists of a 4" diameter scintillator (#1) in front to veto charged particles incident axially (those incident from other directions are blocked by lead shielding), a radiator in which gamma rays convert to electron pairs, a 2" diameter scintillator (#2) to detect the electron pairs and the crystal (c). In normal running the kicksorter sorts the pulses from the crystal counter (suitably amplified) into its 20 channels when gated by an output pulse of the 6 channel coincidence-anticoincidence circuit (the "Keck box") set to respond to the event $2+c-V$, where 2 refers to the 2" scintillator, c to the crystal counter and V effectively to the 4" scintillator (#1).

i) Electronics:

The Keck box is in two parts: 6 discriminators using 6BN6's (synchrotron drawing 10-T-164A) which receive amplified pulses from the several counters and produce standard output pulses for those input pulses above the discriminator bias (which can be set anywhere from about 10 to 100 v); and the 6 channel coincidence-anticoincidence circuit proper which works on the standard output pulses from the discriminators. The 6 channel circuit is actually two 3 channel circuits in parallel. Any channel on a "side" can be put in coincidence or anticoincidence or shut off, simply by throwing switches on the inputs. This versatility simplifies the changing of "signatures" and expedites troubleshooting (which is also aided by cathode follower monitors on the inputs to the discriminators and on the inputs to the several channels of the coincidence circuit). Outputs of each side separately (labelled 123456), and in delayed coincidence (labelled 123(456)*) are available. The delayed coincidence permits monitoring of an accidental coincidence rate. The coincidence resolving time is on the order of 0.3 μ sec (for the approximately 0.2 μ sec output pulses from the discriminators); the anticoincidence dead time is about 0.7 μ sec.

In view of the rather long Keck box anticoincidence dead time it was felt preferable to veto charged particles with a fast coincidence between the two scintillators rather than with the 4" scintillator (#1) itself: instead of requiring the signature (2+c-1), the

equivalent signature $(2+c-(1+2))$ was required.

The "fast" coincidence between the two scintillators was made with a standard Garwin³⁶ circuit (using 6AH6's) with coincidence resolving time of about 40 nsec (for the negative output pulses run over some 80' of RG114 u coaxial cable from the plates of the RCA 6810 photomultiplier tubes which look at the scintillators). The phototube HV's were typically set about 100 v above the value where the Garwin output deteriorated.

Before being fed to the Keck box discriminator (usually channel 6), the pulses from the Garwin were amplified by a standard two loop feedback amplifier Model 522A (10-T-163) with gain continuously adjustable from 0 to 2,500 and risetime of about 0.1 μ sec. The efficiency of the veto was checked by observing "plateaus" in the spectrometer counting rate as the gain of this 522 (or the discriminator setting) was varied. Occasionally the 4" counter (#1) itself was put in veto (after amplification) which made no difference in the gamma ray counting rate for ordinary beam intensities.

Model 522A amplifiers were used also to amplify the output of the #2 scintillator (after inversion and some stretching in the "bias diode" circuit) and of the crystal counter (after preamplification and stretching in the Model 24 preamp) before feeding them to channels 4 and 2 respectively of the Keck box. Pulses from the scintillators (using RCA 6655 10 stage 2" diameter phototubes) used in

the cosmic ray calibration runs were also preamplified with Model 24's for driving the 80' of cable to the 522's.

The kicksorter³⁷ normally sorted the pulses from the crystal counter into 20 pulse height bins when gated by an output of the Keck box. The presence of the 40 msec beam gate could also be required. The pretreatment unit of the kicksorter, in addition to thus gating the input pulse, amplifies it and stretches it to a length of $1\mu\text{sec}$, with height proportional to the input pulse. The converter unit converts this pulse to a standard height pulse whose length is proportional to the input pulse. This pulse (the "analog gate") is used to gate a 500 kc oscillator in the address generator unit thus creating a string of pulses of number proportional to the input pulse. The number of these pulses determines the position of a magnetron beam switching tube which directs a count to one of the 20 channels of temporary storage (EIT decatrons). When the 40 msec beam gate (or an internally generated gate of length adjustable from 3 msec to 30 sec) is over, the temporarily stored counts are transferred to mechanical registers. During this time the kicksorter is insensitive to input pulses. The dead time following a count in channel n is $(50+2n)\mu\text{sec}$. The capacity of the temporary storage is 10 counts per channel. The sum of the counts in the 20 mechanical registers is recorded in the BL (between limits) scaler (Berkeley Model 700A). Similar scalers record the number of pulses above the upper limit

of the 20th channel (UL); the sum of BL and UL (A=accepted); and the total number of input pulses above the lower limit of the first channel (LL). (Also the Keck box outputs 123, 123456, 123(456)*.) Because of dead time losses A is ordinarily slightly less than LL. (And thus serves as a monitor of dead time losses.)

Two pretreatment units were used in this experiment. The first, used during the 60° runs had channel widths adjustable from 1/2 v to 4 v (with a minimum of 5 v or 5 channels off the bottom) but proved subject to serious drifts, mostly due to temperature changes in the characteristics of a few semiconductor diodes. A not completely successful attempt was made to minimize this drift by regulating the temperature of the pretreatment and converter units with a thermostatically controlled air blower. To monitor residual drifts, a precision pulser was used to measure the LL bias and a few channel boundaries periodically (usually at times when data could not be taken, such as synchrotron energy changing time). This data could be used to correct for the effects of drifts to some extent. A second pretreatment unit (also designed by A. Barna and M. Sands) was used for the 120° runs. This had fixed channel widths of 3 v but was somewhat less subject to drift. It, too, was temperature controlled and periodically calibrated.

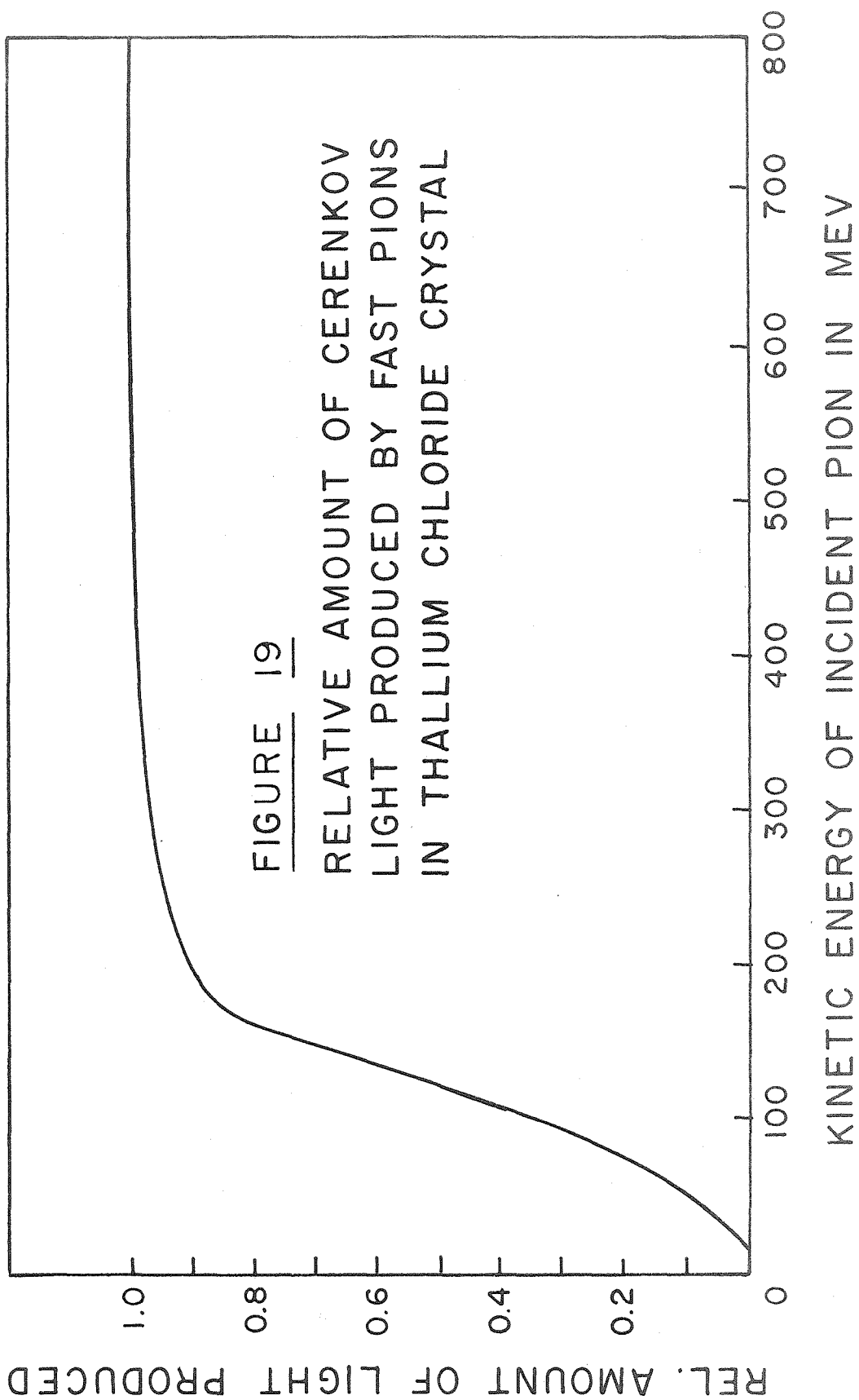
ii) Rejection of Particles Other than Gamma Rays:

The crystal counter itself is sensitive not only to gamma rays but also to fast charged particles. Electrons, of course, produce

showers; electrons above 51 Kev, pions above 14 Mev and protons above 94 Mev produce Cerenkov light. Fast pions ($T \cong 200$ Mev) can pass completely through the crystal (with some probability). Fig. 19 plots (vs. pion kinetic energy, T) the amount of Cerenkov light produced in the crystal relative to a $v=c$ particle passing completely through it (about the same as a 230 Mev shower for an axially travelling muon). Neutrons can cause stars in the crystal which have some probability of producing fast charged particles.

To veto charged particles incident axially, the 4" diameter scintillator (#1) was placed ahead of the crystal and particles incident from other directions blocked by lead shielding. Further rejection of charged particles was accomplished by setting the bias on the 2" scintillator (#2) to correspond to about 2 minimum ionizing particles passing through it, as discussed below, and to some extent by the pulse height in the crystal.

Rejection of neutrons was also accomplished by the combination of the requirements that the incident neutral particle produce a pulse corresponding to about 2 (or more) minimum ionizing particles in the 2" scintillator and at the same time produce a pulse above a bias (typically 130 Mev at 120° and 220 Mev at 60°) in the crystal. Stars created by the neutrons in the crystal itself would be unlikely to trigger the scintillator; stars created in the radiator would be unlikely to transmit enough energy to the crystal to produce



a pulse above its bias. In any case, the flux of neutrons was not expected to be large relative to that of gamma rays, especially at backward angles, since the room background is negligible. That the rejection of neutrons was successful was crudely checked by comparing counting rates as the thickness and atomic number of the radiator was varied (see section iii) and Table 4).

In addition to helping in the rejection of particles other than gamma rays, the requirement of conversion in the radiator and coincidence with the 2" diameter scintillator permitted the rejection of photons incident further than 1" from the crystal axis. Thus the poorer energy resolution for off axis showers was avoided.

iii) Choice of Radiator; Radiator Comparison Runs:

The material and thickness of the radiator were chosen as a compromise between efficiency of photon detection and energy resolution. The thicker and higher Z the radiator, the greater the efficiency but the worse the resolution. Yamagata and Yoshimine²⁷ have performed monte carlo calculations to determine the resolution of a lead glass counter similar in size (measured in radiation lengths) to the crystal, for radiators of varying thickness. They find the resolution deteriorates rapidly for converters of thickness greater than about $1/2$ r.l. and recommend $1/4$ r.l. as a reasonable compromise between efficiency and resolution. Some of the earlier work with this counter was done with a radiator about $1/3$ r.l. thick.³²

TABLE 4

Radiator Comparison Runs*

Radiator	t(in)	t(cm)	t gm/cm ²	Radiators (Diameter 2.26")		Z	ρ (gm/cm ³)	dE/dX minimum
				t(r.l.)	r.l.			
Aluminum	0.4725"	1.200	3.24	0.133	9.05cm	13	2.7	4.5 mev/cm
Copper	0.187	0.475	4.23	0.323	1.47	29	8.9	13.1
Tin	0.155	0.392	2.86	0.320	1.22	50	7.3	8.9
Lead 1	0.030	0.076	0.86	0.134	0.572	82	11.35	12.9
Lead 2	0.073	0.185	2.10	0.32	"	"	"	"
Lead 3	0.146	0.371	4.21	0.65	"	"	"	"
Lead 4	0.285	0.724	8.21	1.27	"	"	"	"

86

Results of Comparison Runs

E _γ	Al/Pb ₄		Cu/Pb ₄		Sn/Pb ₄		Pb ₁ /Pb ₄		Pb ₂ /Pb ₄		Pb ₃ /Pb ₄		
	t = 0.13 r.l.	Meas.	Pred.	Meas.	Pred.	Meas.	Pred.	Meas.	Pred.	Meas.	Pred.	Meas.	Pred.
278	0.154	0.029	0.153	0.346	0.043	0.359	0.405	0.041	0.342	0.382	0.046	0.350	0.154
417	0.191	0.052	0.152	0.402	0.077	0.346	0.474	0.085	0.337	0.511	0.090	0.347	0.153
650	0.110	0.062	0.151	0.479	0.130	0.350	0.272	0.092	0.339	0.304	0.098	0.349	0.152
t = 1/3 r.l.													
278													
417													
650													
t = 2/3 r.l.													
278													
417													
650													

*Much of the computation for this table was done by Mr. R. Diebolt.

Use of the lower density, more spread out gas target for this experiment, rather than the liquid target used for the earlier work, introduced a further resolution deterioration here. Thus it seemed a thicker radiator would not further affect the resolution appreciably: $2/3$ r.l. was chosen. Although an exhaustive analysis of the scattering in the radiator was not carried out, it was felt that the effects of scattering would be minimized by having a radiator with short r.l., so that even showers starting in the front of the radiator would not start far from the crystal. To give at least partial cancellation of scattering in and out of the 2" diameter circle covered by the coincidence scintillator, the radiator was made somewhat larger: $2\frac{1}{4}$ " in diameter.

To verify crudely that the telescope was counting gamma rays, a comparison was made of the counting rates using radiators of Al, Cu, Sn and 4 different thicknesses of lead. The spectrum of gamma rays in the crystal was observed in the kicksorter, the energy scale of which had been calibrated by the cosmic ray and electron runs described above. The counts were grouped into 3 energy bins: $275_{\pm 55}$; $420_{\pm 80}$; $650_{\pm 150}$ Mev. Results were expressed in Table 4 as ratio of counting rate for a particular radiator to that for the thickest lead radiator to cancel errors in beam and kicksorter calibration. The columns labelled "predicted" give the expected ratio calculated from known pair production cross sections.⁴¹ The agreement of predicted and measured ratios within the rather poor statistics

is some evidence that the neutron counting rate is not over perhaps 10% of the photon rate at the lowest energies where it would be expected to be the largest.

iv) Efficiency for Detecting Gamma Rays:

The efficiency of the spectrometer is mainly the probability that a gamma ray convert in the radiator. Corrections were made for electron scattering and energy loss in the lead and for the probability that the incident photon not convert in the matter ahead of the veto scintillator.

Several treatments of the multiple coulomb scattering exist in the literature which are summarized by Rossi,²⁸ Bethe,³⁸ and by Mohr and Tassie.³⁹ The treatments in general assume Rutherford scattering in first approximation but differ somewhat in the treatment of the screening of the nuclear coulomb field by the electrons in the atom, and in the degree to which the individual scatterings are assumed small. None of the treatments is expected to be very good for large angle scattering. All of the formulas quoted by Rossi, for example, would predict mean square angles of scattering on the order of 90° for electrons of energy less than 20 to 30 Mev attempting to traverse a lead radiator $2/3$ r.l. thick.

The probability of radiating a large quantum is also not small. Eyges⁴⁰ has computed the probability that an electron has energy E at depth t if it had E_0 at $t=0$ and loses energy by ionization and by radiation. Dr. A. B. Clegg has used Eyges's result

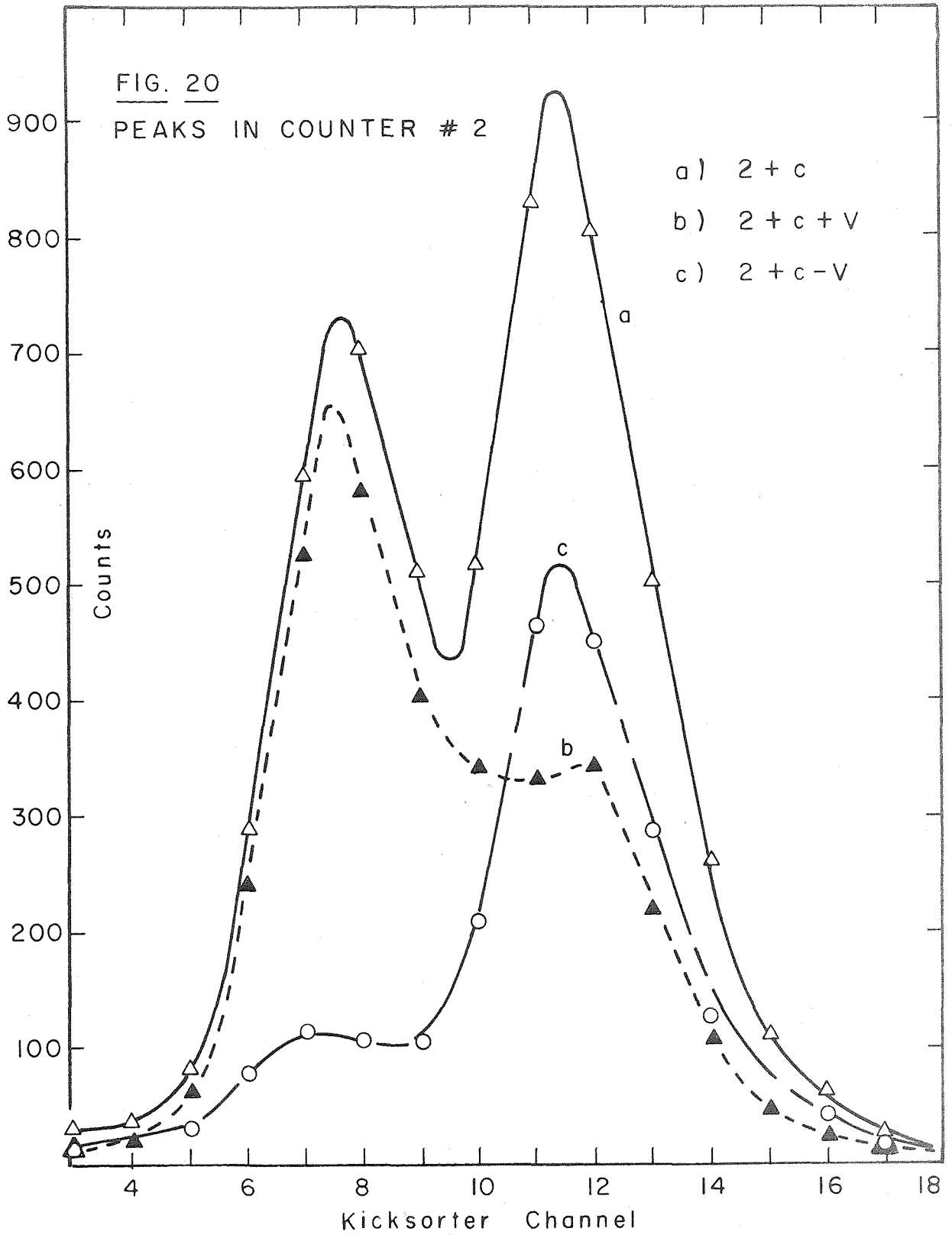
to estimate a correction to the spectrometer efficiency due to this electron straggling, and equation 4, p. 67 of Rossi to estimate the scattering correction, each for several thicknesses of lead and electron energies. Weighting by the pair production probability and integrating numerically over the depth of a lead radiator 2/3 r.l. thick, he finds that within the accuracy of the calculation the radiator efficiency varies with the gamma ray energy (E_γ) as:

$$\frac{E_\gamma - 28 \text{ Mev}}{E_\gamma} (1 - e^{-ut})$$

(Here t is the thickness of the radiator and u the pair production inverse length.) Using UCRL 2426 values for u^{41} , and correcting also for the matter ahead of the veto scintillator (which may convert an incident gamma ray before it reaches the radiator with probability $0.935 (1 \pm 3 \times 10^{-5} E_\gamma)$) one obtains the spectrometer gamma ray efficiency curve plotted in Fig. 3 of Section II, for the 2/3 r.l. thick lead radiator used in this experiment. Back scattering into the veto counter has been neglected.

v) Adjustment of the Spectrometer:

As a further check that the telescope was counting gamma rays, the pulse height spectrum of the #2 scintillator was observed in the kicksorter for various signatures. Fig. 20 shows some typical resulting spectra using a lucite target. Peaks from the gas target itself were similar but were usually taken as the gas was



cooling down so that the gas density was changing gradually from run to run. This does not impede the adjustment of the biases, but makes less evident the relationships of the various peaks.

Curve a shows the spectrum of the #2 scintillator with the radiator in and the coincidence signature $2+c$ (the crystal counter = c) gating the kicksorter. Two distinct peaks are seen. Curve b is obtained by putting the #1 scintillator, which is in front of the radiator, in coincidence as well (actually by requiring the signature $2+c+V$ where $V=1+2$ as discussed above). Note that the upper peak is cut roughly in half. Curve c is obtained with the signature $2+c-V$. Note that the lower peak essentially disappears while about half the upper peak remains. (One can check that curve a = curve b + curve c as might be expected from the signatures.) Thus it seems that the lower peak corresponds to charged particles traversing the two scintillators and enough of the crystal to trigger it: this peak disappears as expected when the front counter is put in veto. The upper peak, corresponding to two or more minimum ionizing particles traversing the 2" scintillator is due roughly half to neutral particles incident on the radiator (curve c) and roughly half to charged particles incident on the radiator (curve b). The neutral component is presumed to be gamma rays since it produces electron pairs in the radiator with the proper radiator Z and thickness dependence, and because it is associated with the largest pulses in the crystal,

presumably those made by showers. The charged component is presumed to be electrons which start showers in the radiator (thus causing 2 or more electrons to traverse the 2" scintillator which continue into the crystal. Note that the energy scale is non-linear (twice minimum particles give less than twice minimum pulse height) presumably because of phototube saturation. A further check is obtained with the signature $2+c-V$ but with the radiator removed. Less than 10% as many coincidences are recorded with the radiator out as with it in. The residual counts are consistent with conversion in the walls of the scintillators and the air between them.

To help the rejection of charged particles, the bias on the Keck box discriminator in the #2 scintillator's channel was set at a point safely below the gamma ray peak but well into the charged particle peak. This bias setting was checked periodically during the course of the experiment by running the $2+c$ peaks with low bias on #2, and the $2+c-V$ peaks with the running bias and noting that the bias setting was safely below the upper peak. In practice the running bias typically corresponded to perhaps $1\ 1/2$ minimum ionizing particles traversing the scintillator.

During the course of the experiment, runs were taken alternately with the radiator in and out with the signature $2+c-V$. The difference in the counting rates was presumed to be due to gamma rays converting in the radiator. Some comparisons were made of IN-OUT

and IN-FRONT yields and no significant difference was found.

(Here "FRONT" refers to the target side of the veto scintillator #1.)

Since the radiator in the front position looks at a considerably different amount of target than it does in the IN position, in the line source geometry used in this experiment, it was not obvious that a more accurate cancellation of accidentals and veto deadtime losses would result from the IN-FRONT subtraction. Since accidentals and deadtime losses were in any case negligible for the counting rates obtained in this experiment, it was decided to adopt the more convenient IN-OUT procedure.

APPENDIX II

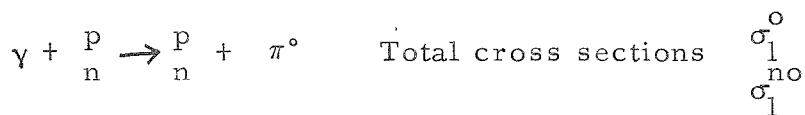
A. SEPARATION OF GAMMA RAYS FROM DIFFERENT

REACTIONS: KINEMATICS: ^{32, 43, 44}

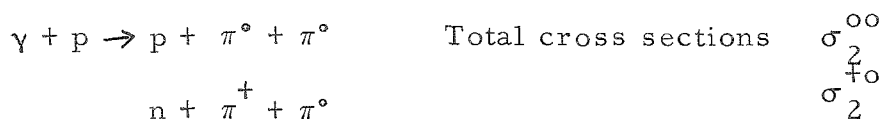
i) Introduction:

The gamma rays counted in the spectrometer, recorded as γ_D and γ_H as discussed above, come from reactions initiated by bremsstrahlung photons of all energies from lower kinematical limits to the endpoint energy; those recorded as the differences $\Delta\gamma$ and $\Delta\gamma$ come from incident photons essentially all within an energy range $E_1 - E_2$ between two bremsstrahlung endpoint energies. In each case, however, the counting rate is "total," i.e., including product gamma rays of all energies (above the bias in the crystal) from all of the reactions which can produce gamma rays at the spectrometer angle. We discuss here what separation of the gamma rays from the several sources is possible because of the different kinematical relations involved and the different resulting gamma ray spectra.

The major source of photons from the target is presumed to be the decay of π^0 's which can be photoproduced singly from nucleons:



and multiply:

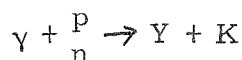


Photons of 1 Bev energy can produce as many as six pions, but production of more than two seems to be rare,¹⁴ for energies below 1 Bev.

Elastic gamma ray scattering (proton Compton effect):



may send photons to the spectrometer, as well, as can the decay of strange particles (Y and K) photoproduced in the reactions:



K meson photoproduction seems to be about an order of magnitude less probable than pion photoproduction for energies around 1 Bev:⁴² In addition not all K decay modes yield π^0 's (perhaps only 30%), nor do all hyperon (Y) decays give gamma rays or π^0 's. Even those decays which do give π^0 's give one or more other particles to carry off energy; thus what gamma rays do come from strange particles are likely to be of low enough energy to be below the crystal counter bias (even more likely below the singles bias). For these reasons K photoproduction is here ignored as a gamma ray source.

Photoproduction of other, as yet unidentified, particles which might decay into gamma rays is also assumed not to contribute to the counting rates.

Since gamma rays are observed in this experiment, in most cases the relevant transformations involve the energy (E), momentum (p) and angle (θ) with respect to the beam of a gamma ray, and the solid angle (Ω) subtended by the spectrometer as defined by gamma rays. Using unprimed letters for these quantities in one frame of reference and primed letters for the corresponding quantities in another frame of reference moving with velocity β relative to the first (in the direction $\theta = 0$), and setting the speed of light equal to one, the appropriate Lorentz transformations can be expressed in the form:

$$\left(\frac{E}{Y}\right)^2 = \left(\frac{p}{p'}\right)^2 = \frac{d\Omega'}{d\Omega} = \frac{1 - \beta^2}{(1 - \beta \cos \theta)^2} = \frac{(1 + \beta \cos \theta')^2}{1 - \beta^2} \quad (1)$$

$$\cos \theta = \frac{\cos \theta' + \beta}{1 + \beta \cos \theta'} \quad (2)$$

In the case of a photon of energy k in the LS (lab system) incident upon a nucleon of mass M at rest the speed of the CMS (system in which the vector sum of the momenta of target nucleon and incident photon is zero) relative to the LS is:

$$\beta_c = \frac{k}{k+M} \quad (3)$$

and the CMS energy of the photon (k') is:

$$k' = \frac{k}{(1 + 2k/M)^{1/2}} \quad (4)$$

The total energy in the LS is:

$$E = k + M$$

and in the CMS:

$$E' = M(1+2k/M)^{1/2} \quad (5)$$

If the incident photon photoproduces a single particle of mass m from a stationary nucleon, the CMS energy of the particle is a constant:

(for given masses and k).

$$E'_m = \frac{E'^2 - M^2 + m^2}{2E'} = \frac{k+m^2/2M}{(1 + 2k/M)^{1/2}} \quad (6)$$

Note that this total CMS energy is a weak function of the particle's mass m , as long as $m \ll M$. This fact makes it difficult to eliminate the possibility that some of the observed gamma rays come from the decay of neutral particles other than π^0 's into two gamma rays.

It is evident that the CMS energy (and thus the LS energy, at least if the target nucleon is at rest) of a scattered gamma ray ($m=0$ in equation 6) is also a constant for a given k . This fact makes it possible to set an upper limit for the proton Compton cross section from the absence of a noticeable "line" near the peak energy in the gamma ray spectra observed from hydrogen.

ii) Expected Pulse Height Spectra from Singly Photoproduced

 π^0 's:

All π^0 's photoproduced singly by photons of a given energy (in the CMS) have the same total energy in the CMS and thus the same velocity β_π , as noted above (equation 6). If we assume for the moment that the pions are emitted isotropically with intensity $n_\pi(\Omega)$ from the origin, then the number emitted into solid angle $2\pi \sin a' da'$ at angle a' is:

$$dn_\pi = n_\pi(\Omega') 2\pi \sin a' da' \quad (7)$$

We consider the RS (π Rest System) to CMS transformation in order to find the gamma ray energy spectrum in the CMS from such a source of π^0 's. (Since only the highest energy gamma rays were in practice used to estimate $\sigma_1(\theta')$, i.e., those emitted by π^0 's travelling within a small angle with respect to the spectrometer's direction, isotropic emission of the parent pions is unessential.)

Since the pion decays into 2 photons isotropically in the RS, it emits $\frac{2\Omega''}{4\pi}$ photons of energy $E''_\gamma = \frac{1}{2} m_\pi$ into solid angle Ω'' in the RS. If a' is the angle of the photon relative to the pion velocity β'_π in the CMS, one sees from equations 1 and 2 that the pion emits

$$\frac{2}{4\pi} \frac{d\Omega''}{d\Omega'} \Omega' = \frac{\Omega'}{2\pi} \frac{1 - \beta'^2_\pi}{(1 - \beta'_\pi \cos a')^2} \quad (8)$$

photons of energy

$$E'_Y = \frac{1}{2} m_\pi \frac{\sqrt{1 - \beta_\pi'^2}}{1 - \beta_\pi' \cos \alpha'} \quad (9)$$

Into the corresponding solid angle Ω' in the CMS. Thus all the photons which are emitted into the direction $\alpha' = 0$ by pions of speed β_π' heading in directions along the generators of a cone of apex half angle α' , have the same energy given by equation (9). Thus for mono-energetic pions, sweeping over α' corresponds to sweeping over E'_Y , and we can eliminate α' in favor of E'_Y . Thus the photon energy spectrum obtained at $\alpha' = 0$ from the pions produced by incident photons of a given energy is:

$$n_Y(E'_Y) = n_\pi(\Omega') \frac{2\sqrt{1 - \beta_\pi'^2}}{m_\pi \beta_\pi'} \Omega' = n_\pi(\Omega') \frac{2\Omega'}{p_\pi'} = \frac{2\Omega' \ln(\Omega')}{E'_Y \max - E'_Y \min} \quad (10)$$

Note that the spectrum is independent of E'_Y . Thus it is a rectangle extending from the minimum photon energy $\frac{1}{2}(E'_\pi - p'_\pi)$ which is about $m_\pi^2/4E'_\pi$ for large E'_π , to the maximum photon energy $\frac{1}{2}(E'_\pi + p'_\pi) \approx E'_\pi$ for large E'_π . (E'_π and p'_π are the CMS total energy and momentum of the pion.)

Applying equations 1 and 2 again with $\beta = \beta_c$ (the velocity of the CMS relative to the LS) one sees that all the photons of angle θ' (relative to the direction of β_c) and energy E'_Y are transformed to photons of E_Y and θ in the LS and the energy scale is expanded or contracted uniformly. Thus the gamma ray energy spectrum in the LS for pions photoproduced by photons in the energy range dk at k is again a rectangle:

$$n_{\gamma}(E_{\gamma}) = \sigma_1(\theta') N_t W \frac{B(k, E_1)}{E_1} \frac{dk}{k} \frac{\sqrt{1 - \beta_c^2}}{1 - \beta_c \cos \theta} \frac{2\Omega}{p_{\pi}'} \quad (11)$$

$\sigma_1(\theta')$ is the CMS differential cross section (ub/ster) for singly photoproducing π^0 's, N_t the number of target nucleons/area of beam, $W = B dk/E_1 k$ the number of incident photons in the energy range dk in a bremsstrahlung beam of endpoint energy E_1 , Ω , the solid angle subtended in the LS by the spectrometer. E_{γ} is:

$$E_{\gamma} = E_{\gamma}' \frac{\sqrt{1 - \beta_c^2}}{1 - \beta_c \cos \theta} = \frac{m_{\pi}}{2} \frac{\sqrt{1 - \beta_{\pi}'^2}}{(1 - \beta_{\pi}' \cos \alpha')} \frac{\sqrt{1 - \beta_c^2}}{(1 - \beta_c \cos \theta)} \quad (12)$$

The gamma ray energy spectrum in the LS from pions photoproduced by a range of incident photon energies $E_1 > k > E_2$ is obtained by integrating equation (11) over this range of k . The resulting gamma ray spectrum is thus approximately a trapezoid, especially if $\Delta k \ll E_1$ and $\sigma_1(\theta')$ varies slowly with k . If one assumes $\sigma_1(\theta')$ varies linearly over the range of k considered the observed spectrum

$S_1(E_{\gamma})$ is:

$$S_1(E_{\gamma}) = \epsilon(E_{\gamma}) n_{\gamma}(E_{\gamma}) = \sigma_1(\theta') N_t 2\Omega \frac{W}{E_1} I(\bar{k}, \theta, E_{\gamma}) = \sigma_1(\theta') N \quad (13)$$

I is the "integrated weighting function":

$$I(\bar{k}, \theta, E_{\gamma}) = \epsilon(E_{\gamma}) \int_{E_2}^{E_1} \frac{\sqrt{1 - \beta_c^2}}{1 - \beta_c \cos \theta} \frac{B(k, E_1)}{p_{\pi}'} \frac{dk}{k} \quad (14)$$

\bar{k} is the average incident photon energy $\approx \frac{1}{2} (E_1 + E_2)$. $\epsilon(E_\gamma)$ is the efficiency of the spectrometer for detecting photons of energy E_γ ; N is the spectrum normalization factor.

Fig. 9 (curve a) shows I/ϵ vs. E_γ for a typical case. Multiplying by the spectrometer efficiency (from Fig. 3) gives curve b, and smearing with the spectrometer energy resolution (Fig. 5) gives curve c. The spectrometer energy resolution is primarily the energy resolution of the crystal counter (assumed to be gaussian with width given by Fig. 18); the angular resolution ($\pm 12^\circ$ or so) contributes a relatively small ($\pm 15\%$ or so) additional effective energy resolution, as does the nucleon motion in deuterium (12% or so).

iii) Expected Pulse Height Spectra from Multiply

Photoproduced π^0 's:

Since multiple pion photoproduction is a three (or more) body process, even for a single incident photon energy, the pions which come out at a given angle in the LS will in general have a distribution of energies. Estimation of the form of this distribution requires a model for the process. As yet no satisfactory model for multiple pion photoproduction exists, although some discussions of simple models have appeared.^{24, 44}

One can, on the other hand, simply assume a set of hypothetical energy spectra $f(E'_\pi)$ and compute from these the corresponding expected gamma ray energy spectra (essentially by integrating the $f(E'_\pi)$

from right to left, multiplying by the spectrometer efficiency and smearing by the counter resolution, as for the singles spectra above:

Some typical cases are plotted in Fig. 21.

$$\frac{1}{c} n_{\gamma m}(E'_{\gamma}, \theta') = \int_{E'_{\pi} \rightarrow E'_{\gamma}}^{E'_{\pi} \text{ max}} \frac{2f(E'_{\pi})dE'_{\pi}}{E'_{\gamma \text{ max}} - E'_{\gamma \text{ min}}} \quad \text{with} \quad \int_0^{E'_{\pi} \text{ max}} f(E'_{\pi})dE'_{\pi} = 1$$

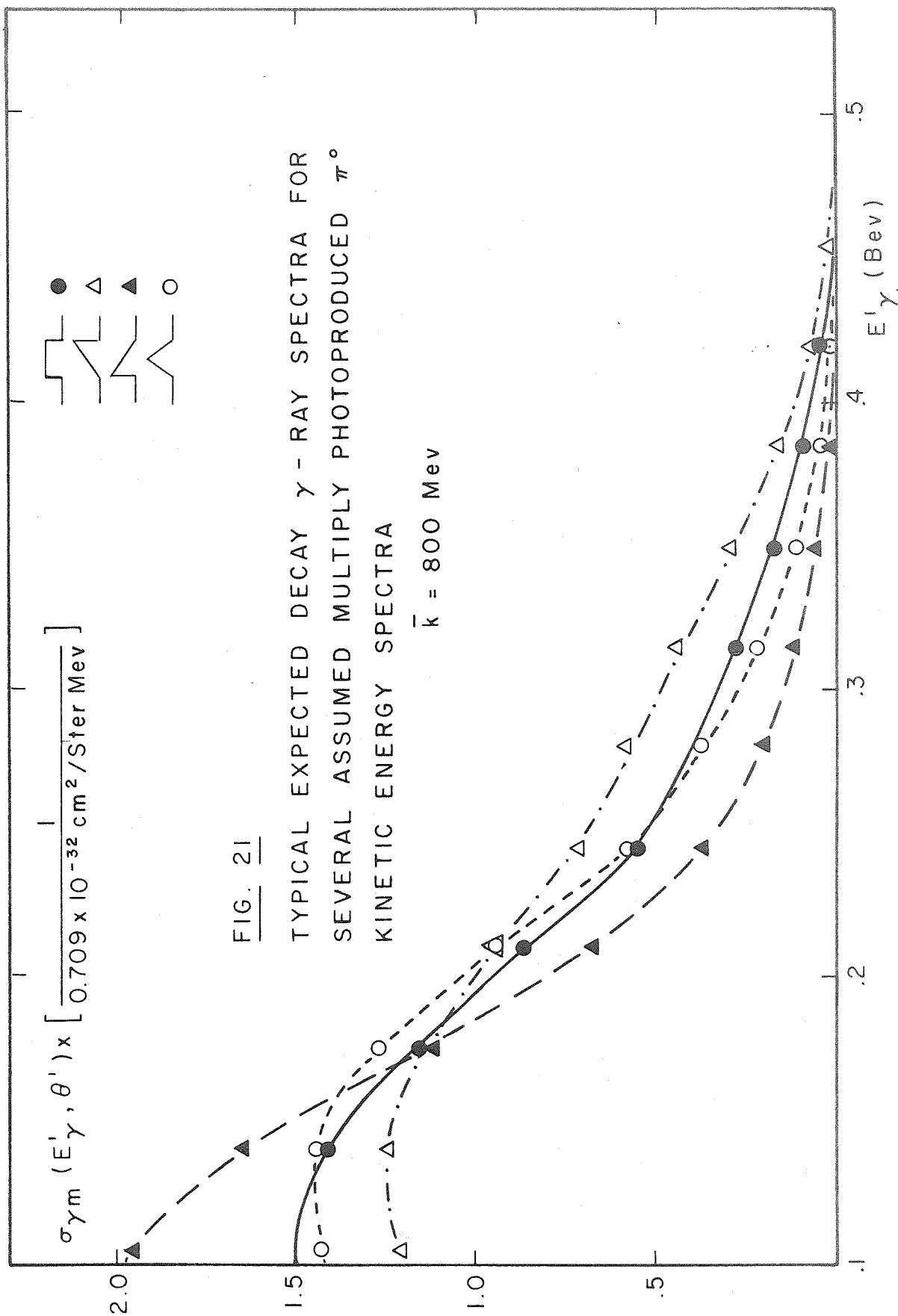
Here $E'_{\gamma \text{ max}}$ is approximately the π^0 energy E'_{π} , as noted above

$$E'_{\gamma \text{ min}} \approx \frac{m_{\pi}^2}{4E'_{\pi}}, \quad \text{if } E'_{\pi} \gg m_{\pi}.$$

The maximum multiple pion energy in the CMS corresponds to the situation where the other pion(s) and the nucleon go off together in the same direction (opposite the observed pion) with the same speed as though they were a compound particle. (To conserve momentum in the CMS the other pion(s) and the nucleon must carry off total momentum equal and opposite to that of the observed pion. They can do this with minimum energy expenditure if they waste no energy in relative momentum.) In the case that the target nucleon is at rest in the LS, equations 3-5 apply, equation 6 with $M+m$ replacing M gives the maximum pion energy in the CMS:

$$E'_{\pi \text{ max}} = \frac{E'^2 - (M+m)^2 + m^2}{2E'}$$

$$c = N_t N_{\gamma} \Omega' \sigma_m(\theta') = N_t N_{\gamma} \frac{d\Omega'}{d\Omega} \Omega \sigma_m(\theta')$$



$$\sigma_m(\theta') = \int_0^{E'_\pi \max} \sigma_{\pi m}(\theta', E'_\pi) dE'_\pi = \frac{1}{2} \int_0^{E'_{\gamma \max}} \sigma_{\gamma m}(\theta', E'_\gamma) dE'_\gamma$$

$$n_{\gamma m}(E_\gamma, \theta) = \frac{dE'_\gamma}{dE_\gamma} \frac{d\Omega'}{d\Omega} n_{\gamma m}(E'_\gamma, \theta') = \frac{dE_\gamma}{dE'_\gamma} n_{\gamma m}(E'_\gamma, \theta') =$$

$$\frac{dE_\gamma}{dE'_\gamma} N_t N_\gamma \Omega \sigma_{\gamma m}(\theta', E'_\gamma)$$

and

$$\epsilon(E_\gamma) n_{\gamma m}(E_\gamma, \theta) = S_m(E_\gamma)$$

iv) Effect of Nucleon Motion in Deuterium:

It was assumed in the computation of the cross sections for single pion photoproduction, and of the deuterium to hydrogen yield ratios, that the smearing effect of the nucleon motion in deuterium on the expected pulse height spectra is not large compared with the rather crude energy and angular resolution of the spectrometer and the broad range of incident photon energies included in the "k bite," $E_1 - E_2$. This section describes a crude estimate of the nucleon motion smearing which supports this assumption.

Since the spectrometer acts like a π° spectrometer with rather broad energy and angular resolution, the nucleon motion is considered in its effect on the pion energy distribution which appears at a given LS angle for a given energy incident bremsstrahlung

photon. For the two body case of single π^0 photoproduction from a nucleon at rest in the LS, equations 1-6 indicate that monoenergetic incident photons send monoenergetic pions to a given LS angle. If the target nucleon may have a distribution of speeds in all directions (as given, for example, by the deuterium momentum wave function), then the outgoing pions will have a momentum distribution (and will have come from a distribution of CMS angles). Assuming a form for the deuterium momentum distribution and for the CMS angular distribution permits the outgoing pion momentum distribution to be computed.

For this calculation the pion CMS angular distribution was assumed to vary linearly over the relevant range of angles, and the deuterium wave function assumed was the simple Hulthen form given in R. Smythe's thesis.⁴⁶ Interpolating from Smythe's values, three values separating equally probable regions of nucleon momentum were chosen:

16.7% of the nucleons in deuterium have momentum less than

34.2 Mev/c

50.0% of the nucleons in deuterium have momentum less than

67.2 Mev/c

83.3% of the nucleons in deuterium have momentum less than

128.4 Mev/c

For the six equally probable directions corresponding to the faces of a cube, the pion energy at $\theta_{LS} = 60^\circ$ was calculated for these three nucleon momentum values for each of three assumed incident photon energies ($k = 500, 800, 1100$ Mev). (For this calculation the nucleon rest mass was erroneously assumed constant in the deuteron independent of its kinetic energy, but this error would not broaden the distribution importantly.*) Although 18 points (per k) are not enough to fix the distribution with any precision, its width was estimated from these results to be some 14% for $k = 500$ Mev, 9% for $k = 1.1$ Bev. Thus the smearing effect from the distribution is much smaller than that due to the energy resolution of the counter itself. (Typically some 30%.) The distribution at $\theta = 120^\circ$ may be somewhat broader* but probably not enough to seriously affect the resolution. A constant smearing of 12% was assumed in correcting the deuterium resolution function, for both 60° and 120° .

*Dr. G. N. Neugebauer, private communication.

B. DATA REDUCTION DETAILS:

i) Errors:

The sources of uncertainty in the results of this experiment can be summarized in the usual three groups: random, partially systematic and systematic. In addition an error can be classified according to whether or not it is "magnified" (i.e., does not cancel and so becomes relatively larger) in the subtractions (such as those leading to $\Delta\gamma$ and σ_1), and whether or not it cancels out in the D/H ratios. Errors listed as "m" below are magnified in the subtractions (typically by about a factor of 7 for $\Delta\gamma$ and $\Delta\gamma$ and by about a factor of 12 for the σ 's). Errors listed as "r" cancel out (at least approximately) in the D/H ratios. Recommendations of Orear⁴⁸ have been used in combining errors.

random

a) Counting statistics (m) - the fundamental known source of uncertainty in most of the results quoted. Typically 2% in γ .

b) Kicksorter drifts (partly m) - partially corrected for by frequent calibrations, but may still contribute 10-20% uncertainty to σ 's. Do not affect γ 's.

partially systematic

c) Spectrometer energy calibration (mostly r) - 10-15% in σ 's, does not affect γ 's. (Crystal counter gain and bias do, of course.)

d) Beam monitor sensitivity - "other target correction" varied at known times, but not under control, thus occasionally m. 1-2%. (Beam monitor temperature and pressure presumably corrected for to better than 1%.)

e) Beam energy - known supposedly to better than 1% and constant. Non-systematic variations, at least, would be m.

f) Gas density - subject to $\frac{1}{2}$ % m type "random" fluctuations (Appendix IB). Varied at known times under control. Thus additional relative error of perhaps 1% (not m unless varied during subtraction). Absolute error of perhaps 3% (not m, partly r).

g) Magnetic fields (m) - mostly varied at known times but not under control. Less than $\frac{1}{2}$ % effect on spectrometer counting rate.

h) Veto (mostly r) - deadtime losses less than 1% and only partly m. No known reason for appreciable veto inefficiency.

i) Counter 2 bias - varied at known times but presumably also subject to random drifts. Possibly 1% and only partially m.

j) Crystal counter bias - perhaps 1% partially m. Does not affect σ_1 's, as kicksorter bias always above crystal counter bias.

k) Bremsstrahlung spectrum shape (r) - primarily affects σ 's and 600 subtractions for $\Delta\gamma$ and $\Delta\sigma$. Known supposedly to better than a few percent, but m for σ 's. The major effects of other targets in the beam are corrected for by the other target correction; residual effects on the spectrum shape due to other targets

are probably not large compared with the rather poor statistics even for the $\sigma_m(\theta')$'s.

systematic

l) Gas composition - supposedly 99% pure, but this was unfortunately not checked (being supposedly negligible for the σ 's).

m) Target length (r) - perhaps 5% (including crude estimate of slit edge penetration). Scattering from slits assumed small, as usually low energy and accompanied by charged particles which would be likely to trigger veto.

n) Solid angle (r) - perhaps 5%.

o) Spectrometer efficiency (r) - depends on energy, typically 10%.

p) Absolute beam calibration (r) - 2%.

Errors quoted in Table I include where applicable (and known):

a, b, d, f, m, n, o, p. The total errors on the results quoted in

Table I should thus possibly be somewhat larger, perhaps typically:

For	γ	about $\pm 3\%$,	(but γ_D/γ_H	about $\pm 2\%$)
	$\Delta\gamma$	" $\pm 20\%$,	(" $\Delta\gamma_D/\Delta\gamma_H$	" $\pm 5\%$)
	$\sigma_1(\theta')$	" $\pm 30\%$,	(" $\sigma_{1D}(\theta')/\sigma_{1H}(\theta')$	" $\pm 15\%$)
	$\sigma_m(\theta')$	" $\pm 40\%$		

REFERENCES

1. M. Gell-Mann and K. M. Watson, The Interactions between π Mesons and Nucleons, Annual Review of Nuclear Science 4, 219 (1954).
2. Koester and Mills, Phys. Rev. 105, 1900 (1957).
3. McDonald, Peterson and Corson, Phys. Rev. 107, 577 (1957).
4. J. M. Blatt and V. F. Weisskopf, Theoretical Nuclear Physics, Wiley, N.Y. (1952).
5. Watson, Keck, Tollestrup and Walker, Phys. Rev. 101, 1159 (1956).
6. A. M. Wetherell, Phys. Rev. 115, 1722 (1959).
7. Bethe and DeHoffman, Mesons and Fields, Vol. II, Row, Peterson, Evanston, Ill. (1955).
8. J. I. Vette, Ph. D. Thesis, CIT (1958), Phys. Rev. 111, 622 (1958).
R. M. Worlock, Ph. D. Thesis, CIT (1958), Phys. Rev.
P. C. Stein and K. C. Rogers, Phys. Rev. 110, 1209 (1958).
DeWire, Jackson and Littauer, Phys. Rev. 110, 1208 (1958).
9. F. Dixon, Ph. D. Thesis, CIT (1959).
F. Dixon and R. L. Walker, Phys. Rev. Lett. 1, 142 (1958).
Heinberg, McClellan, Turkot, Woodward, Wilson and Zipoy,
Phys. Rev. 110, 1211 (1958).
10. M. Moravcsik, Purdue Lectures, BNL 459 (T-100), (March 1957)
R. L. Walker, Lecture Notes (unpublished)
11. G. Neugebauer, Ph. D. Thesis, CIT (1959).
G. Neugebauer and J. Mathews, private communication.
12. M. Moravcsik, Phys. Rev. 104, 1451 (1956).
13. Burrowes et al., Phys. Rev. Lett. 2, 119 (1959).
14. Sellen et al., Phys. Rev. 113, 1323 (1959).

15. Marshak, Meson Physics, McGraw-Hill, N. Y. (1952).
16. Chew and Low, Phys. Rev. 101, 1579 (1956).
17. G. C. Wick, Rev. Mod. Phys. 27, 339 (1955).
18. Chew, Goldberger, Low and Nambu, Phys. Rev. 106, 1337 (1957).
19. K. M. Watson, Phys. Rev. 95, 228 (1954).
M. Gell-Mann and V. L. Telegdi, Phys. Rev. 91, 169 (1953).
20. Bruekner and Goldberger, Phys. Rev. 76, 1725 (1949).
21. Sands, Teasdale and Walker, Phys. Rev. 95, 592 (1954).
22. Keck, Tollestrup and Bingham, Phys. Rev. 103, 1549 (1956)
(includes references to earlier work).
23. Beneventano et al., Nuovo Cimento 10, 1109 (1958).
Hagerman, Crowe and Friedman, Phys. Rev. 106, 818 (1957).
24. M. Bloch, Ph. D. Thesis, CIT (1958).
M. Bloch and M. Sands, Phys. Rev. 108, 1101 (1957).
M. P. Ernstene, Ph. D. Thesis, CIT (1959).
D. D. Elliott, Ph. D. Thesis, CIT (1959).
25. W. Wales, Ph. D. Thesis, CIT (1959).
G. Neugebauer, Ph. D. Thesis, CIT (1959).
G. Neugebauer, Wales and Walker, Phys. Rev. Lett. 2,
429 (1959).
26. Kantz and Hofstadter, Nucleonics 12, #3, 36 (1954).
27. Yamagata and Yoshimine, preprint.
Filosofo and Yamagata, CERN (1956).
28. B. Rossi, High Energy Particles, Prentice-Hall, N. Y. (1952).
29. Boyden, Emery and Walker, Synchrotron Report (unpublished).
30. R. R. Wilson, Nucl. Inst. 1, 101 (1957).
31. Johnston et al., AEC Report MDDC-850 (unpublished).
32. H. H. Bingham and A. B. Clegg, Phys. Rev. 112, 2053 (1958).

33. R. L. Garwin, Rev. Sci. Instr. 23, 755 (1953).
34. E. Breitenberger, Prog. Nuc. Phys. 4, 56 (1955).
35. L. I. Schiff, Quantum Mechanics, McGraw-Hill, N. Y. (1949).
36. R. L. Garwin, Rev. Sci. Instr. 24, 618 (1953).
37. A. Barna and M. Sands, Pulse Height Spectrometer Model 2, (1958), unpublished.
38. H. A. Bethe, Phys. Rev. 89, 1256 (1953).
39. Mohr and Tassie, Aust. J. Phys. 7, 217 (1954).
40. L. Eyges, Phys. Rev. 76, 264 (1949).
41. UCRL 2426
42. Brody, Wetherell and Walker, Phys. Rev. 110, 1213 (1958).
McDaniel, Silverman, Wilson and Cortellessa, Phys. Rev. Lett. 1, 109 (1958).
43. Sternheimer, R., Phys. Rev. 99, 277 (1955).
44. Sternheimer and Lindenbaum, Phys. Rev. 109, 1723 (1958).
45. J. Mathews, Ph. D. Thesis, CIT (1957).
46. R. Smythe, Ph. D. Thesis, CIT (1957).
47. V. Z. Peterson and E. Emery, Gas Target Report (unpublished).
48. J. Orear, UCRL-8417.
49. Cutkosky and Zachariasen, Phys. Rev. 103, 1108 (1956).
50. H. Myers, Ph. D. Thesis, CIT (1959).
51. E. Fermi, Prog. Theor. Phys. 5, 570 (1950).

52. Nambu, Phys. Rev. 106, 1366 (1957).
53. Yuan and Lindenbaum, Phys. Rev. 103, 404 (1956).